ANALYSIS OF THE EXPRESSION AND EFFECTS OF VASCULAR ENDOTHELIAL GROWTH FACTOR FAMILY OF MOLECULES ON FRAGILE X SYNDROME ABNORMALITIES IN A MOUSE MODEL

BY

AMOGH BELAGODU

DISSERTATION

Submitted in partial fulfillment of the requirements
for the degree of Doctor of Philosophy in Neuroscience
in the Graduate College of the
University of Illinois at Urbana-Champaign, 2017

Urbana, Illinois

Doctoral Committee:

Assistant Professor Roberto Galvez, Chair
Associate Professor Robert Wickesberg
Assistant Professor Daniel Llano
Associate Professor Stephanie Ceman

Abstract

Fragile X Syndrome (FXS) is the most common form of inherited mental retardation affecting 1:3600 males and 1:8000 females (Cornish et al., 2008). The primary cause is a silencing of the *FMR1* gene, via increased CGG trinucleotide repeats, which encodes for the Fragile X Mental Retardation Protein (FMRP) (Santoro et al., 2012). The current prevailing theory for the molecular mechanism mediating FXS molecular, physical, and behavioral phenotypes is centered around dysregulation of down-stream products of the metabotropic glutamate receptor (mGluR) (mGluR Theory) (Bear et al., 2004). However recent clinical trials using mGluR inhibitors have all failed, attributing to various factors such as a need for optimized dosage, developmental time for intervention, better metrics for human studies, and most prominently complexity of the mGluR pathway (Scharf et al., 2015). With this ubiquitous failure of mGluR inhibitors, new thrusts have been initiated to determine which of the downstream components of the mGluR pathway is leading to and causing FXS phenotypes.

In the pursuit of isolating and determining potential causes/therapeutic targets for intervention, the current dissertation explored the role of vascular endothelial growth factor A (VEGF-A), a downstream component of mGluR. This dissertation will outline a series of studies where we demonstrate that VEGF-A is elevated in adult FXS mice and that modulation of this elevated VEGF-A can attenuate many FXS abnormalities. In Chapter 2, we obtain developmental expression profiles of the VEGF Family of molecules and their Receptors to help understand where this dysregulation occurs and how it manifests throughout development. Next, Chapter 3 we found that through blocking VEGF-A, Synapsin-1 levels (a presynaptic marker) were reduced to wildtype (WT) levels and resulted in a rescue of physical and behavioral FXS phenotypes (Belagodu et al., 2017). Chapter 4 explored and characterized ultrasonic

vocalization (USV) abnormalities in FXS mice to find more human relevant behavioral metrics to assess potential therapeutic interventions (Belagodu et al., 2016). Utilizing these studies, Chapter 5 assessed the extent to which blocking VEGF-A can rescue many FXS behavioral abnormalities, such as USV production profiles and behavioral measures of locomotion, anxiety, and stereotypy. Finally, to determine which of the VEGF Receptors are driving the beneficial effects of blocking VEGF-A, Chapter 6 utilized VEGF Receptor specific blockers to assess similar molecular and behavioral properties examined following blocking of VEGF-A. Overall these studies will help to provide further insight into which of the downstream components of the mGluR pathway are playing a role in FXS. In particular these studies will establish which of the VEGF Family and Receptors are driving FXS abnormalities and thus may serve as a viable target for future FXS therapeutics.

Dedication

This dissertation is dedicated to my family: my parents Partha and Chithra Belagodu and my brother Akarsh Belagodu, for which without their constant support and encouragement throughout my growth as a scientist, this work would not have been possible.

ACKNOWLEDGMENTS

This work would not have been possible without the continuing support and mentorship of Dr. Roberto Galvez. It is with his patience and guidance that I have been able to progress and succeed in my graduate career. I would also like to thank my committee members whose guidance has allowed my thesis and my graduate career to flourish. I would also like to thank Dr. Stephanie Ceman and her graduate student Geena Skariah for their continued support, guidance, and encouragement with the molecular aspects of my research, as well as BJ Slater for his assistance with slice preparations. Furthermore, I would like to thank Dr. Janice Juraska for her assistance and help with my final year. I would also like to thank my family and my friends who have helped, supported, and encouraged me throughout the years. I would also like to particularly thank all my friends here at the University of Illinois Urbana-Champaign who have made this place a new home for me, creating an environment in which I have been able to develop not only as a graduate student, but a scientist and an adult. I would like to thank all the assistance I have gotten along the way, particularly from the Vet Staff at Beckman, and my numerous undergraduate students who have contributed to various aspects of my research. Finally, I would like to thank the Beckman Institute for providing not only the facilities and equipment which allowed me to complete my thesis, but also providing a multidisciplinary and nurturing environment for me to grow and expand as a scientist.

TABLE OF CONTENTS

CHAPTER 1: INTRODUCTION

Fragile X Syndrome Overview

Fragile X Syndrome (FXS) is the leading form of inherited mental retardation and the most common known single gene cause for autism spectrum disorder (ASD). The syndrome affects roughly 1:3600 males and 1:8000 females (Cornish et al., 2008). FXS is caused by an increase in CGG trinucleotide repeats at the 5' encoding region of *FMR1,* the gene that codes for the Fragile X Mental Retardation Protein (FMRP). This results in hypermethylation and transcriptional silencing of *FMR1*. Normal individuals have less than 50 CGG trinucleotide repeats and thus do not exhibit any deficits in FMRP production. FXS premutations have 50-200 CGG trinucleotide repeats, are able to produce low levels of FMRP and have a different phenotypic profile than FXS full mutations (Santoro et al., 2012). For an extensive review of FXS premutations see (Loesch and Hagerman, 2012). FXS full mutations have more than 200 CGG trinucleotide repeats (McLennan et al., 2011) resulting in hypermethylation, chromatin condensation and transcriptional silencing of *FMR1* (Pieretti et al., 1991; Verkerk et al., 1991). The remainder of this review will focus on this full mutation referred to as FXS, where no FMRP is produced.

FXS is associated with many physical and behavioral characteristics. FXS patents have been shown to have elongated faces, prominent foreheads, macroorchidism in males, prominent ears, soft skin, flat feet, hyperextensible finger joints (McLennan et al., 2011), and hypotonia (Goldstein and Reynolds, 1999). Behavioral phenotypes are more complex. The most common impairments are anxiety, attention deficit hyperactivity disorder, hyperarousal to sensory stimuli, obsessive-compulsive disorder (Cordeiro et al., 2011), general autistic-like behavior (Miller et al., 1999), heightened food selectivity generally based on texture (Raspa et al., 2010), and trouble

sleeping (Kronk et al., 2010). In addition to these abnormalities, FXS patients exhibit numerous molecular and neuronal deficits that many believe are the underlying cause for the behavioral and physical characteristics mentioned above. These molecular and neuronal deficits are discussed in more detail below.

Role of FMRP in FXS

While the lack of FMRP is what drives the FXS phenotype, the cause of the syndrome is the increased number of trinucleotide repeats in concert with hypermethylation (Smeets et al., 1995). During replication, the trinucleotide repeats cause slipping of the three-way DNA junction. This slip causes activation of repair mechanisms that add more repeats into the gene, further increasing the number of CGG trinucleotide repeats (Pearson et al., 2002). However, this expansion of the CGG trinucleotide repeats is not believed to be the sole cause for the transcriptional silencing of *FMR1*, rather the methylation of these CGG trinucleotide repeats results in the transcriptional silencing of *FMR1* (Sutcliffe et al., 1992). These findings were later supported with the discovery of two patients that had expanded CGG trinucleotide repeats without the methylation but normal levels of *FMR1* and its protein product FMRP (Smeets et al., 1995).

Although FMRP can be found in a variety of tissue in the body, it is most abundant in the brain and testes. Within the brain, FMRP is localized mainly to neurons where it can be found in the cell body, dendrites, and dendritic spines (Devys et al., 1993). FMRP's believed primary role in neurons is to down regulate the translation of target messenger RNAs (mRNA; RNA molecules which help communication between DNA and ribosomes) in dendritic spines. However, FMRP has multiple alternatively spliced isoforms suggesting various functions for each (Ashley et al., 1993; Verkerk et al., 1993; Banerjee et al., 2010).

The most prominent FMRP isoform in humans contains three hnRNP K-protein homology domains (KH0, KH1 & KH2) and an arginine-glycine-glycine (RGG) box, totaling four RNA binding domains (Siomi et al., 1993; Hu et al., 2015). Of these KH domains KH2 has been extensively explored, as mutations at this domain results in patients being null for FMRP resulting in a rather extreme manifestation of FXS (De Boulle et al., 1993). This is counter to the majority of FXS patients where the root cause for the lack of FMRP is derived by the excessive presence of CGG trinucleotide repeats and subsequent methylation of the 5' region in the *FMR1* gene (Fu et al., 1991; Oberle et al., 1991; Verkerk et al., 1991; Sutcliffe et al., 1992). These KH2 mutation cases, specifically at I304N, have led to additional investigation of the role of FMRP in mRNA binding. This KH2 domain has been suggested to bind to a "kissing complex motif" which in turn mediates the interaction between KH2 and various polyribosomes found in the brain (Darnell et al., 2005). In exploring these binding interactions, various potential mRNA target structures or sequences for KH2 have been implicated; however, this is a growing research direction with many conflicting findings that need further investigation (Ascano et al., 2012; Anderson et al., 2016).

Alternatively, through co-immunoprecipitation various components of the microRNA (miRNA) pathway that interact with FMRP via the RGG box have been determined (Edbauer et al., 2010). MicroRNAs are small non-coding RNA molecules that have two known functions: RNA silencing and post-transcriptional regulation of gene expression (Ambros, 2004; Bartel, 2004), driving overall regulation and production of various proteins. Interestingly, the RGG box in FMRP, along with the aforementioned miRNAs, also binds to mRNAs containing G-quadruplexes (Darnell et al., 2001). G-quadruplexes are stable secondary structures found on both nucleic acids and are heavily involved with regulation of ribosomal scanning. Through

examination of the domains found in FMRP and screening for targets of those components, extensive lists of its potential targets have been determined, helping to assess FMRP's function such as shuttling of mRNA between the nucleus and cytoplasm, mediating localized synaptic protein synthesis via mRNA modulation (Antar et al., 2005), and inhibition of mRNA translation (Laggerbauer et al., 2001).

In exploration of FMRP as a translation repressor of mRNA targets, it was further found to co-sediment with polyribosomes in subcellular fractions, suggesting that mRNA repression is a result of FMRP binding to polyribosomes. Once bound FMRP is believed to have inhibitory effects on mRNA translation by blocking the eIF4F complex through enlisting of CYFIP1 (Napoli et al., 2008), stalling ribosomes during the elongation phase of translation (Stefani et al., 2004), or by recruiting RNA-induced silencing complex (RISC) (Caudy et al., 2002). As a possible mechanism mediating these different functions, FMRP has been shown to undergo various posttranslational modifications. This allows the protein to slightly change in order to fulfill these different roles of binding to various sites or interacting with different molecules. FMRP exhibits four main post-translational/post-transcriptional modifications, phosphorylation, ubiquitnation, splicing, and methylation. Phosphorylation of FMRP results in the inhibition of translation as it binds to stalled untranslating polyribosomes and RISC, but not with *Dicer* (Zhang et al., 2001; Menon and Mihailescu, 2007; Menon et al., 2008). Ubiquitnation results in increased translation as it causes FMRP to degrade in the synapse, removing its inhibitory affect (Westmark and Malter, 2007). Splicing (the post-transcriptional modification) results in the removal of specific exons, altering FMRP localization (Muddashetty et al., 2007). Finally, methylation alters FMRP's specificity to binding various mRNAs, which can result in the regulation of various proteins throughout the body (Westmark and Malter, 2007).

Although very complex, these molecular deficits are believed to be the underlying cause for FXS dendritic spine abnormalities, resulting in the FXS cognitive and behavioral deficits. The most notable dendritic spine abnormality seen in FXS brains when compared to WT counter parts is the presence of an excess amount of immature looking long dendritic spines (Irwin et al., 2001; Galvez and Greenough, 2005; Grossman et al., 2006). Through developmental analyses these dendritic spine abnormalities were proposed to be due to a lack of properly regulated developmental dendritic spine elimination (Galvez et al., 2003; Galvez and Greenough, 2005), particularly due to elevated formation and elimination rates (Pan et al., 2010). This was further supported in a FXS *Drosophila* model where dFMRP was overexpressed, resulting in a more reduced dendritic spines density, suggesting excessive dendritic spine elimination or reduced dendritic spine production (Zhang et al., 2001; Pan et al., 2004). These studies suggest that the absence of FMRP drives the abnormal dendritic spine morphology and that proper FMRP expression is required for normal network growth and communication.

mGluR Theory of Fragile X Syndrome

The prevailing theory for the molecular mechanism mediating FXS abnormalities revolves around the hyperactivation of metabotropic glutamate receptors (mGluR) resulting in exaggerated protein synthesis downstream of mGluR. To establish a correlation, an extensive review between Group 1 mGluR functionality and behavioral/cognitive tasks was conducted by Mark Bear, from which the major points have been summarized in the table below (Bear et al., 2004) (Table 1.1).

Group 1 mGluR Function	FXS Manifestation
mGluR5 in the Amygdala has been found to help regulate emotionally salient experiences, and helps encode fear and anxiety (Rodrigues et al., 2002).	FXS mice have been observed to have aberrant contextual and conditioned fear responses (Paradee et al., 1999).
Many mGluR5 antagonists reduce anxiety (Tatarczynska et al., 2001).	FXS patients have increased anxiety and autistic-like behavior (Miller et al., 1999; Cordeiro et al., 2011).
Habit formation via corticostriatal synapses is dependent on Group 1 mGluR activation (Graybiel, 1998; Gubellini et al., 2003).	FXS patients have obsessive-compulsive disorders (Cordeiro et al., 2011).
Antagonists to mGluR5 reduce audiogenic seizure sensitivity in mice (Chapman et al., 2000).	FXS patients and mice have increased occurrence and sensitivity to audiogenic seizures (Chen and Toth, 2001; Berry-Kravis, 2002; Incorpora et al., 2002).
Long-term changes in excitability of neocortical layer 5 neurons are mediated by mGluR5 activation. This activation results in long-term potentiation of intrinsic excitability which in turn reduces afterhyperpolarization outward current, allowing the cortical network to be more excitable (Sourdet et al., 2003). Furthermore, increased skin mGluR5 activation increases pain sensitivity (Neugebauer et al., 1999; Walker et al., 2001; Tachibana et al., 2003).	FXS patients have hyperarousal to sensory stimuli and greater sensory evoked potentials (Castren et al., 2003; Cordeiro et al., 2011).
Mice lacking Group 1 mGluRs have reduced pre-pulse inhibition response (Brody et al., 2003).	FXS mice have enhanced response to pre-pulse inhibition (Chen and Toth, 2001; Nielsen et al., 2002).
Maintenance of the circadian rhythm has been linked to activation of Group 1 mGluRs (Park et al., 2003).	The FXS *Drosophila* model have altered circadian rhythms (Dockendorff et al., 2002; Inoue et al., 2002; Morales et al., 2002).

Table 1.1. Overview of correlations between Group 1 mGluRs and FXS that lead to the development of the mGluR theory for FXS.

One of the common neuronal characteristics of FXS is enhanced LTD compared to WT counterparts. The main mechanisms for LTD induction, utilizing NMDA or mGluR receptors, have been characterized in various brains regions. Analyzing these two forms of LTD served as the initial basis for extrapolating the core mechanism driving many of the FXS phenotypes. NMDA induced LTD has been primarily characterized in the hippocampus and traditionally

involves the internalization of AMPA receptors (Carroll et al., 1999). Another key characteristic is that NMDA LTD is entirely independent of protein synthesis during the early stage (Huber et al., 2000; Sajikumar and Frey, 2003). As with NMDA induced LTD, mGluR induced LTD also involves the internalization of AMPA receptors (Snyder et al., 2001). However, mGluR-LTD is protein synthesis dependent and is driven by the translation of preexisting mRNA (Huber et al., 2000).

This dependence on preexisting mRNAs is of particular importance as FMRP has been shown to bind mRNA targets downstream of mGluR, coupled with the direct correlation between mGluR stimulation and FMRP activity, suggesting that proper FMRP expression is critical for driving the protein synthesis dependent mGluR-LTD (Bear et al., 2004; Darnell et al., 2011). Furthermore, as mentioned before, mRNA targets of FMRP have been found in dendritic spines indicating their involvement in the LTD process (Miyashiro et al., 2003; Antar et al., 2005; Huang et al., 2005). Studies have indicated that mGluR is expressed in multiple regions in the brain (Oliet et al., 1997; Huber et al., 2001), and along with FMRP being observed in most neurons (Devys et al., 1993), suggest that a link between the two could result in the deficits seen in FXS, discussed in detail above in Table 1.1.

Validation of the mGluR Theory of FXS as a Treatment Paradigm

In support of the mGluR theory offering a likely site for therapeutic intervention many FXS animal studies provided promising results. FXS *Drosophila* that lacked mGluR displayed a correction of glutamate receptor trafficking, synaptic plasticity, presynaptic ultrastructure, and motor behavior (Pan and Broadie, 2007; Pan et al., 2008; Repicky and Broadie, 2009). Likewise, FXS mice that were heterozygote for the *Grm5* gene, thus only expressing 50% of the normal mGluR5 levels, exhibited decreased sensitivity to audiogenic seizures; reduction in the

presence of immature dendritic spines; increased and heighted response in evoked potentials to contralateral eye depression and ipsilateral eye potentiation following monocular deprivation; reduction in hippocampal protein synthesis; reduction of excessive LTD; and restoration of normal extinction in inhibitory avoidance behavior (Dolen et al., 2007). This drastic reversal of numerous FXS phenotypes was extremely promising, and suggested that modulating mGluR levels can help alleviate FXS abnormalities. As a result of the promising genetic studies, mGluR inhibitors and their efficacies in treating FXS were further explored. 2-methyl-6-(phenylethynyl)-pyridine (MPEP) was initially taken into consideration as it is an allosteric modulator of mGluR5 (the primary Group 1 mGluR receptor that has been suggested to be the key player in the FXS mGluR theory). MPEP can also readily cross the blood brain barrier, making it a viable tool for therapeutic interventions (Gasparini et al., 1999). In FXS *Drosophila* MPEP was found to decrease excitotoxicity induced embryonic lethality (Chang et al., 2008) and rescue olfactory and courtship-related memory (McBride et al., 2005; Bolduc et al., 2008). In the FXS zebrafish model embryos generated in an MPEP enriched medium exhibited rescued neurite morphology and normal craniofacial development (Tucker et al., 2006). In the FXS mouse model MPEP showed a rescue in open field anxiety; reduced audiogenic seizure occurrence rates (Yan et al., 2005); and a rescue in prepulse inhibition deficits (de Vrij et al., 2008). Additional studies found that MPEP also corrected epileptiform discharges; decreased hippocampal protein synthesis levels to that observed in controls (Chuang et al., 2005; Osterweil et al., 2010); decreased hippocampal dendritic filopodia density; rescued mRNA granule expression (Aschrafi et al., 2005); and activity of glycogen synthase kinase-3 (Min et al., 2009). With successes in reversing multiple FXS phenotypes across species, mGluR inhibitors were highly sought after for clinical trials.

Recent Clinical Trials to Establish a Reliable Treatment Scheme

Based on the aforementioned studies, the mGluR theory of FXS, and various phenotypic rescues of MPEP (mGluR5 antagonist), various clinical trials were pursued utilizing mGluR antagonists. Three main antagonists, developed by different pharmaceutical companies, were elected for and pursued, with a fourth that never completed its clinical trial. These consisted of Fenobam developed by McNeil Laboratories, RO4917523/RG7090 (Basimglurant) developed by Roche, AFQ056 (Mavoglurant) developed by Novartis, and finally STX107 developed by Seaside Therapeutics (this clinical trial was halted until further notice).

One of the first mGluR clinical trials conducted (NCT01806415) utilized Fenobam. Fenobam is a nonbenzodiazepine anxiolytic compound that selectively inhibits mGluR5 via negative allosteric modulation (Porter et al., 2005). In NCT01806415, a single dose of Fenobam (50 – 150 mg once a day) was administered to patients ranging from 18 – 35 years of age. A total of 12 males and females were tested with the following endpoints: eye blink inhibition and the Carolina Fragile X Project Continuous Performance Test (Scharf et al., 2015). The Carolina Fragile X Project Continuous Performance Test is a modified version of the Continuous Performance Test (CPT) optimized for FXS, in which the assessment is shorter with a greater focus on auditory/visual attention and impulsivity (Berry-Kravis et al., 2008). NCT01806415 failed to show any real significance on both measures (Berry-Kravis et al., 2009; Scharf et al., 2015).

Basimglurant, another negative allosteric modulator of mGluR5 developed by Roche, had many advantages over Fenobam. It has a longer half-life and can more easily cross the blood brain barrier resulting in improved bioavailability (Lindemann et al., 2015). Currently, there have been three clinical trials utilizing basimglurant; NCT01015430, NCT01517698, and

NCT01750957. The first study, NCT01015430 was conducted to assess safety and tolerability levels over a range of dosages (0.1, 0.5, 1.0, & 1.5 mg once a day). A total of 40 male and female FXS patients ranging from 18 – 50 years of age were utilized in this double blind parallel study. Positive results in safety and tolerance levels from this study (primarily for 0.5 and 1.5 mg doses) then prompted the subsequent two basimglurant studies. These were both proof of concept studies with one focusing on adolescence (NCT01750957) and the other predominately in adulthood with some adolescent subjects (NCT01517698). The first of these two studies, NCT01517698, was conducted on 185 males and females ranging from 14 – 50 years of age. These subjects received one of two dosages (0.5 or 1.5 mg once a day). In this double blind parallel study, both efficacy and viable biomarkers for assessing the drug were pursued. Along with these, a variety of cognitive and behavioral tasks were also assessed, ranging from Anxiety, Depression, Mood Scale, Social Responsive Scale, Clinical Global Impression Rating Scale for both Improvement and Severity, and the Aberrant Behavior Checklist Community Scale. Unfortunately, this study yielded less than ideal results, with no real benefit resulting from basimglurant treatment. In a second attempt, NCT0170957 was designed in a similar fashion with 47 FXS patients ranging from 5 – 13 years of age. This was the first study to explore the effects in a young age group and thus also assessed the safety and tolerance levels of basimglurant in children. As with the aforementioned clinical trial, various cognitive and behavioral tasks were assessed: Anxiety, Depression, Mood Scale, Clinical Global Impression Rating Scale for both Improvement and Severity, General Behavior Assessment Scale, Aberrant Behavior Checklist Community Scale, Repeatable Battery for the Assessment of Neuropsychological Status, and the Visual Analog Scale. Although this study has been completed, no formal results have been made public (Scharf et al., 2015). However, through

press reports from Roche, the results were not promising, and the pursuit of basimglurant as a form of treating FXS has been halted.

Mavoglurant, the mGlur5 inhibitor developed by Novartis, was the most extensive clinically studied inhibitor, ranging over 5 different clinical trials. The first study, NCT00718341, utilized 30 male and female FXS patients ranging from 18 – 35 years of age in a double blind crossover design in which a bi-daily titrated dose (max at 150 mg) was administered. This study was assessing for efficacy and a viable biomarker as a metric of success. A myriad of cognitive assessments (including the Aberrant Behavior Checklist Community Scale, Clinical Global Impression Rating Scale for both Improvement and Severity, Repetitive Behaviors Scale (Revised), Social Responsiveness Scale, Visual Analog Scale, and the Vineland Adaptive Behavior Scale) were also conducted to determine the effectiveness of mavoglurant. Through this trial, tolerance for mavoglurant was found to be acceptable, manifesting mainly as mild fatigue or headaches; unfortunately, none of the cognitive assessments provided significant beneficial results. Interestingly, upon further *post-hoc* analyses, it was determined that patients with a fully methylated *FMR1* gene had significant improvements on the cognitive tests (Jacquemont et al., 2011). Based on these promising findings the next four trials commenced.

The four subsequent mavoglurant trials were both proof-of-concept trials for both FXS adults ranging from 18 – 46 years of age (NCT01253629 & NCT01348087) and FXS adolescence ranging from 12 – 18 years of age (NCT01357239 & NCT01433354). Both studies were double-blind parallel studies utilizing both males and females. A dose response regime was tested with bi-daily 25, 50, or 100 mg doses in the first half (NCT01253629; n=175 for adults & NCT01357239l n=139 for adolescents) in which efficacy, viable biomarkers, and only the

Adaptive Behavior Scale was assessed. The second half of both studies (NCT01348087; n=148 for adults & NCT01433354; n=103 for adolescents) were open label, with bi-daily doses optimized up to 100 mg. These studies conducted the same cognitive assessments as in the first half with the addition of the Clinical Global Impression Rating Scale and the Repetitive Behaviors Scale. The adolescent study also assessed the Social Responsive Scale. Despite being the largest and most extensive clinical trials, and having promising preliminary data with minimal side effects, the trials found no significant improvement in FXS patients (Scharf et al., 2015).

The negative results from the aforementioned clinical trials were less than promising for the FXS field, and put into question the prevailing mGluR theory for FXS. Various explanations have been put forth for the rationale between the overwhelming cross species success in preclinical trials to the negative results in clinical trials. One possible explanation for these results is in the need to assess an optimal dosage time frame. This is of particular importance, as FXS is a developmental disorder, and thus the timing of the intervention can be critical. Other explanations have focused on a need for better metrics in human clinical trials. Many of the end points utilized in these trials were measured and reported by patient caretakers, and thus were variable and subjective. Finally, other explanations have focused on possible compensatory mechanisms masking the effects of inhibiting mGluR I pathways. Furthermore, the mGluR pathway is critically involved in numerous molecular pathways in the body, and thus a global inhibition may not be ideal. This has led to many investigators to explore the modulation/regulation of various mGluR downstream components, in hopes of finding a new therapeutic target.

Breakdown of the mGluR Pathway and New Targeted Treatments

mGluRs are a family of receptors that are involved with functions of the central and peripheral nervous system. Ubiquitously found in both central and peripheral nervous systems, these receptors function ranges from driving aspects of learning and memory, anxiety, and sensory stimuli as well as downstream aspects of protein regulation (Chu and Hablitz, 2000; Ohashi et al., 2002).

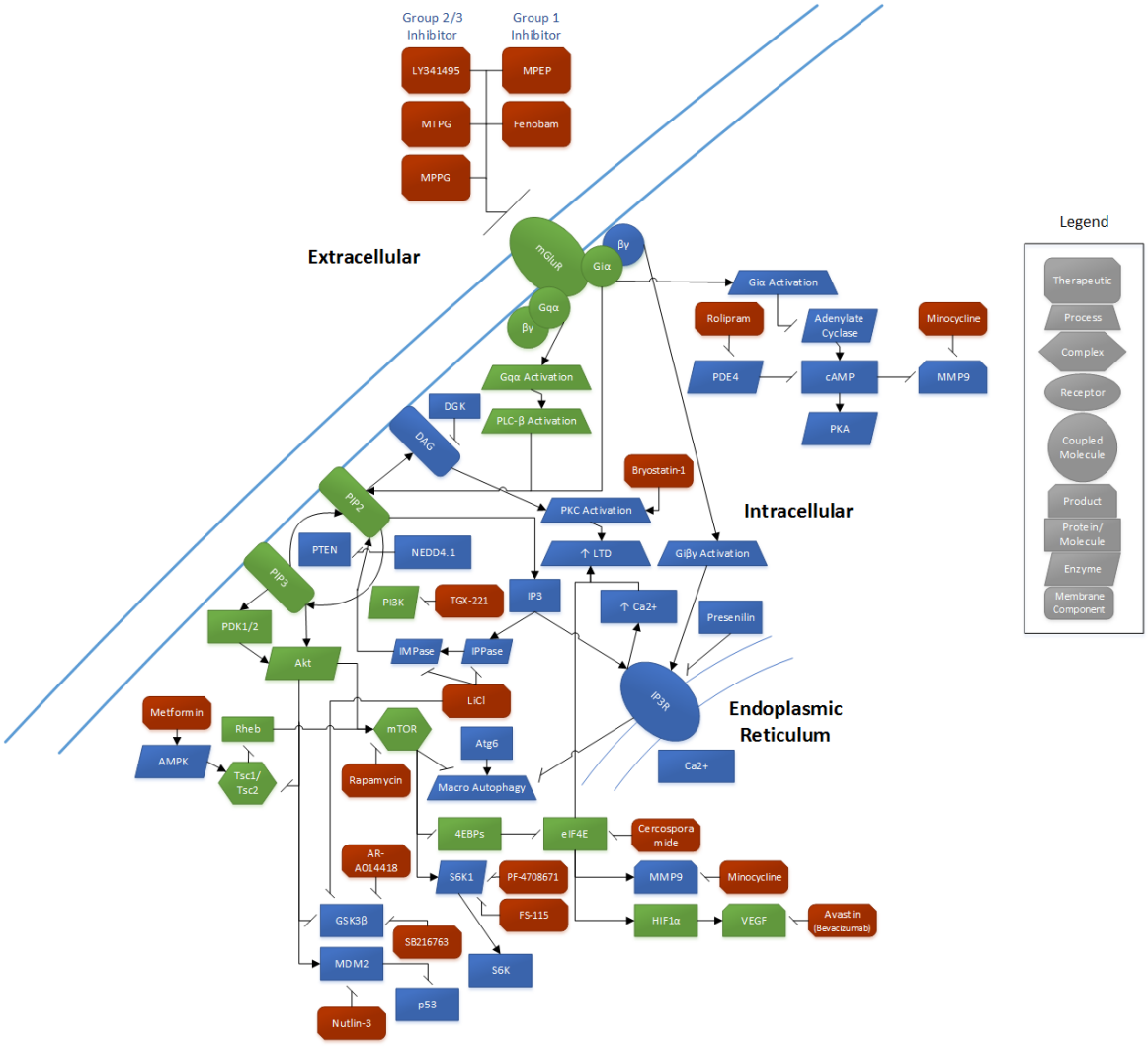

Figure 1.1. Detailed breakdown of the mGluR pathway with therapeutic interventions. Legend denotes the types of molecules found in the pathway. Red blocks are therapeutic interventions, while blue and green blocks are parts of the mGluR pathway. Of particular note, the green blocks indicate the particular downstream pathway of mGluR that results in VEGF production discussed in more detail below.

Table 1.2. Overview of current therapeutics targeting downstream components of the mGluR pathway, and their beneficial effects on FXS.

Therapeutic	Target	Beneficial Effect
Rolipram	Inhibit PDE4	Restores enhanced mGluR LTD to WT levels in FXS mice, memory impairment and structural brain deficits in *Drosophila* model of FXS (Choi et al., 2015).
Bryostatin-1	Enhance PKC Activation	Enhanced PSD-95 expression, rescues PKC and GSK3β to negatively modulate mGluR activity and increases maturation of dendritic spines in FXS mice (Sun et al., 2014).
TGX-221	Inhibit PI3K	Through inhibition of p110β subunit of PI3K, overall protein synthesis in FXS mice derived synaptoneurosomes and patient cells were reduced suggesting regulation of downstream protein synthesis (Gross and Bassell, 2012).
Metformin	Enhance AMPK	Rescued courtship and olfactory memory in FXS *Drosophila* model (Monyak et al., 2016).
LiCl	Inhibit IMPase, IPPase, & GSK3β	Reduction in overall protein synthesis rates in FXS mice, with a marked decrease in phosphorylation of Akt (Liu et al., 2012). Reduces overall GSK3β activity and reduced anxiety behaviors (Mines et al., 2010). Reduced hyperactivity, rescued excessive immature spine morphology, reduced anxiety and normalized impaired social interaction (Liu et al., 2011).
Rapamycin	Inhibit mTOR	Reduced intensity of audiogenic seizures (Osterweil et al., 2010).
AR-A014418	Inhibit GSK3β	Reduced inductance rate of audiogenic seizures (Min et al., 2009).
SB216763	Inhibit GSK3β	Decreased length of dendritic spines and increased hippocampal neurogenesis (Guo et al., 2012). Reduced inductance rate of audiogenic seizures and anxiety like behaviors observed via open field assessment (Min et al., 2009). Improved ability to learn trace fear conditioning and overall spatial memory observed via radial arm maze (Guo et al., 2012).
Nutlin-3	Inhibit MDM2	Reduces neuronal stem cell activation and restores adult neurogenesis in FXS mice. Also rescued performance in novel object recognition and location tests (Li et al., 2016).
PF-4708671	Inhibit S6K1	Reduced overall protein synthesis rates in

		FXS fibroblasts (Kumari et al., 2014). Reduced overall protein synthesis levels, increased performance on novel mouse and object vs mouse behavior, as well increased performance in choice reversal tasks. Furthermore, rescued the increased immature spine morphology, and macroorchidism (Bhattacharya et al., 2016).
FS-115	Inhibit S6K1	Reduced overall protein synthesis levels, increased performance on novel mouse and object vs mouse behavior, as well increased performance in choice reversal tasks, and reduced marble burying activity. Furthermore, rescued the increased immature spine morphology, and macroorchidism (Bhattacharya et al., 2016).
Cercosporamide	Inhibit eIF4E	Through reduction of eIF4E phosphorylation increased social behavior, reduced levels of mGluR induced LTD, hyperactivity, and audiogenic seizure induction rates (Gkogkas et al., 2014).
Minocycline	Inhibit MMP9	Increases maturation of dendritic spines in hippocampal cell culture (Bilousova et al., 2009). Treatment reduced anxiety in elevated plus maze and hyperactivity. Treatment also increased exploration in Y maze and vocalization rates in FXS mice (Bilousova et al., 2009; Rotschafer et al., 2012; Dansie et al., 2013). Improved overall cognition, language, anxiety, and mood in FXS patients as well as reduced irritability (Paribello et al., 2010; Utari et al., 2010; Leigh et al., 2013).

Table 1.2 (cont.). Overview of current therapeutics targeting downstream components of the mGluR pathway, and their beneficial effects on FXS.

VEGF Family Molecules and Receptors Overview

To continue to discern the effects of the downstream components of mGluR, and their effect on FXS, our lab has been exploring the role of Vascular Endothelial Growth Factor (VEGF) in mediating FXS abnormalities. VEGF is one of the most prominent regulators of vascular growth with increased expression being synonymous with increased blood vessel growth (Neufeld et al., 1999). It is critical for proper vascular growth and development, as

genetic knockouts are embryonic lethal (Carmeliet et al., 1996; Ferrara et al., 1996). VEGF is a family of proteins that consist of five main proteins: VEGF-A, VEGF-B, VEGF-C, VEGF-D and placental growth factor (PLGF). Of these five VEGF proteins, VEGF-A is the most studied and the largest driver of angiogenesis (Neufeld et al., 1999; Ferrara et al., 2003). VEGF-B and VEGF-C are known as VEGF related proteins while VEGF-D is also known as c-Fos-induced growth factor (Joukov et al., 1996; Lee et al., 1996). VEGF-B is heavily associated with cell adhesion, migration, and regulation (Olofsson et al., 1998). Although VEGF-C and VEGF-D are not as well understood, they are known to have implications towards regulating lymphatic angiogenesis (Olofsson et al., 1996; Baldwin et al., 2001; Karkkainen et al., 2002). Finally PLGF has been shown to affect angiogenesis, inflammation, would healing, and plasma extravasation (Carmeliet et al., 2001). These five VEGF proteins are known to interact with one of three primary VEGF receptors: VEGFR1, VEGFR2, VEGFR3 (Fig. 1.2).

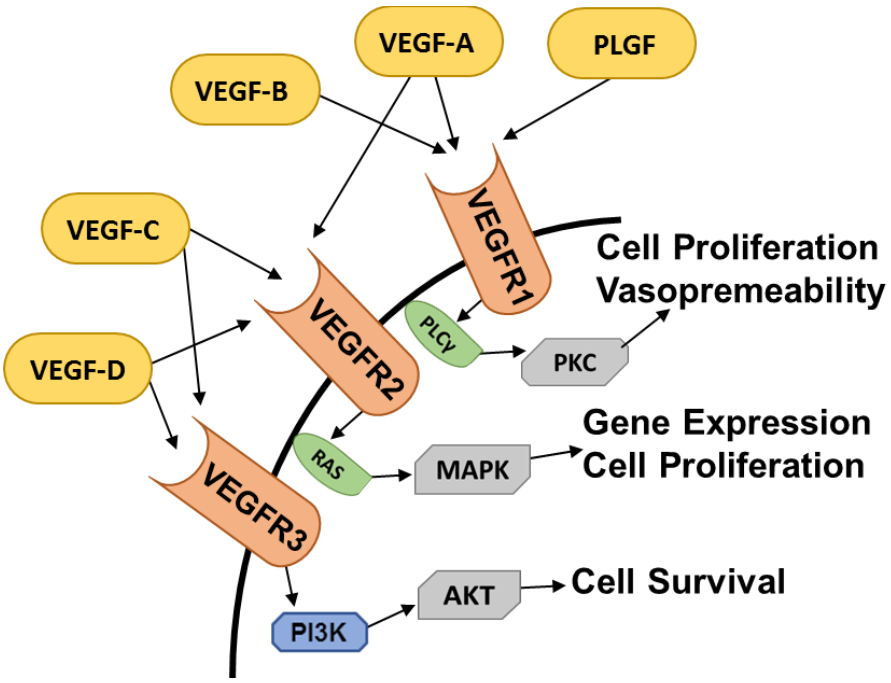

Figure 1.2. Schematic of binding affinities of VEGF Family of molecules to the various VEGF Receptors.

VEGFR1 (Flt-1) is activated by VEGF-A (de Vries et al., 1992), VEGF-B (Olofsson et al., 1998), and PLGF (Park et al., 1994). The loss of VEGFR1 results in abnormal vascular development manifesting through excessive hemangioblast proliferation and a reduction in vascular organization (Fong et al., 1995). VEGFR1 receptor activation can also have pronocicpetive effects through activation of kinases which sensitize reactions to heat, pressure, and various chemicals, but only when stimulated via VEGF-A (Selvaraj et al., 2015). Interestingly, of the 3 family members that target VEGFR1, only VEGF-A targets other VEGF receptors with VEGF-B and PLGF only targeting VEGFR1 (Park et al., 1994). VEGF-A's other and primary target is VEGFR2 (Flk-1) which is the primary driver of angiogenesis and microvascular permeability (Dvorak, 2002) as well as being heavily involved with various aspects of endothelial cells such as proliferation and survival (Millauer et al., 1993; Zeng et al., 2001). VEGFR2 is the more versatile of the VEGF receptors, as it also maintains a weak affinity for VEGF-C and VEGF-D (Joukov et al., 1996; Achen et al., 1998). However there is now growing literature suggesting that VEGFR2 (primarily through VEGF-A stimulation) is heavily involved with neuronal properties such as increased axonal and neurite outgrowth (Silverman et al., 1999; Sondell et al., 1999; Sondell et al., 2000; Jin et al., 2002). Finally, VEGFR3 (Flt-4) has a high affinity for VEGF-C (Joukov et al., 1996) as well as VEGF-D (Achen et al., 1998). As suggested from previously mentioned studies focusing on VEGF-C and VEGF-D, VEGFR3's primary role is lymphangiogenesis, but also plays a role in development of and maintaining the plasticity of vascular networks during embryogenesis (Kukk et al., 1996; Paavonen et al., 2000; Alitalo and Carmeliet, 2002; Laakkonen et al., 2007). Its role in development has been observed to be crucial as homozygotes for VEGFR3 deletion are embryonic lethal (Dumont et al., 1998).

Non-vascular Properties of VEGF-A

VEGF-A is primarily produced by endothelial cells, vascular smooth muscle cells, and neurons (Barleon et al., 1997; Chua et al., 1998; Schiera et al., 2007). VEGF-A acts through VEGFR1, with minor pronocicpetive effects through activation of kinases which sensitize reactions to heat, pressure, and various chemicals (Selvaraj et al., 2015) and vascular reorganization (Fong et al., 1995), but primarily through VEGFR2, which as previously stated is the primary driver of angiogenesis (Dvorak, 2002). VEGFR2 can be found on neurons and endothelial cells and can result in a variety of functions, particularly increasing neurite outgrowth, mitogenesis, angiogenesis, and blood brain barrier permeability-enhancing effects (Ferrara et al., 2003; Jin et al., 2006).

Of particular interest is VEGF-A's ability to interact directly with various neuronal cells. VEGF-A application has been observed to have a neurotropic effect via VEGFR2 in the peripheral nervous system manifesting through stimulation of Schwann cell proliferation (Sondell et al., 1999). Additionally, in the central nervous system, VEGFR2 stimulation yields axonal growth, and enhancing overall cell survival (Sondell et al., 2000). Furthermore, VEGF-A application stimulates cell proliferation in hippocampal *in vitro* cultures as well as neurogenesis in the dentate gyrus of the hippocampus *in vivo* (Jin et al., 2002). VEGFR2 has been found directly on axonal growth cones, and with VEGF-A stimulation, has been shown to increase overall axonal growth (Sondell et al., 1999). Finally, direct application of VEGF-A has been shown to promote overall neurite outgrowth and overall increased neurite branching (Jin et al., 2006). Interestingly, VEGF-A and its interaction with VEGFR2 has been recently implicated in learning and memory. Application of VEGF-A, in concert with NMDA, triggered remodeling of the post synaptic density (PSD), resulting in an overall increase in size of the PSD. This

suggested and was confirmed via fluorescent colabeling that VEGFR2 are also localized on dendritic spines. When these dendritic spine VEGFR2s were genetically silenced, eliminating the ability of VEGF-A to bind and influence these neurons, an impairment in consolidation of fear-related memory was observed (De Rossi et al., 2016). Interestingly, these non-vascular properties of VEGF-A mirror abnormalities seen in FXS and will be discussed in more detail in the following section.

VEGF and Fragile X Syndrome

FXS molecular studies exploring abnormalities in the group 1 mGluR pathway have suggested that VEGF would exhibit elevated expression. As discussed above, group 1 mGluRs in FXS is over active (Bear et al., 2004) resulting in excessive activation of its downstream processes. In support of this, mTOR (an mGluR1 downstream protein (Hou and Klann, 2004)) is over phosphorylated in FXS mice (Sharma et al., 2010). mTOR is a positive regulator of VEGF expression, with increased mTOR activation resulting in increased VEGF expression (Brugarolas et al., 2003). Thus in FXS, increased mTOR activation suggests increased VEGF production.

Interestingly, increasing VEGF expression can cause many abnormalities consistent with those observed in FXS. Increasing VEGF production would increase blood vasculature, subsequently increasing blood flow to brain regions. Likewise, FXS patient have been reported to exhibit abnormal brain blood flow to many brain regions (Kabakus et al., 2006). Furthermore, FXS mice have been shown to exhibit elevated blood vessel density in both primary visual cortex and hippocampus (the only two regions examined) (Galvan and Galvez, 2012). As previously mentioned, VEGF-A application has stimulatory and protective capabilities, which can be observed in FXS. FXS have increased Sertoli cell proliferation and neurogenesis in the dentate gyrus (Hagerman and Hagerman, 2003; Luo et al., 2010). VEGFR2 has been observed

on axonal growth cones, and with stimulation of VEGF-A results in axonal growth (Sondell et al., 1999), mirrored in in the *Drosophila* model of FXS through excessive axonal growth (Pan et al., 2004). Furthermore application of VEGF-A results in excessive neurite outgrowth (Jin et al., 2006) consistent with the immature dendritic spine morphology observed in FXS (Galvez et al., 2003; Galvez and Greenough, 2005). This hallmark phenotype of increased immature dendritic spine numbers is suggested to be due to excessive dendritic spine proliferation (Pan et al., 2010). Thus this dendritic spine abnormality, coupled with increased vascularization and blood flow could result in over active regions, resulting in the cognitive and behavioral deficits observed in FXS (Miller et al., 1999; Kronk et al., 2010; Raspa et al., 2010; Cordeiro et al., 2011; Galvan and Galvez, 2012).

This correlation between excessive VEGF-A and FXS phenotypes suggests that some of the FXS characteristics could be explained via excessive VEGF production. As you will see, our findings suggest that VEGF-A is excessively produced in FXS due to the dysregulated mGluR pathway. Furthermore, this excessive production can be modulated through therapeutics and rescue well known FXS phenotypes, implicating VEGF-A as a potential new target and driver of FXS abnormalities.

CHAPTER 2: CHARACTERIZING NEOCORTICAL DEVELOPMENTAL PROFILES OF VEGF FAMILY MOLECULES, RECEPTORS, AND VASCULAR PROPERTIES IN FRAGILE X MICE

Abstract

The Fragile X Syndrome (FXS) is the most common single gene cause for Autism Spectrum Disorder and the most prevalent form of inherited mental retardation. We have previously demonstrated that adult FXS mice have abnormal Blood Vessel Density (BVD) (Galvan and Galvez, 2012) and elevated Vascular Endothelial Growth Factor A expression (VEGF-A). VEGF-A is one of the most prominent regulators of BVD, and its abnormal expression is the most likely cause for FXS BVD abnormalities. Interestingly, we have also demonstrated that attenuating elevated VEGF-A expression can ameliorate many non-vascular FXS abnormalities (Belagodu et al., 2017). These studies have suggested that abnormal BVD and VEGF-A expression are an underlying cause for some FXS abnormalities. However, FXS is a developmental disorder and VEGF-A expression along with BVD and their potential role in mediating FXS abnormalities during development have never been explored. Furthermore, VEGF-A is one protein in a family of proteins (VEGF-A, VEGF-B, VEGF-C, VEGF-D, & PLGF) that activate one of three primary receptors (VEGFR1, VEGFR2, & VEGFR3). Abnormal expression of any of these proteins could hinder proper neuronal and cognitive development in FXS. The current study demonstrated that FXS mice exhibit abnormal BVD, vascular growth factor and growth factor receptor expression at multiple ages over development. Interestingly, many of these abnormal developmental expression patterns correlated with known FXS age specific neuronal abnormalities. Expanding upon our prior examination of adult BVD and VEGF-A expression, the current study provides additional insight towards potential

mechanisms mediating FXS abnormalities, while offering further sites for age specific therapeutic interventions.

Introduction

The Fragile X Syndrome (FXS) is the most common single gene cause for Autism Spectrum Disorder and the most prevalent form of inherited mental retardation (1:3600 in males and 1:8000 in females) (Cornish et al., 2008). Patients with FXS have various physical, behavioral, and cognitive abnormalities including cluttered speech, hyperactivity, increased seizure susceptibility and difficulty with cognitively demanding tasks (Berry-Kravis, 2002; Van Borsel et al., 2008; Cordeiro et al., 2011). Although the cause for FXS is well understood, transcriptional silencing of *FMR1,* the gene that codes for the Fragile X Mental Retardation Protein (FMRP) (Pieretti et al., 1991; Verkerk et al., 1991; McLennan et al., 2011; Santoro et al., 2012), the mechanism by which an absence of FMRP causes these abnormalities is unknown. Many studies have suggested that these abnormalities are due to a lack of FMRP inhibition of mGluR (metabotropic glutamate receptor) down-stream processes. Specifically, many have suggested that over activation of the down-stream complex mTORC1 (mammalian target of rapamycin complex 1) in FXS results in abnormal expression for various proteins that result in FXS abnormalities (Sharma et al., 2010; Hoeffer et al., 2012).

Our recent studies have demonstrated that one of these proteins, down-stream of mTORC1, that exhibits elevated expression in adult FXS brain is VEGF-A (Vascular Endothelial Growth Factor A) (Belagodu et al., 2017). VEGF-A is one of the most prominent regulators of brain vascular growth and the most likely explanation for our prior observed increased vasculature in adult FXS mice (Galvan and Galvez, 2012). Interestingly, recent studies have demonstrated that in addition to being found on vascular endothelial cells, the prominent VEGF-

A receptor (VEGFR2) is also found on the postsynaptic density of neurons which when genetically removed hinders acquisition for fear conditioning (De Rossi et al., 2016). These studies have suggested that in addition to a prominent role in vascular growth, VEGF-A also plays an active role in learning and memory. VEGF-A stimulation has also been shown to alter many neuronal properties that are disrupted in FXS. For example, increasing VEGF-A induces axonal and dendritic growth consistent with the increased dendritic spine and axonal material observed in FXS (Sondell et al., 1999; Irwin et al., 2000; Pan et al., 2004; Galvez and Greenough, 2005; Antar et al., 2006; Jin et al., 2006). Furthermore, chronic VEGF-A stimulation induces long term depression like conditions (McCloskey et al 2005), a molecular form of learning that is elevated in FXS (Huber et al, 2002). Collectively these studies suggest that increased VEGF-A brain expression mediates more than just FXS vascular abnormalities.

In support of this hypothesis we have recently demonstrated that blocking VEGF-A's ability to bind to its receptor in adult FXS mice attenuates neuronal and cognitive abnormalities. Our studies have shown that blocking VEGF-A decreases adult FXS synapse density in the neocortex and hippocampus to that observed in control mice. Furthermore, our subsequent behavioral analyses using the learning paradigm novel object recognition demonstrated that blocking VEGF-A also ameliorated adult FXS learning deficits, making them indistinguishable from controls (Belagodu et al., 2017). These studies demonstrate that in addition to modulating vasculature, increased VEGF-A expression in adult FXS mice mediates many neuronal and cognitive abnormalities. However, FXS is a developmental disorder and many adult abnormalities could be a result of, or at least exasperated by abnormal brain development (Till et al., 2012; Telias et al., 2013).

Interestingly VEGF-A brain expression during development in FXS is not known. Furthermore, VEGF-A is only one of 5 VEGF family molecules [VEGF-A; VEGF-B; VEGF-C; VEGF-D; and PLGF (placental growth factor)] that activate one of three primary receptors (VEGFR1, VEGFR2, and VEGFR3). In addition, many VEGF receptors can be activated by multiple VEGF family molecules. For example, VEGFR1 can be activated by VEGF-A, VEGF-B or PLGF; VEGFR2 can be activated by VEGF-A, VEGF-C or VEGF-D; and VEGFR3 can be activated by VEGF-C or VEGF-D (Fig. 2.1).

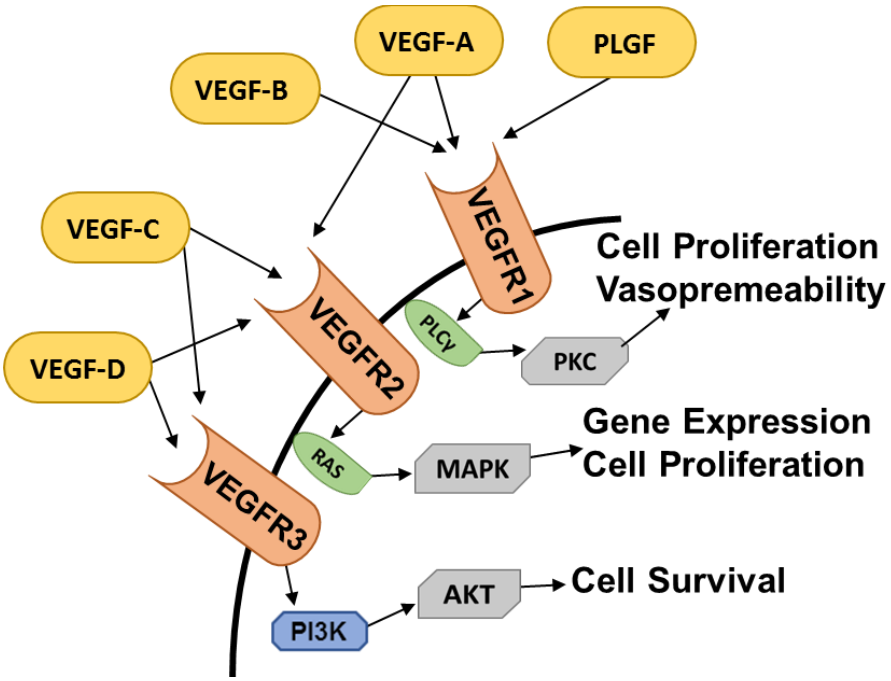

Figure 2.1. Schematic of binding affinities of VEGF Family of molecules to their various VEGF Receptors.

Abnormal developmental expression for any of these receptors, VEGF family molecules, or subsequent blood vessel density could be an underlying cause for FXS abnormalities. Unfortunately, their developmental expression in FXS and potential role in subsequent abnormalities has never been explored. To determine their potential for mediating FXS developmental abnormalities, the current study set out to characterize neocortical vascular

density, vascular growth factor expression, and vascular growth factor receptor expression across development in FXS mice.

Methods & Analysis

All experimental protocols were conducted in accordance with and approved by the Illinois Institution of Animal Use and Care Committee at the University of Illinois at Urbana-Champaign. All studies and analyses were further conducted with the researcher blinded to genotype and animal age to avoid experimenter bias.

Housing and Care of Animals

Male C57/B6 *FMR1* knockout (FXS) and wildtype (WT) mice at postnatal day (PND) 10, 20, 35, and 60 were used for each study. PND 10 has been noted to be the period prior to a significant increase in synaptogenesis in many mouse neocortical brain regions (De Felipe et al., 1997). PND 20 was chosen as it corresponds to the beginning of a rise in synaptic plasticity for many regions in the brain (Greenough and Chang, 1988; White et al., 1997; Hanover et al., 1999; Huang et al., 1999; Dahlhaus et al., 2011; Levelt and Hubener, 2012). PND 35 is representative of a mid-adolescent time point, where the period of rapid increased dendritic and synaptic plasticity in most brain regions has ended (Vergouwen et al., 1993; Adriani et al., 2004). Finally, PND 60 was chosen as it corresponds to a young adult and is the age when our prior VEGF-A and blood vessel analyses were conducted (Galvan and Galvez, 2012; Belagodu et al., 2017). Mice were housed in standard laboratory conditions (12 hrs -12 hrs light/dark cycle with food and water provided *ad libitum*).

Blood Vessel Density

Once mice reached the appropriate aforementioned ages, an overdose of sodium pentobarbital (100 mg/kg) was intraperitoneally administered followed by subsequent transcardial perfusion with 1x PBS followed by 4% paraformaldehyde. Brains were then

extracted and post-fixed for 24 hrs in 4% paraformaldehyde followed by 30% sucrose at 4º C. The brains were then sectioned into 30 µm coronal sections, and stored at -20º C in cryoprotectant (30% ethylene glycol & 30% sucrose in PBS) until ready for Immunohistochemistry.

For staining and visualizing blood vessels, a modified protocol from (Galvan and Galvez, 2012) was utilized. After PBS washes, sections were incubated in pepsin (1 mg/ml) at 37^0 C for 10 min for antigen-unmasking. Sections were then incubated for 30 min in 0.6% hydrogen peroxide followed by a 1 hr incubation in TBS-X blocking solution (0.1% Triton X, 5% normal goat serum in PBS). Sections were then incubated for 48 hrs at 4^0 C in anti-Collagen IV antibody (1:300 Millipore in TBS-X). Following the primary antibody incubation, sections were incubated in anti-rabbit secondary antibody (1:100 Vector, Burlingame, CA) for 2 hrs followed by incubation in avidin-biotin (Vector, Burlingame, CA) for 1 hr at room temperature. Finally, the antigen was visualized through an incubation in a diaminobenzidine (DAB) solution (0.5 mg/ml DAB, 6.95 mg/ml nickel ammonium sulfate, 0.033 µl/ml 30% hydrogen peroxide). Anatomical landmarks were used to locate the neocortical visual cortex (Paxinos, 2008). Stained sections were imaged on an Olympus BX50 microscope with a Zeiss AxioCam ICc1 camera at 4x magnification with AxioVision ver 4.8.1. Once imaged, a 400 x 400 μm^2 area in each subdivision of the neocortical visual cortex [V1, $V1_M$ (monocular), & $V1_B$ (binocular)] was analyzed. The visual cortex was chosen as it correlates with previous FXS studies of blood vessel density (Galvan and Galvez, 2012) and dendritic spine abnormalities (Irwin et al., 2001; Irwin et al., 2002). Collagen IV positive staining was examined using the particle analysis tool on ImageJ (http://rsbweb.nih.gov/ij/docs/guide/146-30.html) to determine the percent area fraction of blood vessels. To control for any tears or damage in the tissue, the "white space" was

calculated through the same particle analysis procedure and taken out of the area percent calculation, resulting in a more accurate representation of the total blood vessel density.

Volumetric Analysis

To calculate the size of the regions being examined over development, evenly spaced sections were then nissl stained using a standard 25% cresyl violet staining protocol. Using standard non-biased stereological techniques, the area of V1, $V1_M$, and $V1_B$ were calculated with AxioVision ver 4.8.1 for each section and then used to determine the volumes of each region for each mouse using the following equations: Σ[(section area * section thickness) * distance to next section].

Growth Factor and Receptor Expression

To determine expression levels of VEGF family molecules (VEGF-A, VEGF-B, VEGF-C, VEGF-D and PLGF) and their subsequent receptors (VEGFR1, VEGFR2, and VEGFR3), dissected cortical hemispheres, including white matter and hippocampus were utilized. Samples were processed as described in (Belagodu et al., 2017) for large gels to allow for comparison across developmental ages. From each developmental time point FXS (n=3) and WT (n=3) mouse brains were homogenized and protein concentration estimated via bicinchonic acid assay (Thermo Scientific). Each sample (40 µg of protein) in a 1:1 loading buffer (475 µl Laemmli + 25 µl βME) ratio were loaded and run on a large 10% electrophoresis gel at 150 V for 1 hr followed by 200 V for 4 hrs. The separated proteins were then transferred to a nitrocellulose membrane at 20 V at 100 mA overnight in 4^0 C. The resulting protein embedded membranes were then blocked with 5% milk in TBS-T (Tris Buffered Saline with 0.05% Tween 20) and probed with a primary antibody for the molecules of interest (VEGF-A 1:1000; Santa Cruz, VEGF-B 1:1000; Abcam, VEGF-C 1:1000; Abcam, VEGF-D 1:1000; Abcam, PLGF 1:1000;

Abcam, VEGF Receptor 1 (Flt-1) 1:1000; Abcam, VEGF Receptor 2 (Flk-1) 1:1000; Santa Cruz, or VEGF Receptor 3 (Flt-4) 1:1000; Abcam). The membrane was then washed and incubated in anti-rabbit or anti-mouse secondary antibody (1:1000; Cell Signaling Technology) for 2 hr prior to chemiluminescent substrate exposure for 5 min and imaged via a BioRad ChemiDoc Touch Gel Imaging System (BioRad). After imaging, the blots were reprobed for GAPDH (1:1000; Santa Cruz) as a loading control. The relative intensity of the protein of interest was calculated by dividing its optical density by that of GAPDH. The optical densities were determined through Image Lab v5.2.1 (BioRad).

Statistical Analysis

Comparisons across developmental time points were conducted with a two-way mixed model ANOVA on SAS 9.4 (http://www.sas.com) with age and genotype as between subject factors and Bonferroni correction for multiple comparisons. As noted below, some comparisons at specific ages across genotype were further explored with a pair-wise t-test on SAS 9.4.

Results

Examination of the total V1 region ($V1_T$) blood vessel density (BVD) for WT mice demonstrated an expected increase in vascular density over development with a sharp reduction at PND 35 (Fig. 2.2a; $F_{(3,52)}=3.76$; $p<0.05$), a time point that correlates with an end to the rapid synaptic plasticity observed at PND 20 (Greenough and Chang, 1988; White et al., 1997; Hanover et al., 1999; Huang et al., 1999; Dahlhaus et al., 2011; Levelt and Hubener, 2012). Interestingly, this increase with subsequent reduction was not observed in FXS mice. Rather, in FXS mice the overall BVD maintains a general increase throughout development (Fig. 2.2a). Further comparisons across age demonstrated that FXS mice had significantly reduced BVD at PND 20 and elevated BVD at PND 60 compared to WT mice (Fig. 2.2). Our findings at PND 60

are consistent with our prior Galvan and Galvez (2012) study demonstrating elevated BVD in FXS mice.

Upon obtaining these initial findings $V1_T$ was further sub-divided into three regions: V1, $V1_M$ and $V1_B$. In V1 and $V1_M$, WT mice exhibited a similar increase in BVD at PND 20 (V1: Fig. 2.2b; $F_{(3,48)}=3.81$; $V1_M$: Fig. 2.2c; $F_{(3,51)}=3.96$; $p<0.05$) that was not observed in FXS mice. In $V1_B$ WT mice also exhibited elevated BVD at PND 20; however, it did not reach statistical significance (age*genotype $p=0.0561$) (Fig. 2.2d). Interestingly, in $V1_M$, FXS mice exhibited significantly elevated BVD at PND 60 (Fig. 2.2c; $F_{(3,51)}=3.96$; $p<0.05$) similar to that observed in $V1_T$. These findings are consistent with our prior study examining BVD in FXS mice (Galvan and Galvez, 2012).

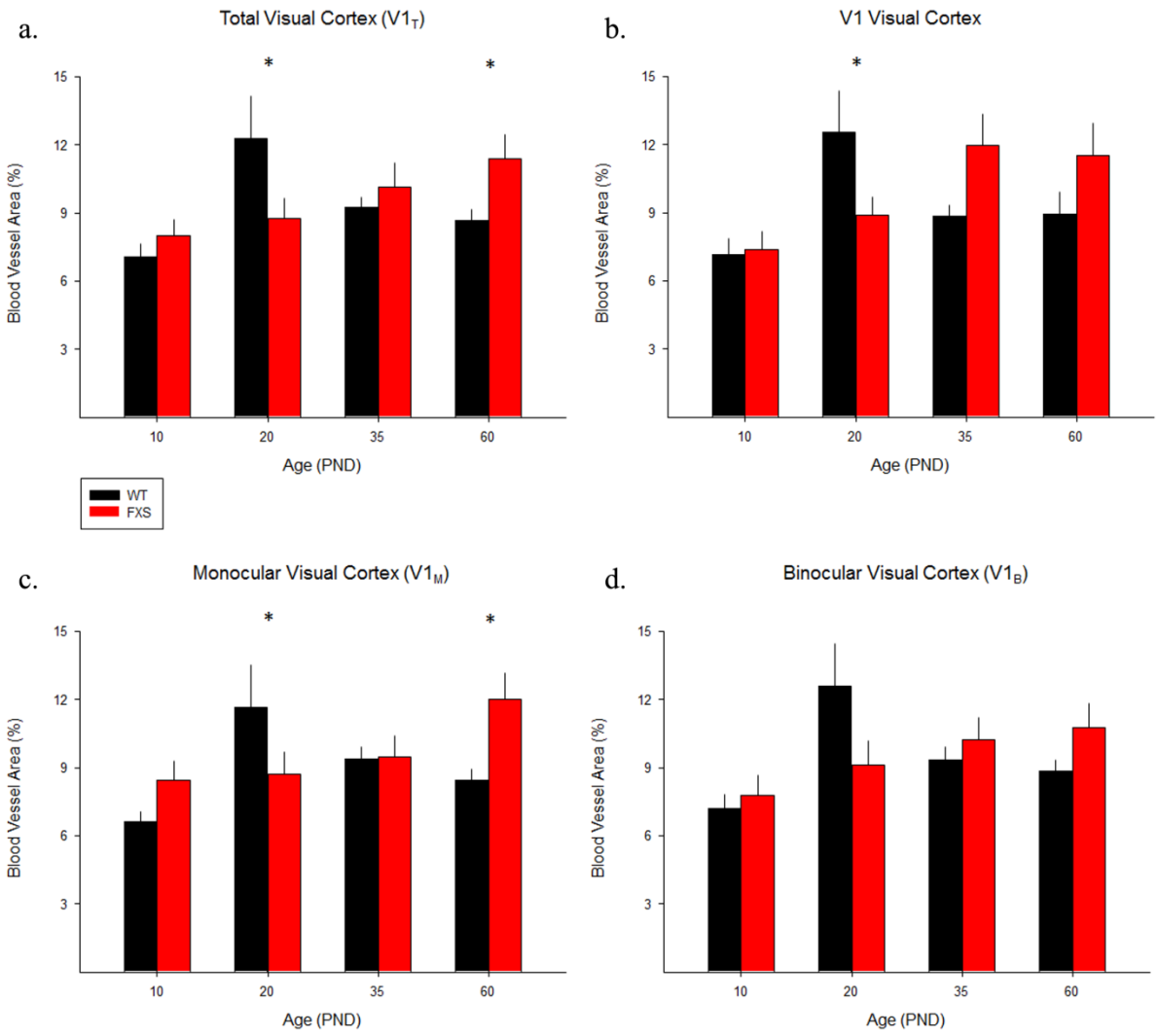

Figure 2.2. Fragile X mice (FXS) display a dysregulated growth and development of blood vessel density in the visual cortex compared to their wildtype (WT) counterparts. a. Quantification of blood vessel density in total visual cortex ($V1_T$ is a sum of V1, V1 Monocular, and V1 Binocular) across all developmental time points. b. Quantification of blood vessel density in mouse V1 visual cortex across all developmental time points. c. Quantification of blood vessel density in mouse monocular visual cortex ($V1_M$) across all developmental time points. d. Quantification of blood vessel density in mouse binocular visual cortex ($V1_B$) across all developmental time points. Note: $V1_B$ displayed elevated BVD at PND 20, but did not reach significance: age*genotype p=0.0561. *<0.05

To determine which of the major angiogenic factors are driving these changes in blood vessel density, Western Blot analyses was performed for each VEGF family molecule at the different ages. An overall ANOVA demonstrated a significant age*geno differences for VEGF-A (Fig. 2.3a; $F_{(3,16)}$=11.91; p<0.05), VEGF-B (Fig. 2.3b; $F_{(3,16)}$=21.11; p<0.05), and PLGF (Fig.

2.3e; $F_{(2,12)}$=4.81; p<0.05). Individual pair-wise comparisons will now be discussed at each age to further elucidate specific FXS developmental abnormalities.

At PND 10, the period prior to increased synaptogenesis in the neocortex (De Felipe et al., 1997), no differences were seen in VEGF-A or VEGF-C; however, a pair-wise t-test revealed that VEGF-D was significantly reduced in FXS mice ($t_{(4)}$=-2.82; p<0.05) (Fig. 2.3d). Interestingly, FXS mice also exhibited elevated expression of VEGF-B (Fig. 2.3b; $F_{(3,16)}$=21.11; p<0.05) and there was no expression of PLGF in either genotype.

The expression profiles at PND 20, the period that marks the peak of dendritic and synaptic plasticity (Greenough and Chang, 1988; White et al., 1997; Hanover et al., 1999; Huang et al., 1999) varied from those at PND 10. At this age, FXS mice exhibited significantly reduced expression of VEGF-A (Fig 2.3a; $F_{(3,16)}$=11.91; p<0.05) and VEGF-B (Fig. 2.3b; $F_{(3,16)}$=21.11; p<0.05) compared to WT mice. Interestingly, WT mice also demonstrated a significant reduction in VEGF-B expression from PND 10; however, the reduction in FXS mice was more pronounced (Fig. 2.3b; $F_{(3,16)}$=21.11; p<0.05). VEGF-C, VEGF-D and PLGF did not show any differences between genotypes.

At PND 35, the time point corresponding to the end of the rapid neuronal plasticity observed at PND 20 (Adriani et al., 2004), FXS and WT mice exhibited an age dependent reduction in VEGF-A ($F_{(3,16)}$=35.18; p<0.05) and VEGF-B ($F_{(3,16)}$=218.38; p<0.05), with pair-wise t-test analyses demonstrating a similar reduction in VEGF-C ($F_{(3,16)}$=22.06; p<0.05) and an increase in VEGF-D ($F_{(3,16)}$=10.22; p<0.05). Further analyses demonstrated that FXS mice exhibited significantly elevated amounts of VEGF-A (Fig. 2.3b; $F_{(3,16)}$=11.91; p<0.05); however, VEGF-B and PLGF did not exhibit any significant differences compared to WT mice.

Interestingly, FXS mice had significantly elevated VEGF-C expression (Fig. 2.3c; $t_{(4)}$=3.67; p<0.05) and reduced VEGF-D expression (Fig. 2.3d; $t_{(4)}$=-4.37; p<0.05) compared to WT mice.

Consistent with our prior studies in adult FXS mice (Galvan and Galvez, 2012; Belagodu et al., 2017), the current study found that PND 60 FXS mice exhibited significantly elevated VEGF-A expression compared to WT mice (Fig. 2.3a; $F_{(3,16)}$=11.91; p<0.05). Interestingly, VEGF-B (Fig. 2.3b; $F_{(3,16)}$=21.11; p<0.05) and PLGF (Fig. 2.3e; $F_{(2,12)}$=4.81; p<0.05) were both significantly reduced in FXS mice. Contrary to that observed at PND 35, VEGF-C and VEGF-D showed no significant differences at this age.

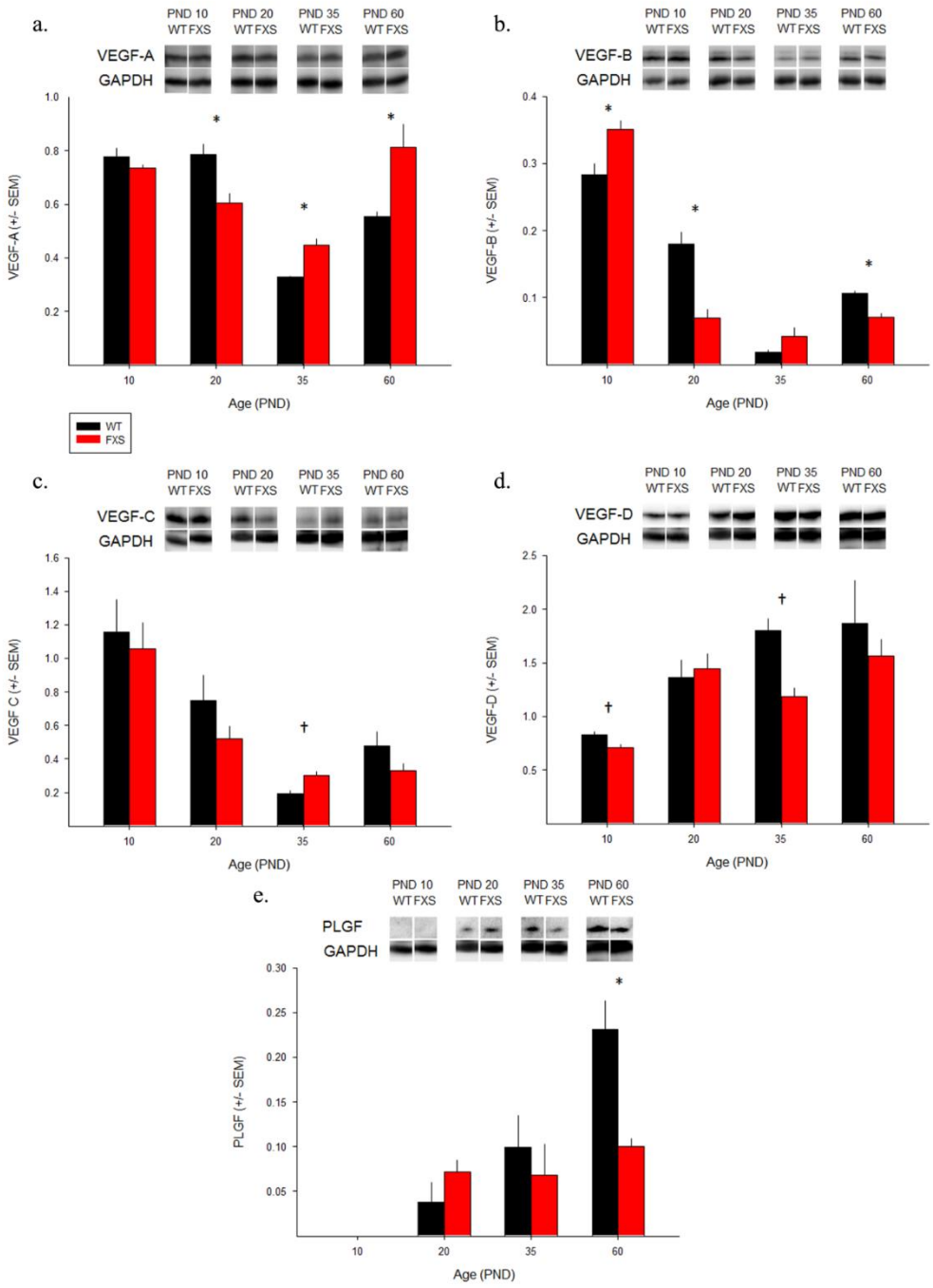

Figure 2.3. VEGF Family Growth Factors' expression is dysregulated in Fragile X mice (FXS) compared to their wildtype (WT) counterparts at key developmental time points (PND 10, 20, 30, & 60). All samples were run on the same gel to allow for direct comparison between time points. a. VEGF-A expression in dissociated cortical hemispheres at developmental time points. b. VEGF-B expression in dissociated cortical hemispheres at developmental time points. c. VEGF-C expression in dissociated cortical hemispheres at developmental time points. d. VEGF-D expression in dissociated cortical hemispheres at developmental time points. e. PLGF expression in dissociated cortical hemispheres at developmental time points. *<0.05 for age*genotype overall effect, †<0.05 when each time point is individually analyzed.

With this dysregulation of the VEGF family members, each of the three primary receptors were also analyzed. Interestingly, besides a change with age [VEGFR1 (Fig. 2.4a; $F_{(3,16)}=9.99$; $p<0.05$), VEGFR2 (Fig. 2.4b; $F_{(3,16)}=55.36$; $p<0.05$), VEGFR3 (Fig. 2.4c; $F_{(3,16)}=12.84$; $p<0.05$)], there were not many notable differences across genotypes for any of the three main VEGF receptors . VEGFR3 was the only receptor that demonstrated a significant age*geno interaction (Fig. 2.4c; $F_{(3,16)}=4.45$; $p<0.05$). As above we will now discuss individual pair-wise comparisons at each age to further elucidate specific FXS developmental abnormalities.

At PND 10 FXS had significantly elevated VEGFR3 expression (Fig. 2.4c; $F_{(3,16)}=4.45$; $p<0.05$). At PND 20 there were no significant differences in any of the receptors in FXS mice. At PND 35 individual pair-wise t-tests demonstrated that both VEGFR1 (Fig. 2.4a; $t_{(4)}=5.56$; $p<0.05$) and VEGFR2 (Fig. 2.4b; $t_{(4)}=2.8$; $p<0.05$) were significantly elevated in FXS compared to WT mice. There were no significant differences at PND 60 or for any other receptors at the different ages.

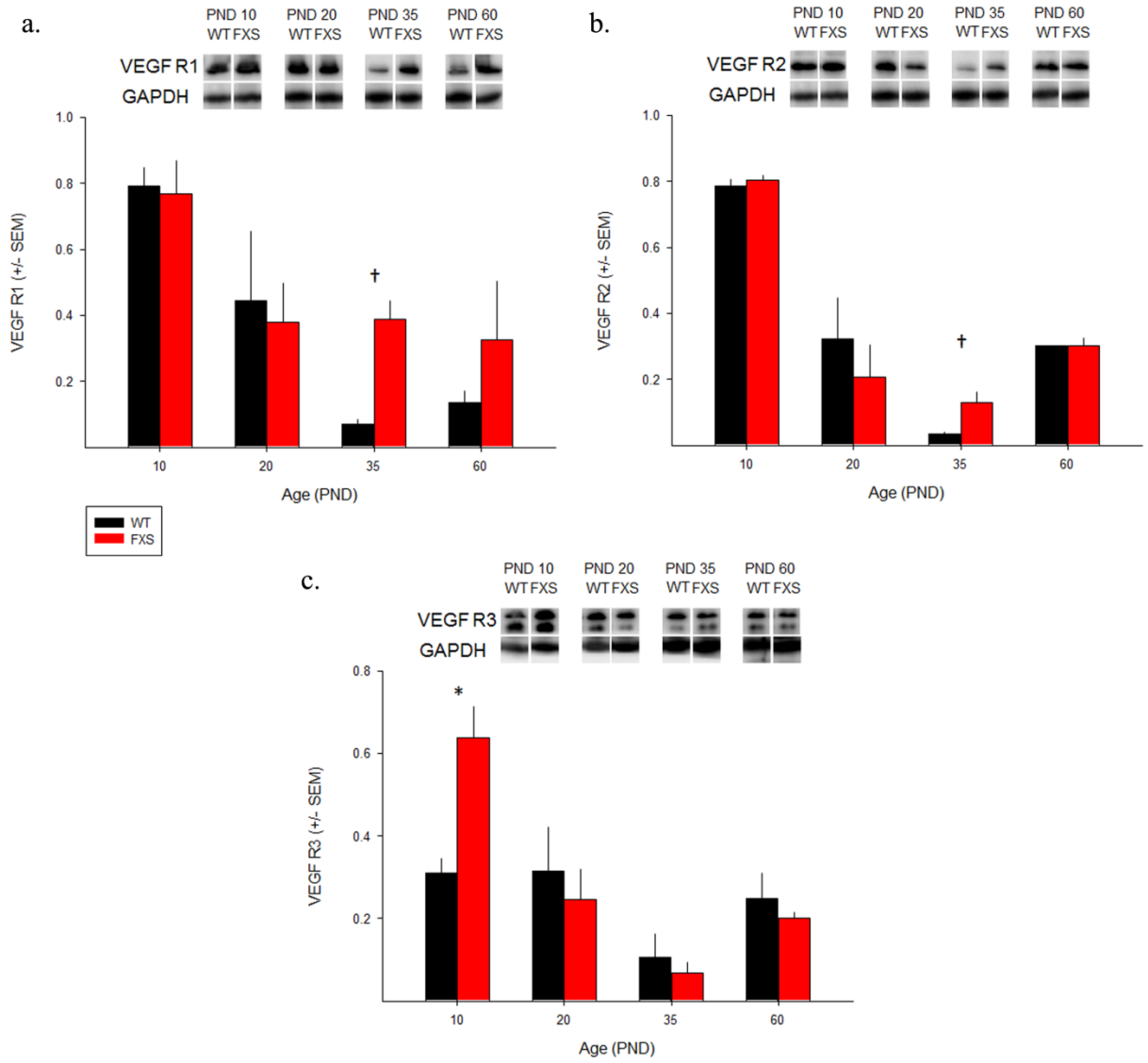

Figure 2.4. . VEGF Family Receptors' expression is dysregulated in Fragile X mice (FXS) compared to their wildtype (WT) counterparts at key developmental time points (PND 10, 20, 30, & 60). All samples were run on the same gel to allow for direct comparison between time points. a. VEGFR1 expression in dissociated cortical hemispheres at developmental time points. b. VEGFR2 expression in dissociated cortical hemispheres at developmental time points. c. VEGFR3 expression in dissociated cortical hemispheres at developmental time points. *<0.05 for age*genotype overall effect, †<0.05 when each time point is individually analyzed.

Discussion

Our prior studies have demonstrated that FXS is associated with adult abnormalities in both vascular density and VEGF-A expression (Galvan and Galvez, 2012; Belagodu et al., 2017). More importantly, we have shown that decreasing VEGF-A to WT levels can alleviate

some FXS abnormalities (Belagodu et al., 2017). However, FXS is a developmental disorder and there are multiple VEGF proteins and receptors that could mediate FXS abnormalities at these developmental time points. The current study set out to examine the developmental expression for these VEGF proteins, their receptors, and the underlying neocortical vascular density in FXS to determine their potential for mediating FXS abnormalities.

At PND 10 we did not observe any significant differences in BVD in FXS mice but did detect several interesting differences in the various VEGF family members and receptors. VEGF-D was found to be reduced in FXS compared to WT mice (Fig. 2.3d). Interestingly, VEGF-D is believed to primarily affect lymphangiogenesis and only have a minor role in vasculogenesis (Jeltsch et al., 1997; Veikkola et al., 2001; Karkkainen et al., 2002). Although it was previously believed that the brain does not have lymphatic vasculature (Galea et al., 2007), recent studies have demonstrated the presence of lymphatic vasculature in the meninges (Aspelund et al., 2015; Louveau et al., 2015). This lymphatic vasculature has been proposed to function in concert with the glymphatic system to act as a drainage for clearing by-products through CSF draining across the parenchyma (Iliff et al., 2012). Collectively these studies suggest that the development of this drainage system may be impaired in FXS. Interestingly, our study also found that VEGFR3 (Flt-4), a VEGF-D receptor (Joukov et al., 1996; Achen et al., 1998), was upregulated in FXS mice. This increased VEGFR3 expression could be an indication of a compensatory mechanism initiated by the reduced VEGF-D expression. VEGFR3's primary role is with lymphangiogenesis, but also plays a critical role in the development and plasticity of vascular networks during embryogenesis (Dumont et al., 1998) (Kukk et al., 1996; Paavonen et al., 2000; Alitalo and Carmeliet, 2002; Laakkonen et al., 2007).

In addition to altered expression of VEGF-D and VEGFR3, VEGF-B was found to be significantly elevated in FXS mice at PND 10 (Fig. 2.3b). VEGF-B has been shown to be heavily involved in cell adhesion, migration and regulation of the extracellular membrane degradative process (Olofsson et al., 1998). This reduced VEGF-B expression could result in a lack of or abnormal cellular migration in FXS, hindering proper neuronal development. Interestingly, studies have demonstrated that the developmental switch of GABAergic transmission from depolarizing to hyperpolarizing is delayed during this time period (WT at ~PND 9 and FXS at ~PND 14) (He et al., 2014). Although the current study does not allow for a detailed analysis of the effects of reduced VEGF-B expression at this age, these findings suggest that this expression profile could hinder appropriate migration and formation of necessary neuronal connections delaying neuronal development in FXS.

At PND 20 WT mice exhibited a significant increase in BVD that would directly correlate with and provide the appropriate nutrient levels for the robust global dendritic and synaptic plasticity occurring at this time point (Greenough and Chang, 1988; White et al., 1997; Hanover et al., 1999; Huang et al., 1999; Dahlhaus et al., 2011; Levelt and Hubener, 2012). Interestingly, FXS mice did not exhibit this developmental increase and had significantly reduced BVD compared to WT mice at this age (Fig. 2.2). This absence of increased BVD in FXS was consistent with our subsequent examination of VEGF expression. At PND 20, both VEGF-A and VEGF-B were significantly reduced in FXS compared WT mice (Fig. 2.3a & Fig. 2.3b). VEGF-A is the most prominent regulator of vascular growth, with increased expression inducing angiogenesis and vasculogenesis (Neufeld et al., 1999; Josko et al., 2000; Kunkel et al., 2001; Carmeliet and Storkebaum, 2002). Likewise, as discussed above, VEGF-B is critically involved in cell adhesion, migration and membrane degradation (Olofsson et al., 1998), cellular

processes that are critically involved in various aspects of vascular growth. Consistent with our findings, WT mice have been shown to exhibit a drastic increase in neuronal brain VEGF expression at PND 20 (Ogunshola et al., 2000). Interestingly, our examination of VEGF receptor expression failed to detect any differences at this age. These findings suggest that the reduced VEGF-A and VEGF-B expression in FXS are resulting in a dysregulation, overall decrease rate of vascularization, and the observed decrease BVD at this time point. Reduced BVD, potentially starving neurons of needed nutrients for proper neuronal development, could be an underlying cause for neuronal and cognitive abnormalities in FXS. Future studies will need to explore this relationship and the potential beneficial effects of modulating VEGF expression at this early developmental time point.

Unlike the distinct vascularization properties observed at PND 20, at PND 35 there were no significant differences in BVD between genotypes (Fig. 2.2). PND 35 in male rodents is a complex time point as it corresponds to mid-adolescence, a time of sexual maturity, an end to ocular dominance critical period plasticity, and the end of the extensive neuronal plasticity observed at PND 20 (Vergouwen et al., 1993; Adriani et al., 2004; Dahlhaus et al., 2011; Levelt and Hubener, 2012). Interestingly, VEGF-A, the main angiogenic factor, was significantly elevated in FXS mice at this time point (Fig. 2.3a). This VEGF-A over expression in FXS could be a result of compensatory mechanisms originating from the lack of increased BVD expression at PND 20 or due to delayed neuronal development in FXS (Till et al., 2012; He et al., 2014). Consistent with the increased VEGF-A expression, FXS mice also exhibited increased expression of both VEGFR1 and VEGFR2 (Fig. 2.4a & Fig. 2.4b) [receptors that are activated by VEGF-A (de Vries et al., 1992)]. VEGFR1 has been shown to be important for normal vascular development as genetic knockouts result in excessive hemangioblast proliferation and a

reduction in the organization of vascular components (Fong et al., 1995). VEGFR1 is also found on astrocytes, and is suggested to aid in overall astroglial expression of various growth factors (Krum et al., 2008; Koyama et al., 2014). Interestingly, non-endothelial VEGF production shifts to a more glial origin at this time, and progresses through development (Ogunshola et al., 2000). This shift in origin and production could account for the harmonious increase in astrocyte VEGFR1 receptors and its subsequent activators. Furthermore, this observation could suggest a dysregulation in glial/neuron ratios during FXS development, warranting further investigation. VEGFR2 has been shown to be the primary driver of angiogenesis, microvascular permeability (Dvorak, 2002), and is heavily involved with various aspects of endothelial cells such as proliferation and survival (Millauer et al., 1993; Zeng et al., 2001). There is also growing evidence that VEGFR2 (primarily through VEGF-A stimulation) is heavily involved with modulating neuronal properties such as increased axonal and neurite outgrowth (Silverman et al., 1999; Sondell et al., 1999; Sondell et al., 2000; Jin et al., 2002). Interestingly, our study also found that FXS mice exhibited increased VEGF-C (Fig. 2.3c) but decreased VEGF-D (Fig. 2.3d) expression. Both VEGF-C and VEGF-D can have similar functions as they both bind to VEGFR2 and VEGFR3 (Jeltsch et al., 1997; Veikkola et al., 2001; Karkkainen et al., 2002). Thus this bi-directional expression could be a form of reciprocal compensatory mechanisms.

Consistent with our prior studies in young adults (Galvan and Galvez, 2012; Belagodu et al., 2017), the current study found that FXS mice had significantly elevated BVD and VEGF-A expression at PND 60 (Fig. 2.2 & Fig. 2.3). As discussed in our prior studies (Belagodu et al., 2017), FXS increased VEGF-A expression is the most likely cause for the elevated BVD density; however, various FXS abnormalities also exist at this age and could be either caused by or contribute to these VEGF-A and BVD abnormalities. At this age numerous studies have

demonstrated an excess presence of long immature appearing dendritic spines with decreased presence of short mature appearing dendritic spines in various brain regions (Irwin et al., 2001; Galvez and Greenough, 2005). Furthermore, studies have suggested that this dendritic spine abnormality is a direct result of increased dendritic immature spine turnover in FXS mice (Pan et al., 2010). Interestingly, excessive dendritic spine motility would result in elevated metabolic demands and subsequent angiogenesis (Zhang et al., 2010) consistent with what we observed in FXS mice. Furthermore, as discussed above and in our prior study (Belagodu et al., 2017), elevated VEGF-A has been shown to induce neurite outgrowth and may play a role in stimulating increased FXS dendritic spine motility. These findings, along with our prior studies (Belagodu et al., 2017) suggest that the FXS vascular and VEGF-A abnormalities are a result of or cause for many FXS abnormalities. Interestingly, in addition to exhibiting elevated VEGF-A expression, FXS mice were found to have significantly reduced VEGF-B and PLGF expression compared to WT mice (Fig. 2.3b & Fig. 2.3d). Although it is difficult to discern the cause for this reduction, it could be due to compensatory mechanisms as a result of the elevated BVD and VEGF-A expression. Additional studies will be needed to better elucidate the cause for and effect of these altered growth factor expressions on FXS abnormalities.

The current study elegantly demonstrates that BVD, the growth factors mediating vascular growth and their subsequent receptors exhibit a complex expression pattern that is often disrupted in FXS. As discussed above, this abnormal developmental expression pattern in FXS could be a result of or cause many FXS abnormalities; thus providing a better understanding of FXS abnormalities over development. Furthermore, as we have previously demonstrated with VEGF-A (Belagodu et al., 2017), correction of these abnormal developmental expression patterns in FXS can provide new sites and time points for therapeutic interventions.

CHAPTER 3: BLOCKING ELEVATED VEGF-A ATTENUATES NON-VASCULATURE FRAGILE X SYNDROME ABNORMALITIES

Abstract

Fragile X syndrome (FXS) is the most common form of inherited mental retardation. In exploring abnormalities associated with the syndrome, we have recently demonstrated abnormal vascular density in a FXS mouse model (Galvan and Galvez, 2012). One of the most prominent regulators of vascular growth is VEGF-A (Vascular Endothelial Growth Factor A), suggesting that FXS is associated with abnormal VEGF-A expression. In addition to its role in vascular regulation, VEGF-A also induces cellular changes such as increasing cell proliferation, and axonal and neurite outgrowth independent of its effects on vasculature. These VEGF-A induced cellular changes are consistent with FXS abnormalities such as increased axonal material, dendritic spine density, and cell proliferation. In support of these findings, the following study demonstrated that FXS mice exhibit increased expression of VEGF-A in brain. These studies suggest that increased VEGF-A expression in FXS is contributing to non-vascular FXS abnormalities. To explore the role of VEGF-A in mediating non-vascular FXS abnormalities, the monoclonal antibody Bevacizumab was used to block free VEGF-A. Bevacizumab treatment was found to decrease FXS Synapsin-1 expression, a presynaptic marker for synapse density, and reduce FXS testicle weight to control levels. Blocking VEGF-A also alleviated FXS abnormalities on novel object recognition, a test of cognitive performance. These findings demonstrate that VEGF-A is elevated in FXS brain and suggest that its expression promotes non-vascular FXS abnormalities. Note this study has already been published (Belagodu et al., 2017).

Introduction

Fragile X Syndrome (FXS) is the leading form of inherited mental retardation and the most common known single gene cause for autism spectrum disorder (Cornish et al., 2008). Although the cause for the syndrome [transcriptional silencing of *FMR1*, the gene that codes for the Fragile X Mental Retardation Protein (FMRP)] is known (Pieretti et al., 1991; Verkerk et al., 1991), our current understanding of the mechanisms mediating the behavioral and anatomical deficits are not understood. In exploring FXS abnormalities, studies in a mouse model of the syndrome have demonstrated increased neocortical blood vasculature (Galvan and Galvez, 2012). These findings are consistent with reports from FXS patients demonstrating abnormal cerebral blood profusion (Balci et al., 2006; Kabakus et al., 2006) and suggest abnormal vascular development in FXS. One of the most prominent regulators of vascular growth, with increased expression being synonymous with increased vasculature, is VEGF-A (Vasculature Endothelial Growth Factor A) (Neufeld et al., 1999). These studies suggest that VEGF-A expression is elevated in FXS.

In support of this hypothesis, molecular studies have further suggested that VEGF-A expression is elevated in FXS. One of the most prominent theories of FMRP function has suggested that it regulates mGluR (metabotropic glutamate receptor) dependent synthesis of various proteins through mTORC1 (mammalian target of rapamycin) activation (Bear et al., 2004; Sharma et al., 2010). mTORC1 is a complex of proteins that mediate activation of various cellular substrates and exhibits elevated phosphorylation in FXS (Sharma et al., 2010; Hoeffer et al., 2012). Interestingly, mTORC1 has been shown to mediate activation of HIF1α (hypoxia inducible factor 1, alpha), a transcription factor that promotes VEGF-A transcription (Brugarolas et al., 2003; Dodd et al., 2015). Consistent with these findings, blocking mTORC1 in cancer

cells decreases VEGF-A expression (Li et al., 2015). These findings suggest that in FXS, an absence of FMRP, resulting in increased mTORC1 phosphorylation, would subsequently phosphorylate HIF1α resulting in increased VEGF-A production. This mechanism would further suggest that VEGF-A expression is elevated and the most likely cause for increased vasculature in FXS (Galvan and Galvez, 2012).

In addition to its primary role in angiogenesis, recent studies have demonstrated that VEGF-A can alter neuronal properties independent of vasculature. Specifically, studies have shown that VEGF-A can increase neuronal survival and proliferation (Sondell et al., 1999; Matsuzaki et al., 2001; Jin et al., 2002). Furthermore, VEGF-A stimulation of cultured neurons, in the absence of blood vessels, induces axonal outgrowth (Sondell et al., 1999; Sondell et al., 2000) and dendritic/neurite growth (Silverman et al., 1999; Jin et al., 2002). In further support of a neuronal role for VEGF-A, anatomical studies have characterized VEGF-A receptors (VEGFR2/Flk-1) on dorsal root ganglia neurons and HN33 cells (an immortalized hippocampal neuronal cell line), suggesting that VEGF-A can directly alter neuronal properties independent of its role on vasculature (Jin et al., 2000; Sondell et al., 2000; Jin et al., 2002). These studies suggest that in addition to its prominent role in vascular growth, VEGF-A also acts directly on neurons altering various neuronal properties such as cell proliferation, axonal sprouting, and neurite outgrowth.

Interestingly, these VEGF-A induced cellular properties are consistent with many FXS abnormalities. Studies have demonstrated that similar to VEGF-A induced increased cell proliferation (Sondell et al., 1999; Matsuzaki et al., 2001; Jin et al., 2002), FXS has been associated with increased proliferation of Sertoli cells (Slegtenhorst-Eegdeman et al., 1998) and hippocampal neurons (Luo et al., 2010). Furthermore, consistent with VEGF-A induced

increased axonal and neurite outgrowth (Silverman et al., 1999; Sondell et al., 1999; Sondell et al., 2000; Jin et al., 2002), excessive axonal growth and increased dendritic material have been observed in a drosophila and mouse model of FXS (Galvez et al., 2003; Antar et al., 2005). Also in line with these finding FXS neurons have been shown to exhibit an abundance of long-thin dendritic spines (Irwin et al., 2002; Galvez and Greenough, 2005; Grossman et al., 2006). Interestingly, two photon FXS studies have further demonstrated that this increase in dendritic spine density is due to an increase in dendritic spine formation, suggesting that an unknown factor is actively stimulating dendritic spine production in FXS (Pan et al., 2010). These findings, along with the fact that VEGF-A stimulates neurite outgrowth (Silverman et al., 1999; Jin et al., 2002), suggests that elevated VEGF-A expression in FXS is stimulating dendritic spine production and possibly other neuronal anatomical abnormalities.

The following study demonstrates that VEGF-A is elevated in FXS brains and suggests that this increase is due to an mTORC1 dependent pathway. To explore the role of VEGF-A in mediating non-vascular FXS abnormalities, VEGF-A was blocked and found to alleviate both behavioral and anatomical FXS abnormalities. These studies provide the first account for the role of VEGF-A in contributing towards FXS abnormalities.

Methods & Analysis

Housing and Care of Animals

Adult (PND 60) male C57/B6 *FMR1* knockout (FXS) and wildtype (WT) mice were used. Mice were housed in standard laboratory conditions (12 hr-12 hr light/dark cycle with food and water provided *ad libitum*).

VEGF-A Expression

For analysis of VEGF-A expression, dissected cortical hemispheres, including cortical white matter and hippocampus (referred to as cortical hemispheres from this point on) from FXS (n=3) and WT (n=3) mice were homogenized and protein concentration estimated via bicinchonic acid assay (Thermo Scientific). Protein (40 µg) in a 1:1 loading buffer (475 µl Laemmli + 25 µl βME) ratio was loaded and run on a 4-15% electrophoresis gel (Biorad) at 100 V for 10 min followed by 200 V for 35 min. The separated proteins were then transferred to a nitrocellulose membrane at 100 V for 1 hr, blocked with 5% milk in TBS-T (Tris Buffered Saline with 0.05% Tween 20) and probed with VEGF-A antibody (1:1000; Santa Cruz) overnight at 4°C. The membrane was then washed and incubated in anti-rabbit secondary antibody (1:1000; Cell Signaling Technology) for 2 hr prior to chemiluminescent substrate exposure for 5 min and imaged via a BioRad ChemiDoc Touch Gel Imaging System (BioRad). Once imaged, blots were re-probed for GAPDH (1:1000; Santa Cruz) as a loading control. The relative intensity of VEGF-A was determined by dividing its optical density, determined using Image Lab v5.2.1 (BioRad), by GAPDH. GAPDH has been used in previous FXS studies as an effective loading control (Yu et al., 2013; Pretto et al., 2014; von Leden et al., 2014).

To explore the proposed mechanism for the increased VEGF-A expression and the dependency on mTORC1 activation in FXS, brain slices from FXS (n=3) mice were treated with rapamycin followed by Western Blot analysis of VEGF-A expression. For collection of brain slices, mice were transcardially perfused with an ice cold high sucrose slicing solution (206 mM sucrose, 10.0mM $MgCl_2$, 11.0 mM glucose, 1.25 mM NaH_2PO_4, 26 mM $NaHCO_3$, 0.5 mM $CaCl_2$, and 2.5 mM KCl at ph 7.4) and brains sectioned via vibrating tissue slicer (300 microns) into a holding chamber with oxygenated artificial cerebrospinal fluid (126 mM NaCl, 2.0 mM $MgCl_2$, 10.0 mM glucose, 1.25 mM NaH_2PO_4, 26 mM $NaHCO_3$, 2.0 mM $CaCl_2$, and 2.5 mM

KCl at ph 7.4). The sections were also cut in half and stored in separate chambers to allow for within animal control of rapamycin treatment. After a 3-4 hour incubation at 37°C in a cell culture incubator maintained at >80% humidity and 5% CO_2, half of each brain section was treated with 50 nM rapamycin or equivalent DMSO vehicle for 30 min. After drug treatment, the sections from each animal and hemisphere were pooled, homogenized and examined for VEGF-A expression with Western Blot detection as described above.

Blocking VEGF-A

To determine the role of VEGF-A in mediating FXS abnormalities, its ability to bind to its receptor was blocked using Bevacizumab (Genentech). Bevacizumab is a monoclonal antibody that binds to free-floating VEGF-A preventing it from binding with its receptor. To determine Bevacizumab's ability to block VEGF-A in brain, WT (n=6) and FXS (n=6) mice were given 5 mg/kg Bevacizumab or Saline IP every other day for 10 days. This dose has been shown to attenuate VEGF-induced angiogenesis in mouse brain (Lu et al., 2012; Walker et al., 2012). VEGF-A expression in dissected cortical hemispheres was then examined with Western Blot analyses. Samples were prepared and processed as described above on a large 10% electrophoresis gel at 150 V for 1 hr followed by 200 V for 4 hrs. The separated proteins were then transferred to a nitrocellulose membrane at 20 V at 100 mA overnight. The membrane was then probed for VEGF-A and GAPDH with Western Blot detection as described above.

Synapse Expression

To examine the role of VEGF-A in mediating synapse density, mice were given Bevacizumab as outlined above. The day following the last injection, mice were either processed for Western Blot analyses of VEGF-A as described above or transcardially perfused for Immunohistochemical analyses. For Western Blot analyses dissected cortical hemispheres

were examined from WT (n=6) and FXS (n=6) mice for Synapsin-1 expression. Synapsin-1 is a synaptic vesicle binding protein whose expression correlates with synapse number (Sudhof et al., 1989; Cesca et al., 2010). Synapsin-1 antibody (Sigma) was probed at 1:1000 dilution, incubated overnight and imaged along with GAPDH to control for loading differences. For Immunohistochemical analyses six sections (30 μm) spanning primary visual cortex (V1) (FXS Saline n=5, FXS Bevacizumab n=4, WT Saline n=5, WT Bevacizumab n=4) and CA1 of hippocampus (FXS Saline n=4, FXS Bevacizumab n=5, WT Saline n=5, WT Bevacizumab n=5) were examined. V1 was selected because in rodents it exhibits many forms of experience-induced plasticity that were previously believed to only be found in higher processing regions of the cortex. For example V1 neurons exhibit stimulus familiarity (Sawtell et al., 2003; Frenkel et al., 2006; Cooke and Bear, 2010), reward-timing prediction (Shuler and Bear, 2006; Chubykin et al., 2013), and spatiotemporal sequence learning (Gavornik and Bear, 2014). As a result studies have recently utilized plasticity in V1 as an indicator of cognitive health for various neurological disorders (Cooke and Bear, 2012; Gavornik and Bear, 2014). Furthermore, V1 is the brain region where FXS neuronal and vascular abnormalities have been the most extensively examined (Irwin et al., 2002; Galvan and Galvez, 2012) making it a suitable structure for examining FXS abnormalities. CA1 was selected due to its well established link with cognition (Zola-Morgan et al., 1986) and the fact that it exhibits FXS dendritic spine abnormalities (Grossman et al., 2006).

For staining, sections were incubated in Synapsin-1 antibody (1:500; Sigma) overnight at 4°C followed by a 2 hr biotinulated anti-rabbit secondary antibody incubation at room temperature (1:100; Jackson ImmunoResearch). Synapsin-1 expression was visualized through avidin-biotin amplification (Vector) and nickel enhanced DAB detection (0.5 mg/ml DAB, 6.95 mg/ml nickel ammonium sulfate, 0.033 μl/ml 30% hydrogen peroxide). Sections were imaged

on an Olympus BX50 microscope with a Zeiss AxioCam ICc1 camera at 20x magnification with AxioVision ver4.8.1. The number of Synapsin-1 positive puncta per area was quantified across all layers in V1 and in the apical dendritic field of CA1 of the hippocampus using the particle analysis tool on ImageJ (http://rsbweb.nih.gov/ij/docs/guide/146-30.html). To accurately determine the density of Synapsin-1 staining in the neuropil the area with blood vessels was removed from the analysis. To determine if the absence of FMRP altered the size of V1 or CA1, volumetric analyses were conducted. Briefly, the total area of the region was determined on adjacent evenly spaced cresyl violet stained sections from each brain by tracing the region on ImageJ. These areas were then multiplied by the distance between each section to create an estimation of the volume between sections. This number was then summed with each volume between each of the sections, to provide an overall estimation of the total volume of V1 and CA1.

Testicle Weight

To elucidate the role of VEGF-A in modulating FXS testicle weight, FXS (n=10) and WT (n=5) mice were given Bevacizumab or Saline via the dosing scheme outlined above. The day following the last injection, testicles were removed and post-fixed in 4% paraformaldehyde for 24 hr. FXS males exhibit macroorchidism as a result of increased Sertoli cell proliferation (Slegtenhorst-Eegdeman et al., 1998). After post-fixing, testicles were desiccated for 2 days and weighed. Testicular weight has been shown to be a viable metric to assess macroorchidism in adult FXS mice (Kooy et al., 1996). For statistical analyses each testicle was considered an individual unit.

Behavioral Analyses

To determine the contribution of VEGF-A to FXS behavioral and cognitive deficits, mice were given Bevacizumab or Saline (FXS Saline n=7, FXS Bevacizumab n=9, WT Saline n=7, WT Bevacizumab n=9) as outlined above and tested for hyperactivity and novel object recognition. Using a modified protocol (Ventura et al., 2004), mice were habituated to the training chamber (16.5"L x 8.5" W x 8" H) with no objects for 10 min on the day following the last injection. Between trials, to decrease the influence of scent marking, the cage was wiped down with 70% ethanol and allowed to dry before starting the next trial. Hyperactivity was assessed during habituation. To assess hyperactivity, video recordings of the mice were obtained and the distance traveled over 10 minutes was measured with Anymaze (v4.98). The following day (Training), mice were exposed to two of the same objects (randomly assigned, two beakers or two plastic egg shells) for 10 min. Percent time exploring the objects (direct whisking or sniffing) was determined using the following calculation: (time exploring the objects/total training time)*100. Preference for a specific side of the training chamber (Left vs. Right) was determined using the following calculation: (time spent on each side/total training time)*100. On the third day (Testing), one of the objects was randomly replaced with a novel object and the time spent interacting with each (direct whisking or sniffing) was recorded for 10 min. Percent interaction time for each object was determined via: (interaction with object/sum of total interaction with both objects)*100. Note 50% delineates equal exploration of both objects. On average mice spent 32.9 sec interacting with the objects. Finally the discrimination index for the novel object was determined via: [(interaction with novel object–interaction with familiar object)/interaction with familiar object]*100. Four mice (1 from each group) spent less than 10 sec interacting with any of the objects during the Testing Stage and were thus removed from the study.

Statistical Analyses

The analysis of VEGF-A expression in WT vs FXS and FXS rapamycin treated vs non-treated were conducted with a paired T-Test with equal variance on SAS (http://www.sas.com/en_us/home.html). All additional statistical analyses were conducted with a 2-way mixed model ANOVA on SAS with either genotype and/or drug as between subject factors. For novel object recognition, object (novel vs. familiar) was treated as a within subject factor.

Results

VEGF-A brain expression in FXS was found to be elevated compared to WT mice. FXS dissected cortical hemispheres were found to have 45.6% more VEGF-A expression than WT mice (Fig. 3.1a; $t_{(4)}=3.06$; $p<0.05$). Note, there was no significant difference in GAPDH (loading control) expression in the Western Blot analysis or any of the subsequent analyses across any of the groups (data not shown). This increased VEGF-A expression in FXS is consistent with the proposed molecular pathway (Fig. 3.1c). To further investigate the proposed molecular pathway, FXS brain sections were treated with rapamycin to block mTORC1 activation followed by analysis of VEGF-A expression. This study found that blocking mTORC1 activation for 30 minutes decreased VEGF-A expression in FXS brain 13% (Fig. 3.1b; $t_{(4)}=3.10$; $p<0.05$). These findings, although cannot discount a possible mTORC1 independent pathway contributing towards FXS VEGF-A expression, suggest that the increased VEGF-A expression in FXS is at least partially mediated by mTORC1 activation (Fig. 3.1c).

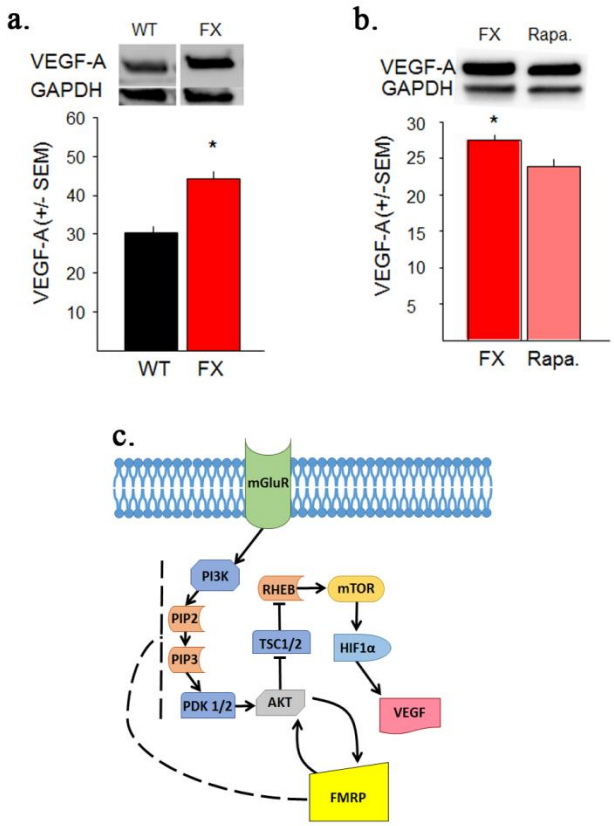

Figure 3.1. VEGF-A expression is elevated in Fragile X brain. a. VEGF-A expression in dissected cortical hemispheres. Adult FXS mice have significantly more VEGF-A expression than WT mice. GAPDH was used as a loading control. b. VEGF-A expression in FXS is mediated by an mTORC1 dependent pathway. Treatment of adjacent coronal hemispheres with Rapamycin to block mTORC1 activity for 30 min significantly decreased VEGF-A expression in FXS brain slices. GAPDH was used as a loading control. Rapa.=Rapamycin c. Schematic of a proposed molecular pathway for VEGF-A production involving the Fragile X Mental Retardation Protein (FMRP), the protein that is absent in FXS. Arrows=activation. Perpendicular line=inhibition. Solid lines=known interactions. Dotted lines=proposed interactions. For a detailed description of the mGluR/FMRP pathway see (Bear et al., 2004; Santoro et al., 2012). *<0.05

To explore the role of VEGF-A in mediating FXS abnormalities, VEGF-A's ability to bind to its receptor was blocked with Bevacizumab. Blocking of VEGF-A was found to significantly reduced VEGF-A expression in dissected cortical hemispheres of FXS mice (Fig. 3.2a; $F_{(3,11)}$=12.72; p<0.05). These findings demonstrate that Bevacizumab can be used to explore the role of VEGF-A in FXS brain abnormalities.

One of the most prevalent FXS neuronal abnormality is increased dendritic spine density. To examine synapse properties, we demonstrated with Western Blot analyses, that Synapsin-1 was significantly increased in FXS dissected cortical hemispheres compared to WT mice (Fig. 3.2b; $F_{(3,8)}$=6.66; p<0.05). Subsequent region specific analyses demonstrated that Synapsin-1 was significantly increased in FXS V1 (82%) and CA1 (60%) compared to WT controls. Interestingly, these findings are not consistent with a prior study examining Synapsin staining in FXS (Li et al., 2002). Possible differences could be due to the quantification methods used; however, our findings are consistent with previous FXS anatomical dendritic spine studies (Irwin et al., 2002; Galvez and Greenough, 2005; Grossman et al., 2006; Pan et al., 2010). In addition to replicating the FXS dendritic spine abnormality, our Synapsin-1 analyses demonstrated that Bevacizumab treatment significantly decreased Synapsin-1 density in FXS cortical hemispheres, V1 and CA1 [Fig. 3.2b; Cortex $F_{(3,8)}$=6.66; p<0.05; Fig. 3.2e; V1 ($F_{(3,12)}$=4.10;p<0.05); Fig. 3.2f; CA1 ($F_{(3,15)}$=3.86;p<0.05)]. Note, Bevacizumab did not have a significant effect on Synapsin-1 in WT mice. Furthermore, volumetric analyses of V1 and CA1 demonstrated no significant differences between treatment groups (V1 Fig. 3.2g & CA1 Fig. 3.2h), demonstrating that the observed differences in Synapsin-1 density are not due to Bevacizumab induced changes in the volume of these brain regions. These findings strongly suggest that elevated VEGF-A expression is a contributing factor towards FXS dendritic spine abnormalities.

Figure 3.2. Bevacizumab decreases VEGF-A and Synapsin-1 (SYN) in Fragile X. a. VEGF-A expression in dissected cortical hemispheres following 10 days of Bevacizumab treatment.

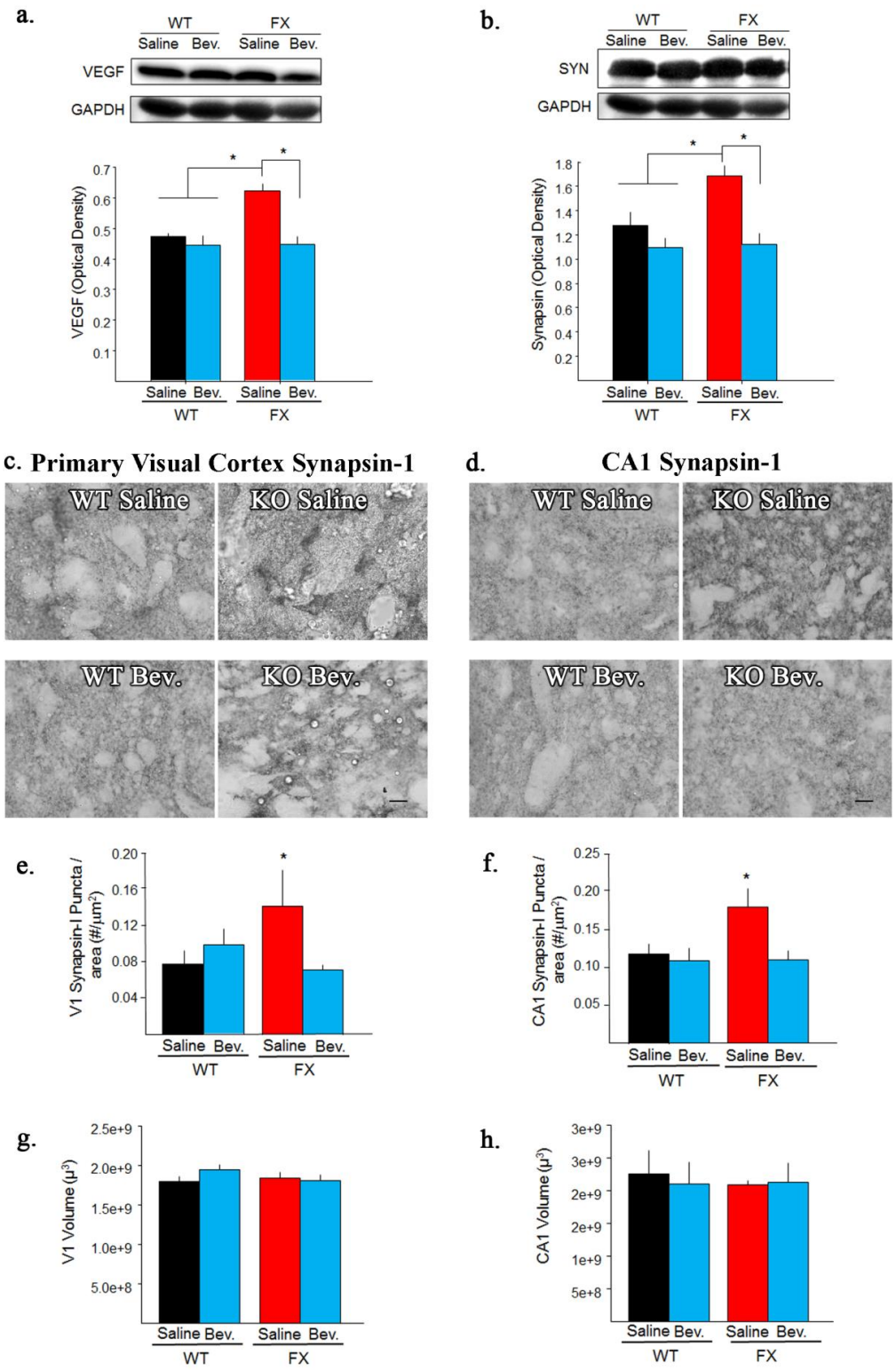

Figure 3.2 (cont.). Bevacizumab decreases VEGF-A and Synapsin-1 (SYN) in Fragile X. a. VEGF-A expression in dissected cortical hemispheres following 10 days of Bevacizumab treatment. Bevacizumab treatment significantly reduced VEGF-A expression in adult FXS mice. GAPDH was used as a loading control. b. Synapsin-1 expression in treatment groups. Bevacizumab treatment significantly reduced SYN expression in adult FXS mice. GAPDH was used as a loading control. c. Immunohistochemical expression of Synapsin-1 (dark punctated staining pattern) in primary visual cortex (V1) from treatment groups. Note, FXS saline treated have more dark punctated staining than WT mice and Bevacizumab treatment decreases that amount of dark punctated staining to WT levels. d. Immunohistochemical expression of Synapsin-1 (dark punctated staining pattern) in CA1 from treatment groups. Note, FXS saline treated have more dark punctated staining than WT mice and Bevacizumab treatment decreases that amount of dark punctated staining to WT levels. e. Quantification of Synapsin-1 density in V1 following treatment with Bevacizumab. Bevacizumab significantly decreased the density of V1 Synapsin-1 positive puncta in adult FXS mice. f. Quantification of Synapsin-1 density in CA1 following treatment with Bevacizumab. Bevacizumab significantly reduced the density of CA1 Synapsin-1 positive puncta in adult FXS mice. Note, Bevacizumab did not significantly alter Synapsin-1 expression in WT V1 or CA1. g. Volumetric analysis of V1 following treatment with Bevacizumab. h. Volumetric analysis of CA1 following treatment with Bevacizumab. Bevacizumab did not significantly alter the volume of V1 or CA1. Scale bar =10µm Bevacizumab=Bev. *<0.05

In addition to neuronal abnormalities, macroorchidism has also been characterized as a prominent abnormality in FXS subjects. Consistent with previous studies (Slegtenhorst-Eegdeman et al., 1998) FXS mice exhibited a significant 20% increase in testicle weight compared to WT controls. However, Bevacizumab treatment decreased FXS testicle weight 11%, making them statistically indistinguishable from WT mice (Fig. 3.3a; $F_{(3,26)}=6.87$;$p<0.05$). Note, Bevacizumab did not have a significant effect on testicle weight in WT mice. These findings strongly suggest that elevated VEGF-A expression also contributes towards FXS testicle abnormalities.

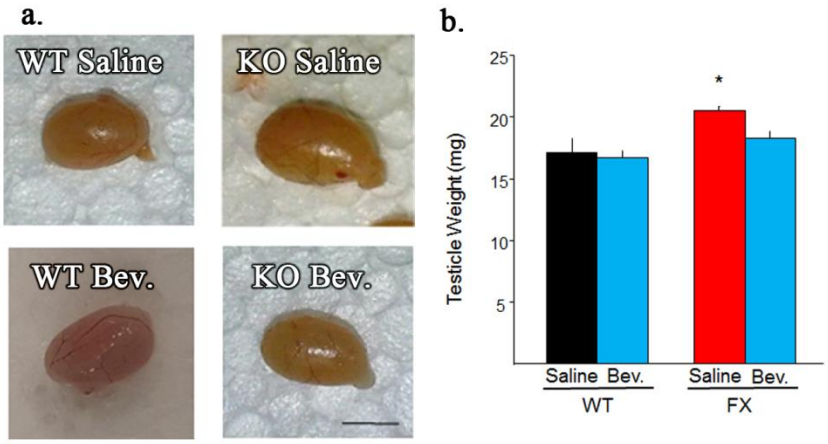

Figure 3.3. Blocking VEGF-A decreases FXS testicle weight. a. Representative testicles from treatment groups. Scale bar=5 mm. b. Quantification of testicle weight from adult mice treated with Bevacizumab. Bevacizumab significantly reduced testicle weight in FXS mice. Note, Bevacizumab did not significantly alter testicle weight in WT mice. Bevacizumab=Bev. *<0.05

Finally, to assess VEGF-A contribution towards FXS behavioral and cognitive abnormalities, mice were given Bevacizumab as outlined above and tested for hyperactivity and novel object recognition. In line with previous findings (Bakker et al., 1994), FXS mice exhibited increased hyperactivity compared to WT mice (Fig. 3.4b; $t_{(26)}$=3.00;p<0.05). Bevacizumab did not significantly alter activity levels in either FXS or WT mice. For novel object recognition, WT controls exhibited expected preferential exploration towards the novel vs. familiar object. Likewise, consistent with previous studies, FXS Saline mice did not exhibit preferential exploration towards either object (Ventura et al., 2004; Bhattacharya et al., 2012; Seese et al., 2014). However, Bevacizumab treated FXS, like WT mice, preferentially explored the novel vs. familiar object, suggesting that they remembered which object had been previously explored [Fig. 3.4c; Percent Interaction Time ($F_{(1,14)}$=11.36;p<0.05), Fig. 3.4f; Discrimination Index ($F_{(3,19)}$=4.68;p<0.05)].

As a behavioral control it was further determined that during training mice did not significantly differ in percent time exploring the objects (Fig. 3.4d). However, all groups

exhibited a significant preference for the left side of the training chamber (Fig. 3.4c; $t_{(48)}$=3.20;p<0.05), with no significant side by group interaction; suggesting that this could not account for any group differences. These findings collectively suggest that blocking VEGF-A can alleviate some FXS cognitive abnormalities.

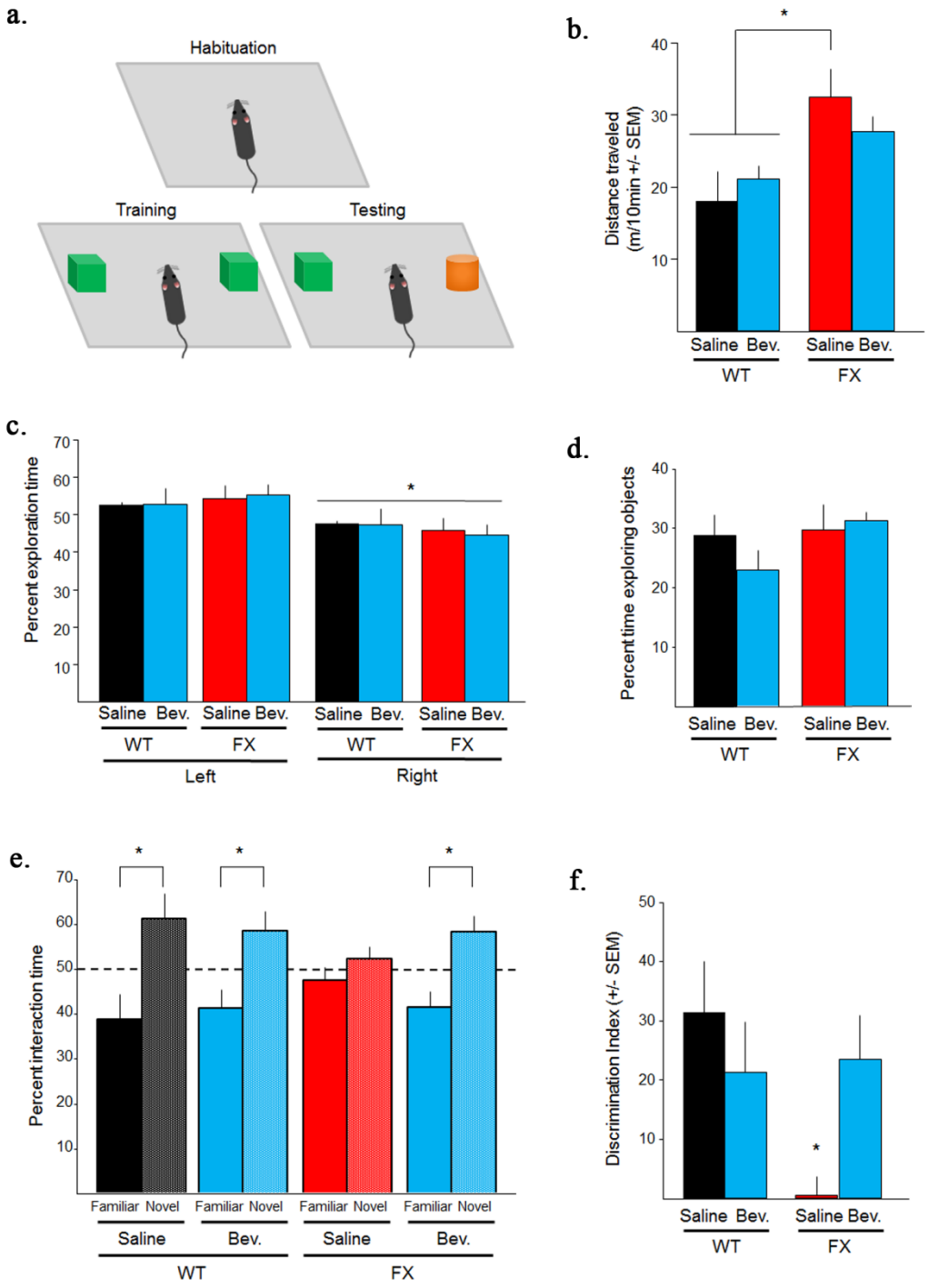

Figure 3.4. Blocking VEGF-A alleviates FXS novel object recognition (NOR) deficits. a. NOR training protocol. b. Amount of movement during habituation. FXS mice had significantly more movement than WT mice. Bevacizumab did not significantly alter the amount of movement for any of the groups. c. Percent time spent in each side of the training chamber during training. Mice in all groups preferred the right side of the training chamber. This preference was controlled for by randomly placing the novel object on either side of the training chamber during testing. d. Percent time mice spent exploring objects during training. There were no significant

Figure 3.4 (cont.): differences across groups. e. Percent time spent interacting with each object during testing. Bevacizumab increased adult FXS preference for the novel object, similar to WT mice. Dotted line represents no preference. f. Discrimination index for novel object interaction across treatment groups. Bevacizumab alleviated FXS discrimination index deficit. Note, Bevacizumab did not significantly alter any measured behaviors in WT mice. Bevacizumab=Bev. *<0.05

Discussion

Fragile X Syndrome is the leading form of inherited mental retardation. It is caused by transcriptional silencing of a single gene, *FMR1*; however, the specific mechanisms by which this genetic mutation causes FXS abnormalities are currently unknown. The current study explored a novel mechanism contributing towards FXS abnormalities, VEGF-A modulation. Historically VEGF-A has been shown to play a prominent role in vascular regulation, with increased expression being synonymous with increased vasculature (Josko et al., 2000). Consistent with these studies we previously demonstrated vascular abnormalities in V1 of adult FXS mice (Galvan and Galvez, 2012). However, in addition to its vascular role, recent studies have demonstrated that VEGF-A can increase axon growth, cell survival and neurite outgrowth, consistent with abnormalities observed in FXS (excessive axonal material, increased neurogenesis, and increased number of immature dendritic spines); suggesting a role for VEGF-A in mediating non-vascular FXS abnormalities (Slegtenhorst-Eegdeman et al., 1998; Silverman et al., 1999; Sondell et al., 1999; Jin et al., 2002; Pan et al., 2004; Pan et al., 2010).

In exploring this mechanism, the current study demonstrated that VEGF-A expression is elevated in the cortex of FXS mice (Fig. 3.1a). These findings, although novel for FXS and VEGF-A, are consistent with our current molecular understanding of FMRP function. In FXS mTORC1 has been shown to exhibit increased phosphorylation/activation (Sharma et al., 2010). Furthermore, mTORC1 is a critical regulator of VEGF-A, with increased mTORC1 activation resulting in increased VEGF-A expression (Brugarolas et al., 2003; Dodd et al., 2015) (Fig.

3.1c). Consistent with these findings, we demonstrated that blocking mTORC1 in FXS decreases VEGF-A expression (Fig. 3.1b), suggesting that increased mTORC1 phosphorylation in FXS would result in increased VEGF-A expression. These studies collectively support our current finding of increased VEGF-A expression in FXS and suggest a role for VEGF-A in mediating FXS abnormalities.

To explore the role of VEGF-A in mediating FXS abnormalities, our subsequent studies blocked VEGF-A and demonstrated decreased synapse density in FXS mice (Fig. 3.2b-h). Note, these studies did not discern the effect of blocking VEGF-A on dendritic spine morphology in FXS. Current studies in the lab are actively exploring this research direction. However, our findings demonstrate that blocking VEGF-A can decrease elevated synapse density in FXS. Synapse abnormalities have been well documented in FXS (Irwin et al., 2002; Galvez and Greenough, 2005; Grossman et al., 2006); with studies suggesting that adult dendritic spine abnormalities are a result of increased dendritic spine proliferation (Pan et al., 2010). These studies have suggested that an unknown factor stimulates dendritic spine proliferation in FXS. Consistent with these findings, VEGF-A stimulation of cultured neurons in the absence of blood vessels increases dendritic growth, axon length and axon density (Silverman et al., 1999; Sondell et al., 1999; Jin et al., 2002). These findings collectively suggest that excessive brain VEGF-A in FXS stimulates dendritic spine proliferation, inducing FXS dendritic spine abnormalities.

Many studies have suggested that FXS neuronal abnormalities such as increased dendritic spine density are an underlying cause for behavioral and cognitive abnormalities. Based upon this rational, we demonstrated that blocking VEGF-A can alleviate FXS cognitive abnormalities using novel object recognition (Fig. 3.4e & f). When provided with a choice, mice normally explore a novel object over a familiar object. However, FXS mice do not preferentially explore

either object, suggesting that they do not remember prior exposure to the familiar object (Busquets-Garcia et al., 2013). Blocking VEGF-A alleviates this behavioral abnormality in FXS. Furthermore, this behavioral effect cannot be explained due to changes in the total number of object interactions or hyperactivity, as blocking VEGF-A did not alter either of these behaviors (Fig. 3.4b & d). These findings suggest that excessive VEGF-A production, possibly via VEGF-A induced synapse abnormalities, contributes to FXS cognitive abnormalities.

Although the mechanism for VEGF-A induced neuronal growth is still not fully understood, VEGF-A has been shown to predominantly bind to VEGFR1 and VEGFR2. Upon VEGF-A binding to VEGFR1, it activates PLC gamma (phospholipase C) that then phosphorylates DAG (diacylglycerol), which phosphorylates PKC (protein kinase C). PKC then alters various cellular processes including cell proliferation and vasopermeability. In contrast, when VEGF-A binds to VEGFR2 it activates Shc (SH2 domain protein C1) that then phosphorylates RAS (Rat sarcoma), which phosphorylates MAPK. This activation then also alters various cellular processes including gene expression and cell proliferation. More importantly, neuronal studies have suggested that activation of VEGFR2 and the MAPK pathway are primarily responsible for VEGF-A's ability to modulate neuronal processes. For example, VEGF-A stimulation of superior cervical ganglia neurons which predominantly express VEGFR2 and neurophilin-1, induce axonal outgrowth and cell survival (Sondell et al., 1999). Furthermore, inhibiting VEGFR2 or MAPK prevents VEGF-A induced axon growth (Sondell et al., 1999; Sondell et al., 2000). These studies suggest that VEGF-A is mediating its neuronal effects in FXS through VEGFR2 and the MAPK pathway.

Although VEGF-A has been shown to directly alter neuronal properties independent of vascular changes (Sondell et al., 1999), it is possible that the observed attenuation of FXS

abnormalities are not due to direct neuronal modulation, but rather due to indirect Bevacizumab induced VEGF-A modulation of vascular properties. Blocking VEGF-A (via Bevacizumab) decreases VEGF-induced angiogenesis in control brains (Walker et al., 2012); however, its effect on already established vascularization in FXS has not been explored. If decreasing VEGF-A expression decreases vascular density in FXS brain, decreased nutrients and other signaling factors being delivered via the blood stream could mediate some or all of the benefits observed. Interestingly, it should be noted that our prior studies demonstrated increased vasculature in aged FXS brains with only mild increases in adults (Galvan and Galvez, 2012), the age group examined in this study. The mild increased vasculature observed in adult FXS brains suggests that abnormalities in vascular density alone could not completely account for the extensive FXS neuronal abnormalities observed at this age. However, this does not preclude VEGF-A from acting directly on neurons. Furthermore, our finding of increased VEGF-A expression in the absence of excessive vascular growth (Galvan and Galvez, 2012) suggests that a compensatory mechanism is reducing vasculature in FXS brains. Current studies in the lab are actively exploring this and other possible mechanisms for the role of VEGF-A in FXS abnormalities. Although further studies will be needed to determine the specific mechanism by which blocking VEGF-A is able to attenuate these FXS abnormalities, the current studies strongly suggest that increased VEGF-A expression plays a role in mediating FXS neuronal abnormalities. Additionally, these studies demonstrate that reducing VEGF-A binding, irrespective of the mechanism, helps alleviate some FXS neuronal abnormalities.

In addition to playing a role in FXS neuronal abnormalities, our studies suggest that excess VEGF-A expression is mediating other FXS abnormalities such as macroorchidism. Studies have shown that FXS is associated with increased testicle weight, due to increased

Sertoli cell proliferation (Slegtenhorst-Eegdeman et al., 1998). Consistent with these findings, VEGF-A stimulation increases neuronal survival rate and proliferation of Schwann cells (Xiao et al., 2007). These studies suggest that abnormal VEGF-A expression in FXS is mediating the increased Sertoli cell proliferation. In support of this hypothesis, we demonstrated that blocking VEGF-A in FXS significantly reduced testicle weight (Fig. 3.3b). These findings further suggest that excessive VEGF-A production in FXS plays a role in mediating both neuronal and non-neuronal FXS abnormalities.

The aforementioned experiments demonstrate that blocking VEGF-A can alleviate FXS abnormalities in testicle weight, synapse density, and cognition. Although the specific mechanism mediating these effects is still not fully understood, these studies elucidate a potential novel mechanism, VEGF-A modulation, for FXS abnormalities. Furthermore, it is worth noting that the benefits following blocking of VEGF-A were observed in adult FXS, further suggesting that VEGF-A modulation could be used to help alleviate adult FXS abnormalities.

CHAPTER 4: CHARACTERIZATION OF ULTRASONIC VOCALIZATIONS OF FRAGILE X MICE

Abstract

Fragile X Syndrome (FXS) is the leading form of inherited intellectual disability. It is caused by the transcriptional silencing of *FMR1*, the gene which codes for the Fragile X Mental Retardation Protein (FMRP). Patients that have FXS exhibit numerous behavioral and cognitive impairments, such as attention-deficit/hyperactivity disorder, obsessive compulsive disorder, and autistic-like behaviors. In addition to these behavioral abnormalities, FXS patients have also been shown to exhibit various deficits in communication such as abnormal sentence structures, increased utterances, repetition of sounds and words, and reduced articulation. These deficits can dramatically hinder communication for FXS patients, exacerbating learning and cognition impairments while decreasing their quality of life. To examine the biological underpinnings of these communication abnormalities, studies have used a mouse model of the Fragile X Syndrome; however, these vocalization studies have resulted in inconsistent findings that often do not correlate with abnormalities observed in FXS patients. Interestingly, a detailed examination of frequency modulated vocalizations that are believed to be a better assessment of rodent communication has never been conducted. The following study used courtship separation to conduct a detailed examination of frequency modulated ultrasonic vocalizations (USV) in FXS mice. Our analyses of frequency modulated USVs demonstrated that adult FXS mice exhibited longer phrases and more motifs. Phrases are vocalizations consisting of multiple frequency modulated ultrasonic vocalizations, while motifs are repeated frequency modulated USV patterns. Fragile X mice had a higher proportion of "u" syllables in all USVs and phrases while their wildtype counterparts preferred isolated "h" syllables. Although the specific

importance of these syllables towards communication deficits still needs to be evaluated, these findings in production of USVs are consistent with the repetitive and perseverative speech patterns observed in FXS patients. This study demonstrates that FXS mice can be used to study the underlying biological mechanism(s) mediating FXS vocalization abnormalities. Note this study has already been published (Belagodu et al., 2016).

Introduction

Fragile X Syndrome (FXS) is the leading form of inherited intellectual disability and the most common known single gene cause for Autism Spectrum Disorder (ASD) (Maenner et al., 2013). FXS is an X-linked disorder that generally results from the transcriptional silencing of *FMR1*, the gene which codes for the Fragile X Mental Retardation Protein (FMRP). Normally the 5′ untranslated region of *FMR1* contains a CGG trinucleotide repeat of less than 50 repeats, whereas in FXS it contains more than 200 CGG repeats. This extended trinucleotide repeat leads to hypermethylation and transcriptional silencing of *FMR1* (McLennan et al., 2011; Santoro et al., 2012). As a result, FXS patients exhibit many behavioral abnormalities consistent with those commonly observed in ASD, such as poor eye contact, hand flapping and/or hand biting, hyperactivity, impulsivity, and social anxiety (Miller et al., 1999; Kronk et al., 2010; Cordeiro et al., 2011).

In addition to these behavioral deficits, many studies have characterized various communication abnormalities in FXS patients. For example, FXS patients exhibit a greater number of articulation errors often associated with dyspraxia as well as dysprosody (Borghgraef et al., 1987; Spiridogliozzi et al., 2000; Mirrett et al., 2003; Roberts et al., 2005). They also often speak in rapid bursts of repeated words (Largo and Schinzel, 1985; Tierney et al., 2012), although they do not significantly differ from controls in the number of vocalizations produced

(Borghgraef et al., 1987). Furthermore, FXS patients have been shown to exhibit a form of stuttering (disfluency) where they repeat components of speech (Lubs et al., 1984; Opitz and Sutherland, 1984; Rhoads, 1984; Vilkman et al., 1988). These disfluencies typically manifest in the initial component of the phrase or sentence resulting in a subpar structuring of sentences (Lubs et al., 1984; Opitz and Sutherland, 1984). Such deficits in speech production can dramatically hinder communication with FXS patients, having detrimental consequences on subsequent learning, cognition and quality of life (Cornish et al., 2004).

In recent years the FXS mouse model has provided a vital tool for understanding the anatomical and molecular bases for many deficits in FXS (Zeidler et al., 2015), suggesting that it could also be used to better understand the biological mechanism(s) underlying FXS vocalization deficits. Unfortunately there have only been a few studies examining FXS mouse vocalizations and most have characterized abnormalities that either only exist at one developmental time point or do not correlate with abnormalities observed in FXS patients, questioning the neuroethological relevance towards FXS vocalization abnormalities (Lubs et al., 1984; Opitz and Sutherland, 1984; Rhoads, 1984; Borghgraef et al., 1987; Vilkman et al., 1988; Van Borsel et al., 2008). To induce vocalizations most FXS studies have examined pup ultrasonic vocalizations (USV) due to maternal separation. These studies have demonstrated that postnatal day (PND) 7 FXS mice exhibit an increase in the number of frequency jump USVs compared to controls. However this increase was transient and found to return to control levels by PND 8-10 (Roy et al., 2012; Lai et al., 2014). Studies in adult mice have further demonstrated FXS mice produce fewer USVs during courtship than control mice (Rotschafer et al., 2012); however, this study had the added confound of recording when both male and female mice were present, making detailed mouse specific analyses of USVs properties difficult.

Interestingly, as mentioned above, none of these studies observed vocalization deficits to the extent of those observed in FXS patients (Lubs et al., 1984; Opitz and Sutherland, 1984; Rhoads, 1984; Borghgraef et al., 1987; Vilkman et al., 1988; Van Borsel et al., 2008). Although these studies examined many USV properties such as number, duration, rate, mean frequency, and bandwidth (Rotschafer et al., 2012) a detailed investigation of USV spectral properties, particularly frequency modulated USVs that many believe are reminiscent of bird song vocalizations in their spectral complexity referred to as syllables (Arriaga and Jarvis, 2013), has not been conducted. These syllables have complex patterns and frequency jumps that are organized into phrases and motifs. Phrases are vocalizations consisting of multiple syllables, while motifs are repeated syllable patterns (Holy and Guo, 2005). Due to the complexity of these vocalization patterns and spectral properties, it has been argued that syllable production provides a better assessment of rodent vocal communication, especially when examining models of neurological disorders (Zampieri et al., 2014). Given that FXS vocal abnormalities are predominately observed in deficits with communication, a detailed analysis of USV syllable production and spectral properties in FXS mice would provide a better assessment of their neuroethological relevance towards understanding FXS vocalization abnormalities. The current study conducted a detailed analysis of USV syllable production and spectral properties in adult FXS mice following courtship separation.

Methods & Analysis

Housing and Care of Animals

Adult (2-3 month) male C57/B6 *fmr1* knockout (FXS) (n=10) and wildtype (WT) (n=10) mice were used. Mice from the same liter were housed together by gender in standard laboratory

conditions (12 hr-12 hr light/dark cycle with food and water provided *ad libitum*). All mice had prior exposure to the opposite sex before testing.

USV Recording

There were 3 main stages in the social encounter used to elicit and record USVs: Habituation, Interaction and Removal. The Habituation step consisted of introducing the male mouse to the testing chamber for 5 minutes to minimize stressors from a novel environment. The Interaction step involved introducing a randomly assigned receptive female mouse into the testing chamber. The male and female were allowed to interact for up to one minute, or until the male mouse mounted the female. If mounting occurred, the female was immediately removed. The final stage, Removal, occurred immediately upon removing the female from the testing chamber. Male mice were left in the testing chamber without the female for 2 minutes before returning to their home cage. USVs were only recorded during the Removal stage to ensure no female vocalizations were recorded.

All social encounters and USV recordings were performed in a testing chamber (7”x11”x5”) placed inside a larger sound attenuating chamber. An ultrasonic microphone (UltraSoundGate CM16/CMPA, Avisoft Bioacoustics) with a relatively flat frequency response (< 3 dB variability) up to 130 kHz was suspended 2 inches above the top of the testing chamber. The acoustic signal from the microphone was digitized at 375 kHz, 16 bits (UltraSoundGate 416H, Avisoft Bioacoustics) and saved as a wav file (Avisoft-RECORDER, Avisoft Bioacoustics) for later analysis.

Courtship Behavior

Each social encounter was video recorded for later offline assessment of courtship behavior. The videos were hand scored for courtship behaviors (total time until first mount; time to first interaction; interaction occurrences and time; percent time interacting; duration of time not interacting; and percent time not interacting) (Rotschafer et al., 2012).

USV Examination

The audio recordings from the Removal stage were processed and analyzed for USVs using a custom MATLAB program written by Holy and Guo (2005). First, spectrograms were created with a 512 FFT-length and 50% frame overlap, then bandpass filtered to remove sounds below 25 kHz and above 110 kHz. Background noise was removed with an intensity threshold. Potential USV syllables were automatically identified and extracted based on mean frequency, spectral purity, and spectral discontinuity of neighboring spectrogram bins (see Holy 2005 for details). Next, these extracted sounds were identified as a USV syllable if they had a minimum duration of 5 ms, a spectral purity of 0.25 (at least 25% of the power in a single frequency, consistent with the narrow-band whistle of USVs vs. the broad-band noise associated with movement), and a spectral discontinuity of less than one, indicating a frequency change within the range previously reported for USV syllables frequency modulation.

Frequency and temporal acoustic parameters of each extracted USVs were automatically calculated. From the frequency contour, average peak frequency (the frequency which had the most power), mean frequency, maximum frequency, minimum frequency, frequency bandwidth, and the difference between the starting and ending frequencies were extracted. Additionally, overall duration of each USV as well as the time between USVs was calculated. Bout analysis was conducted utilizing the time between USVs. Bouts were defined as a series of calls separated

by a 4 standard deviation change from the mean time between WT USVs, resulting in a value of ~ 1 second.

Additionally, Holy et al. have shown that male USVs in response to female separation exhibit a song-like characteristic (Fig. 4.1) that can be classified into three defined syllables (h, d, & u) based on an abrupt jumps between low (35-50 kHz) and high (70-90 kHz) frequencies. The syllable "h" is a jump to a high frequency, "d" is a downward jump to a low frequency, and "u" is an upward jump from a low frequency (Holy and Guo, 2005). Note, the MATLAB code for isolating and classifying USVs into these three defined syllables and the subsequent syllable analyses are provided in Holy et al. (2005). A single USV could be comprised of a single syllable or of multiple syllables (phrase). Syllables that ended and began within 30 ms of each other were considered to be part of a single phrase (Fig. 4.1c). Those USVs that did not meet the classification for a pre-determined syllable (referred to as "remainder" by Holy) were further classified based upon Zampieri et al (2014) into one of the following (Fig. 4.1a): short (<10 ms), flat (<5kHz modulation), upswing (increasing in frequency over the course of the USV), downswing (decreasing in frequency over the course of the USV), chevron/hill (a frequency increase then decrease in a symmetrical pattern with a starting and ending frequency within 5 kHz), U (a frequency decrease then increase in a symmetrical pattern with a starting and ending frequency within 5 kHz), and finally unclassified.

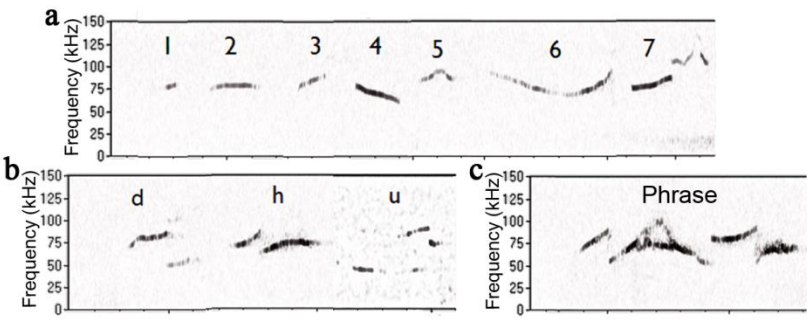

Figure 4.1. Spectrogram representations of analyzed USVs. a. Representative SS calls [1 = short (<10 ms); 2 = flat (<5kHz modulation); 3 = upswing (increasing in frequency over the course of the USV); 4 = downswing (decreasing in frequency over the course of the USV); 5 = hill/chevron (a frequency increase then decrease in a symmetrical pattern with a starting and ending frequency within 5 kHz); 6 = U (a frequency decrease then increase in a symmetrical pattern with a starting and ending frequency within 5 kHz); & 7 = unclassified]. b. Representative Syllable calls [based on an abrupt jumps between low (35-50 kHz) and high (70-90 kHz) frequencies "d" = (a downward jump to a low frequency); "h" = (a jump to a high frequency); & "u" = (an upward jump from a low frequency). c. Representative Phrase. Phrases = vocalizations consisting of multiple syllables.

Statistical Analyses

All data collection and analyses were conducted using a blind procedure to eliminate experimenter bias. Statistical analyses were conducted using a mixed model ANOVA on SAS (http://www.sas.com/en_us/home.html) with genotype as a between subject factor and call properties such as time between calls or percent of a certain type of call as within subject factors.

Results

Courtship Characteristics

During the interaction phase, the courtship was recorded to explore any genotype specific differences in male/female interaction. There was no significant differences between FXS and WT mice in the total time to first mount, time to first interaction or number of interaction instances (Fig. 4.2a & 4.2c). However, the total time spent interacting [Fig. 4.2a Interaction ($F_{(1,11)}$=6.94;p<0.05)] and percent time interacting [Fig. 4.2b Interaction ($F_{(1,11)}$=9.63;p<0.05)] was significantly higher in FXS. Subsequently WT mice spent significantly more time not

interacting [Fig. 4.2a No Contact ($F_{(1,11)}$=9.52;p<0.05) & Fig. 4.2b No Contact ($F_{(1,11)}$=9.63;p<0.05)]. Note, percent time was assessed to normalize the specific behavior to the total amount of time each male mouse had with a female as this varied depending upon the time until first mount, when the female was removed.

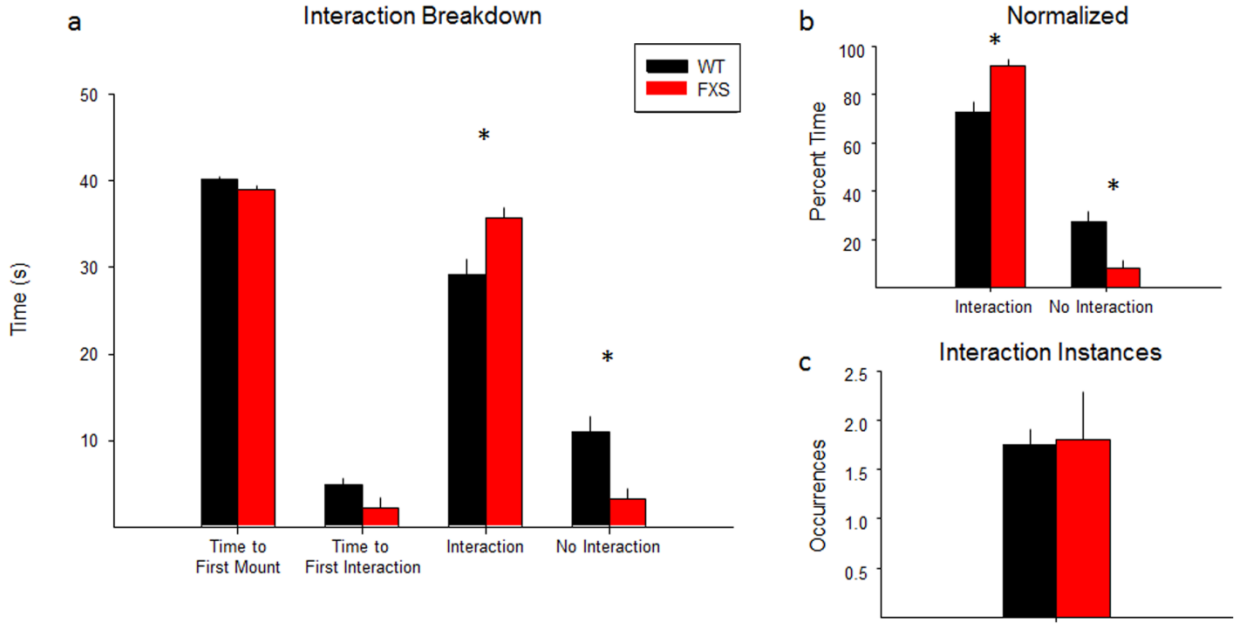

Figure 4.2. Fragile X male mice spend significantly more time interacting with the female mice. a. Raw time distribution of total time of courtship (Time to First Mount), time to first interaction (Time to First Interaction), amount of time the male mouse spent interacting with the female mouse (Interaction) and amount of time spent not interacting (No Interaction). FXS male mice spent significantly more time interacting with the females, and conversely, WT male mice spent significantly more time not interacting. b. The amount of time spent interacting or not interacting normalized to the total testing time [(Percent time = time spent interacting or not interacting / time to first mount) *100]. FXS male mice spent significantly more time interacting compared to their WT counterparts who spent significantly more time not interacting with the female. c. FXS male mice did not significantly differ in the number of times it interacted with the female (Interaction Instances). *<0.05

USV Characterization

Two WT mice, and three FXS mice were removed from the study for not producing vocalizations. FXS male mice did not exhibit any significant differences in the number of USVs

or in the frequency and temporal acoustic parameters (Fig. A1-4). Prior studies have demonstrated that FXS mice exhibit significantly fewer USVs in distinct bouts (Lai et al., 2014). In this study a bout was defined as "age-dependent minimum values in the distribution of the natural log of the [intercall interval]" (Lai et al., 2014). In our study we were unable to reliability define a bout using this criteria. Thus in an attempt to replicate these findings, a bout was defined as a series of calls being separated by a 4 standard deviation change from the mean time between WT USVs; however, no significant difference in the number of USVs per bout were detected (Fig. A5-6). Note there was also no significant difference in the mean time between USVs in FXS mice (Fig. A7-9).

Three FXS mice vocalized but did not exhibit syllables and thus were moved from the syllable analysis. Upon examination of the syllables, FXS mice were found to produce significantly more "u"s [Fig. 4.3c All "u" ($F_{(1,10)}$=7.85;p<0.05)] and more overall syllables which contained "u"s [Fig. 4.3c All USVs containing "u" ($F_{(1,10)}$=9.72;p<0.05)] compared to WT mice. FXS mice also exhibited significantly fewer isolated "h" syllables [Fig. 4.3b Isolated h ($F_{(1,10)}$=8.61;p<0.05)]. Upon examination of the spectral properties for each syllable it was determined that there were no differences in bandwidth or length for isolated "d" or "u" syllables; however, isolated "h" syllables were longer and had a greater bandwidth in FXS mice [Fig. 4.3e "h" Length ($F_{(1,10)}$=17.73;p<0.05) & Fig. 4.3h. "h" Bandwidth ($F_{(1,10)}$=6.13;p<0.05)]. Furthermore, there were no significant differences in the average peak, mean, or max frequencies for "d" and "u" syllables; however, FXS mice had a significantly higher average max frequency for "h" syllables [Fig. 4.3k Average Max ($F_{(1,10)}$=7.61;p<0.05)].

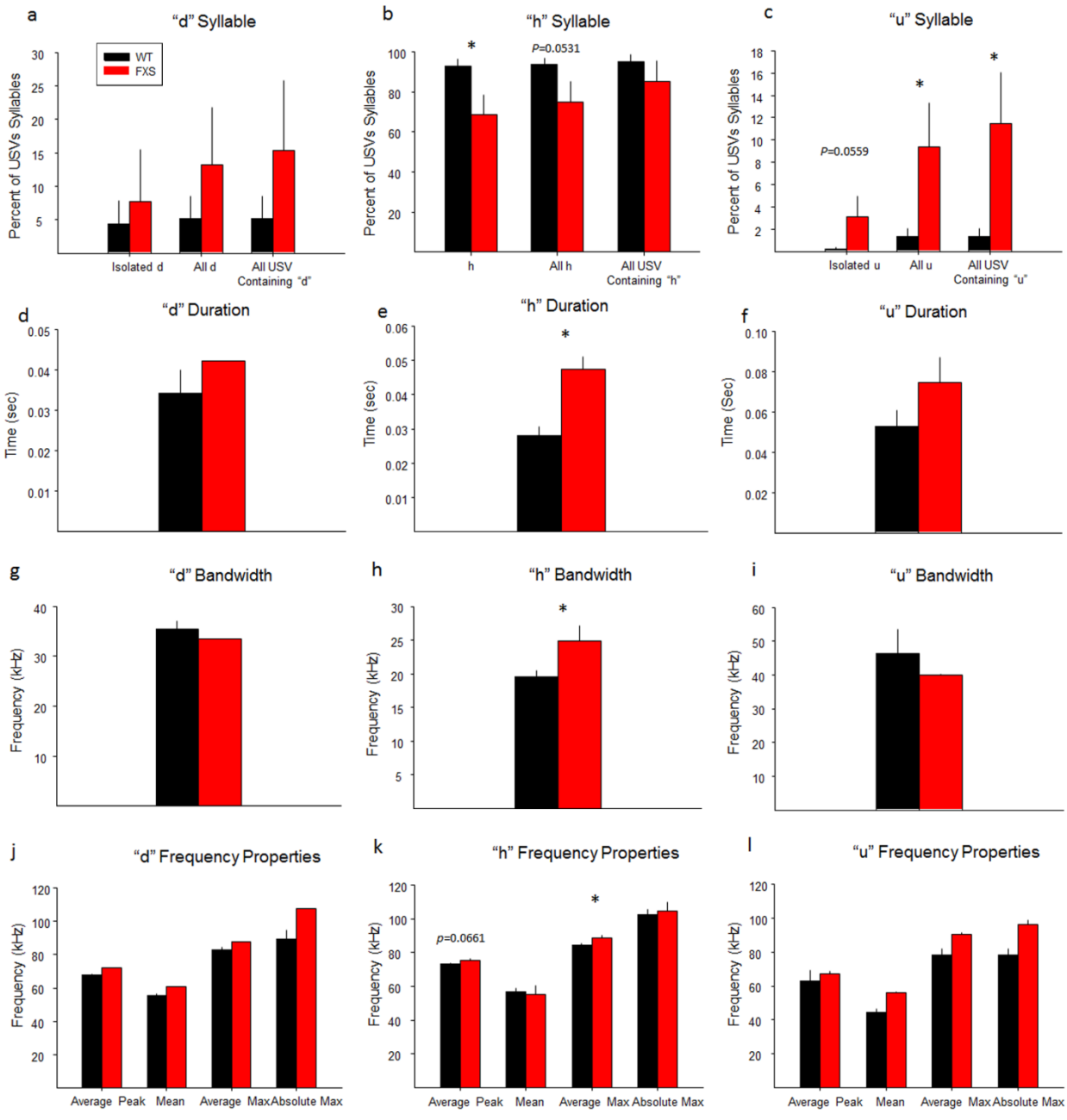

Figure 4.3. Occurrence rate and spectral properties for syllable production in Fragile X mice. a. Occurrence rate of "d" to total syllable production (isolated "d" = individual syllable; All "d" = all instances of syllable; All USV containing "d" = all USVs that contain syllable). b. Occurrence rate of "h" to total syllable production (see above for description of figure labeling). WT mice expressed more isolated "h" USVs compared to FXS mice and had a trend in expressing more "h" syllables in all calls. c. Occurrence rate of "u" to total syllable production (see above for description of figure labeling). FXS mice expressed more "u" syllables in all calls, utilized more "u"s in their calls, and had a trend to produce more isolated "u"s. d. Duration

Figure 4.3 (cont.): of isolated "d" syllables. e. Duration of isolated "h" syllables. FXS mice generated significantly longer isolated "h" syllables. f. Duration of isolated "u" syllables. g. Bandwidth (frequency range) of isolated "d" syllables. h. Bandwidth (frequency range) of isolated "h" syllables. FXS mice exhibited significantly larger frequency jumps with isolated "h" syllables. i. Bandwidth (frequency range) of isolated "u" syllables. j. General frequency properties of "d" syllables (average peak, mean, average max, and absolute max frequencies). k. General frequency properties of "h" syllables (average peak, mean, average max, and absolute max frequencies). FXS mice had significantly higher average max frequency and a trend towards a higher peak frequency with their "h" syllables. l. General frequency properties of "u" syllables (average peak, mean, average max, and absolute max frequencies). *<0.05

Interestingly, in addition to these individual syllable differences, FXS mice also generated more phrases and they were longer compared to their WT counterparts [Fig. 4.4a Syllable/Phrase Length ($F_{(1,10)}$=26.33;p<0.05) & Fig. 4.4b Percent of Phrases in USVs ($F_{(1,10)}$=8.22;p<0.05)]. FXS mice produced more phrases compared to individual syllables and within those phrases FXS mice exhibited more motifs [Fig. 4.4c Percent Syllable USVs which are Phrases ($F_{(1,10)}$=79.82;p<0.05) & Fig. 4.4d Percent Motifs in Phrases ($F_{(1,10)}$=9.73;p<0.05)]. This pattern of repeated vocalization is consistent with the repetitive, perseverative speech pattern observed in FXS patients (Herbst, 1980; Ferrier et al., 1991; Belser and Sudhalter, 2001).

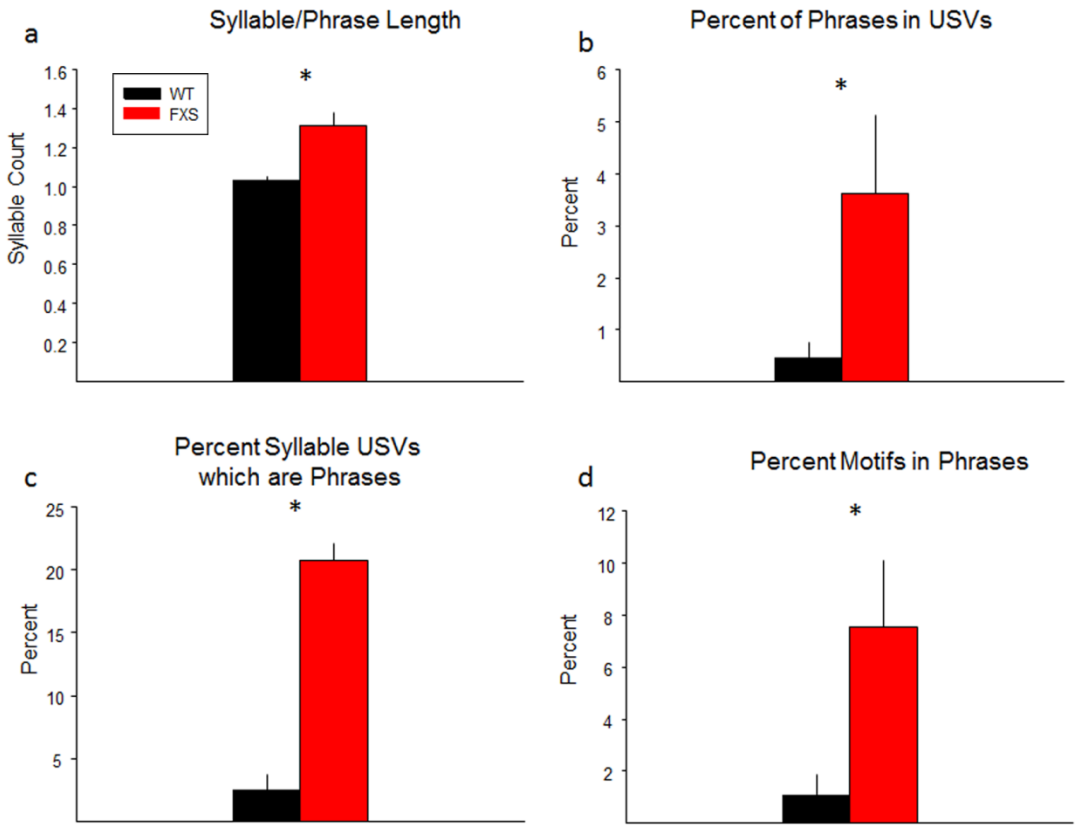

Figure 4.4. Fragile X mice exhibit more longer phrases than WT mice. a. The average number of syllables in USVs containing syllables. FXS mice produced USVs with a significantly greater number of syllables. b. The percent of phrases in all USVs. FXS mice exhibited significantly more phrases compared to WT mice. c. The percent of syllable USVs that are phrases. FXS mice had significantly more syllable USVs phrases. d. Motif occurrence in phrases. FXS mice had significantly more motifs in their phrases compare to their WT counterparts. *<0.05

A summary of the percent break down of each of these types can be found in Table 1. Finally, there were no significant differences observed in any of the SS USVs properties, except for the overall bandwidth in the Hill/Chevron calls, in which WT mice had significantly larger bandwidth compared to their FXS counterparts (Fig. A24 Hill/Chevron Bandwidth ($F_{(1,5)}$=8.47;p<0.05).

	WT	FXS
SS Short (1)	41.7 ± 5.73	40.9 ± 6.58
SS Flat (2)	3.6 ± 0.52	3.9 ± 0.42
SS Upswing (3)	5.4 ± 2.08	6.7 ± 0.90
SS Downswing (4)	0.4 ± 0.36	1.3 ± 0.81
SS Chevron/Hill (5)	0.2 ± 0.10	0.5 ± 0.34
SS U (6)	0.2 ± 0.09	0.1 ± 0.07
SS Unclassified (7)	33.9 ± 4.46	34.9 ± 3.61
h	13.9 ± 2.39	7.3 ± 3.13
d	0.2 ± 0.08	1.5 ± 1.48
u	0.1 ± 0.04	0.4 ± 0.38
Phrases	0.4 ± 0.31	2.2 ± 1.05 *

Table 4.1. Distribution of all USV classifications (average +/- SEM). No significant differences were seen in production of each classification between WT and FXS mice except for phrases. FXS male mice produced significantly more phrases than WT mice. *<0.05

Discussion

The current study demonstrated that adult FXS mice exhibit syllable vocalization abnormalities (longer phrases and more motifs) that are consistent with those observed in FXS patients (repetitive and perseverative speech), suggesting that FXS mice can be used to examine the underlying biological mechanism(s) and assess therapeutic interventions for FXS vocalization abnormalities. Although the syndrome is associated with many abnormalities, a prominent characteristic in fragile X patients that can dramatically affect learning and cognition are speech vocalization abnormalities (repetitive, cluttered and perseverative speech patterns) (Herbst, 1980; Ferrier et al., 1991; Belser and Sudhalter, 2001; Cornish et al., 2004). Until now FXS vocalization studies have been unable to characterize abnormalities that are consistent with those observed in FXS patients, thus hindering examination of the underlying cause for FXS vocalization deficits.

Consistent with human FXS studies demonstrating repetitive, perseverative speech patterns, our studies demonstrated that FXS mice exhibited increased number of repeated-syllable motifs. Interestingly, this increase was not consistent across all syllables. FXS mice

exhibited more “u” syllables, while WT mice exhibited more “h” syllables. The overall use of “u” in all syllables and phrases was significantly higher in FXS mice. This was noted by the increased number of USVs that contained “u” as well as an increased presence of “u” in phrases. It was also observed that FXS mice generated more isolated “u” syllables than WT, but not enough to reach significance. WT mice, on the other hand, generated more “h” syllables, as they vocalized significantly more isolated “h” syllables than FXS mice. There was also a tendency for WT mice to have more “h” syllables in their phrases, but this did not reach statistical significance. Studies have suggested that calls spanning 50 kHz (a major frequency component of syllables) results in a positive rewarding state in rodents (Burgdorf et al., 2011), suggesting that these syllables have a behavioral and biological significance. Unfortunately the behavioral and biological implications of vocalizing more of one syllable vs another, along with its relevance towards the human condition, is currently unknown. However, these studies demonstrate that FXS mice exhibit syllable vocalization abnormalities consistent with those observed in FXS patients, indicating that they may be a viable model for studying repetitive vocalization abnormalities in FXS.

Consistent with human FXS studies demonstrating repetitive, perseverative speech patterns, our studies demonstrated that FXS mice exhibited increased number of repeated-syllable motifs. Interestingly, this increase was not consistent across all syllables. FXS mice exhibited more “u” syllables, while WT mice exhibited more “h” syllables. The overall use of “u” in all syllables and phrases was significantly higher in FXS mice. This was noted by the increased number of USVs that contained “u” as well as an increased presence of “u” in phrases. It was also observed that FXS mice generated more isolated “u” syllables than WT, but not enough to reach significance. WT mice, on the other hand, generated more “h” syllables, as they

vocalized significantly more isolated “h” syllables than FXS mice. There was also a tendency for WT mice to have more “h” syllables in their phrases, but this did not reach statistical significance. Studies have suggested that calls spanning 50 kHz (a major frequency component of syllables) results in a positive rewarding state in rodents (Burgdorf et al., 2011), suggesting that these syllables have a behavioral and biological significance. Unfortunately the behavioral and biological implications of vocalizing more of one syllable vs another, along with its relevance towards the human condition, is currently unknown. However, these studies demonstrate that FXS mice exhibit syllable vocalization abnormalities consistent with those observed in FXS patients, indicating that they may be a viable model for studying repetitive vocalization abnormalities in FXS.

Although the neuroanatomical brain regions/mechanism mediating rodent vocalization patterns are not fully understood, imaging and tracing studies have begun to delineate some critical brain regions and neuronal pathways. Vocalizing in mice and not auditory stimulation has been shown to increase immediate early gene activation in primary motor cortex, premotor cortex, anterior cingulate cortex and anterodorsal striatum (Arriaga et al., 2012). Tracing studies have further demonstrated projections from the cricothyroid and laryngeal muscles to the vocalizing-activated region in primary motor cortex. Subsequent tracing analyses demonstrated that this region of primary motor cortex also projects directly to the brainstem nucleus ambiguus (Arriaga et al., 2012). In mammals the brainstem nucleus ambiguus directly innervates the larynx and when lesioned abolishes the animals ability to vocalize (Kirzinger and Jurgens, 1985; Jurgens, 1998; Floody and DeBold, 2004; Jurgens and Ehrenreich, 2007). For a detailed discussion of mouse vocalization patterns, neuroanatomical connections and possible homology to vocalization regions in song birds and humans see (Arriaga and Jarvis, 2013).

Although studies have not specifically examined FXS neuronal abnormalities in response to vocalization properties in the motor cortical, limbic, and striatal regions mentioned above, studies have characterized some FXS abnormalities in these brain regions that could contribute towards abnormal vocalization patterns. At a gross anatomical level, the caudate has been shown to be enlarged in FXS (Gothelf et al., 2008; Hallahan et al., 2011; Hazlett et al., 2012), suggesting underlying neuronal abnormalities. Likewise, the primary motor cortex, consistent with other brain regions previously studied (Irwin et al., 2002; Galvez and Greenough, 2005), has been shown to exhibit increased dendritic spine proliferation and elimination (Padmashri et al., 2013). Furthermore, FXS mice exhibit disrupted learning-induced changes in LTP in the motor cortex (Padmashri et al., 2013) and impaired pre-synaptic LTP in anterior cingulate cortex (Koga et al., 2015). Although it is difficult to speculate how these abnormalities can result in the observed FXS repetitive vocalization, these studies demonstrate that brain regions known to mediate rodent vocalizations exhibit many neuronal and biochemical abnormalities in FXS. In further support of a role for FMRP in proper vocal production the avian ortholog to FMRP (TGuFmr1) has been shown to be upregulated in prominent song nuclei of the male zebra finch brain immediately prior to song learning (Winograd et al., 2008). These studies collectively suggest that FMRP plays a critical role in vocalization and when absent, results in various abnormalities that could disrupt that process resulting in the observed FXS syllable abnormalities.

Although this study is the first to examine syllable production in FXS mice, prior studies have looked at other vocalization properties. For example, studies utilizing maternal separation to generate vocalizations have demonstrated that USV production rate was significantly increased in FXS mice; however, this was shown to only occur at PND 7 (Lai et al., 2014).

Contrary to these findings, Rotschafer et al., (2012) demonstrated that FXS mice exhibit a reduced vocalization rate during courtship compared to WT mice. Interestingly, it has recently been shown that both males and females undergo interaction-induced USVs during courtship behavior (Neunuebel et al., 2015). Thus, it is difficult to determine if the reduced vocalization rate from Rotschafer et al., (2012) is due to FXS vocalization abnormalities, differences in interaction-induced female vocalizations or a combination of both. In support of there being differences in the courtship behavior, our study demonstrated that FXS mice spent significantly more time interacting with the female than controls (Fig. 4.2). Unfortunately we are unable to determine if this is due to FXS increased hyperactivity (Bakker et al., 1994) or a consequence of not being able to properly communicate. To control for possible differences during courtship altering vocalization patterns, USVs were only examined after the female was removed. Interestingly, after removing the female we did not detect a significant difference in the vocalization rate in FXS mice (Fig. A11), suggesting that the decreased vocalization rate observed in Rotschafer et al was due to abnormalities in communication and not an inability to vocalize. Furthermore, these findings, along with prior studies suggesting that mouse syllable vocalizations have a behavioral significance (Burgdorf et al., 2011), suggest that our observed repetitive syllable production in FXS hinders effective communication and is an underlying cause for FXS decreased vocalization during courtship (Rotschafer et al., 2012).

Abnormalities in vocalization production are a prevalent disorder that exists in various types of ASD including FXS. Difficulties in speech production can often have dramatic effects on both social and cognitive development. Although many mouse models of ASD have demonstrated vocalization abnormalities such as decreased USVs production, FXS mice have not reliably been shown to exhibit vocalization abnormalities that are consistent with those observed

in FXS patients such as repetitive, cluttered and perseverative speech patterns (Borghgraef et al., 1987; Jamain et al., 2008; Radyushkin et al., 2009; Gaub et al., 2010; Kurz et al., 2010; Wohr et al., 2011). The current study demonstrated that adult FXS mice exhibit a repetitive USV syllable production that is consistent with that observed in FXS patients. These findings further strengthen the neuroethological relevance of FXS mice and suggest that examination of perseverative syllable production can be used in future analyses of FXS mice vocalization abnormalities. Furthermore, the current study provides a means for future investigations into the underlying biological mechanism(s) mediating FXS repetitive speech patterns.

CHAPTER 5: BLOCKING ELEVATED VEGF-A ALTERS A MYRIAD OF PHENOTYPICAL CHARACTERISTICS OF FRAGILE X MICE

Abstract

Fragile X Syndrome (FXS) is the most common form of single gene inherited mental retardation. We have recently demonstrated that Vascular Endothelial Growth Factor A (VEGF-A) is not only elevated in FXS mice, but its modulation can lead to molecular and behavioral rescue of some FXS abnormalities (Belagodu et al., 2017). These findings suggest that VEGF-A modulation can be used to alleviate FXS abnormalities. This study set out to determine the extent in which blocking VEGF–A can alleviate many well established behavioral FXS phenotypes such as locomotor activity, anxiety-like behavior, stereotypy, and USV deficits. The current study found, consistent with those from other studies, that FXS mice exhibit increased locomotor activity and hyperactivity, reduced anxiety-like behavior, increased stereotypy, and increased production of phrases and motifs in USV profiles. Interestingly, blocking VEGF-A with Bevacizumab was found to not alleviate any of these deficits. Although these findings are disappointing, they are not surprising given our prior analyses of hyperactivity following Bevacizumab treatment, in which the increased hyperactivity in FXS was unaltered with Bevacizumab treatment. Many of the measures of anxiety-like behavior and stereotypy can be influenced/driven by hyperactivity and thus would be unaltered with this type of intervention. Interestingly, blocking VEGF-A did not have a drug treatment effect on USV production profiles (Belagodu et al., 2016). Rather much to our surprise both Saline and Bevacizumab alleviated FXS USV abnormalities. These findings suggest that this vocalization deficit could be altered through handling and warrants further exploration into the neuronal mechanism mediating USV production in mice. Overall, these findings, along with our prior studies, demonstrate that

blocking VEGF-A has beneficial effects on specific FXS abnormalities, and that further exploration into the specific types of behaviors that can be alleviated along with optimization of drug dosage will be needed.

Introduction

Fragile X Syndrome (FXS) is the leading cause of inherited genetic autism spectrum disorder with higher incidence rates in males (1:3600) than females (1:8000) (Cornish et al., 2008). The transcriptional silencing of *FMR1*, the gene which encodes the Fragile X Mental Retardation Protein (FMRP) is known to be the primary cause of FXS (Pieretti et al., 1991; Verkerk et al., 1991); however, its exact mode of action in mediating behavioral and anatomical abnormalities are not well understood. A prevailing theory on changes induced by the lack of FMRP is the unregulated activation of metabotropic glutamate receptor (mGluR) downstream components, such as the mammalian target of rapamycin (mTORC1) (Bear et al., 2004; Sharma et al., 2010; Hoeffer et al., 2012). mTORC1 plays a critical role in regulating levels of numerous downstream proteins. One of these proteins of interest is vascular endothelial growth factor A (VEGF-A). We have previously shown that VEGF-A, under the regulation of mTORC1, exhibits elevated brain expression in FXS (Belagodu et al., 2017).

VEGF-A has historically been classified as a prominent regulator of vascular growth with increased expression being synonymous with increased vasculature (Neufeld et al., 1999). Consistent with these findings FXS patients have been shown to exhibit blood profusion abnormalities (Balci et al., 2006; Kabakus et al., 2006) and our findings have shown that adult FXS mice have increased vasculature (Galvan and Galvez, 2012). Interestingly, in addition to modulating vasculature, recent studies have demonstrated that VEGF-A can alter many neuronal properties. Treatment with VEGF-A has yielded neuroprotective properties, by increasing overall

survival rates of nerve cells in the CNS and Schwann cells in the PNS (Sondell et al., 1999), as well as increasing neurogenesis in the dentate gyrus (Jin et al., 2002). This is mirrored in FXS, with increased proliferation rate of sertoli cells (Hagerman and Hagerman, 2003) and BrdU positive cells in the dentate gyrus of the hippocampus (Jin et al., 2002). Furthermore, VEGF stimulation has led to axonal outgrowth and increased neurite outgrowth and branching (Jin et al., 2006) with one of its receptors (VEGFR2) being found on axonal growth cones (Sondell et al., 1999; Sondell et al., 2000) and dendritic synapses (De Rossi et al., 2016). Interestingly, the FXS *Drosophila* model exhibits excessive axonal growth in length and arborization complexity (Pan et al., 2004). Furthermore, FXS has been shown to result in increased number of dendritic spines due to excessive spine proliferation and turn over (Pan et al., 2010). This collectively suggests that VEGF-A plays a critical role in neuronal properties, and could potentially be a venue for alleviating FXS neuronal abnormalities.

To better understand the potential role for VEGF-A in mediating FXS abnormalities, our subsequent studies explored the beneficial effects of blocking VEGF-A binding to its receptor. Using the anti-cancer medication Bevacizumab (Genentech), a humanized monoclonal antibody (Lu et al., 2012; Walker et al., 2012), we were able to reduce VEGF-A levels in FXS brain to those observed in control mice (Belagodu et al., 2017). More importantly, this same drug treatment alleviated FXS macroorchidism and reduced Synapsin-1 brain expression, a marker for synapse density (Sudhof et al., 1989; Cesca et al., 2010), to control levels. To explore the beneficial behavioral effects of blocking VEGF-A, Bevacizumab treated mice were then assessed on Novel Object Recognition. Novel Object Recognition is a cognitive learning task that has been shown to be sensitive to FXS, resulting in impaired performance. Our behavioral analyses

demonstrated that blocking VEGF-A binding to its receptor was able to alleviate the FXS cognitive impairment observed with Novel Object Recognition.

These initial studies exploring the effects of blocking VEGF-A binding on FXS behavioral abnormalities have been very promising; however, the full implications of VEGF-A modulation on FXS abnormalities are still unknown. The following study set out to assess the effect of blocking VEGF-A on various behavioral abnormalities commonly associated with FXS. Specifically, the follow study set out to examine measures of anxiety (Hagerman and Hagerman, 2003; Cordeiro et al., 2011; Bailey et al., 2012), repetitive behaviors such as self-grooming (McNaughton et al., 2008; Pietropaolo et al., 2011) and marble bury (Spencer et al., 2011; Veeraragavan et al., 2012; Gholizadeh et al., 2014), and vocalization deficits (Rotschafer et al., 2012). We have recently shown that FXS mice exhibit ultrasonic vocalizations deficits consistent with abnormalities observed in patients (Belagodu et al., 2016). Through such a wide spectrum analysis of the effects of VEGF-A modulation on FXS abnormalities, the following study will provide a better assessment of the potential benefits of VEGF-A modulation for therapeutic interventions.

Methods & Analysis

Housing and Care of Animals

Adult (PND 60) male C57/B6 *FMR1* knockout (FXS) and wildtype (WT) mice were used. Mice were housed in standard laboratory conditions (12 hr-12 hr light/dark cycle with food and water provided *ad libitum*).

Blocking VEGF-A

Based upon our prior study exploring the beneficial effects of VEGF-A modulation on FXS abnormalities (Belagodu et al., 2017), FXS (n=30) and WT (n=39) mice were given 5

mg/kg Bevacizumab or Saline IP every other day for 10 days. Prior to and following drug treatment various behavioral assessments outlined below were conducted.

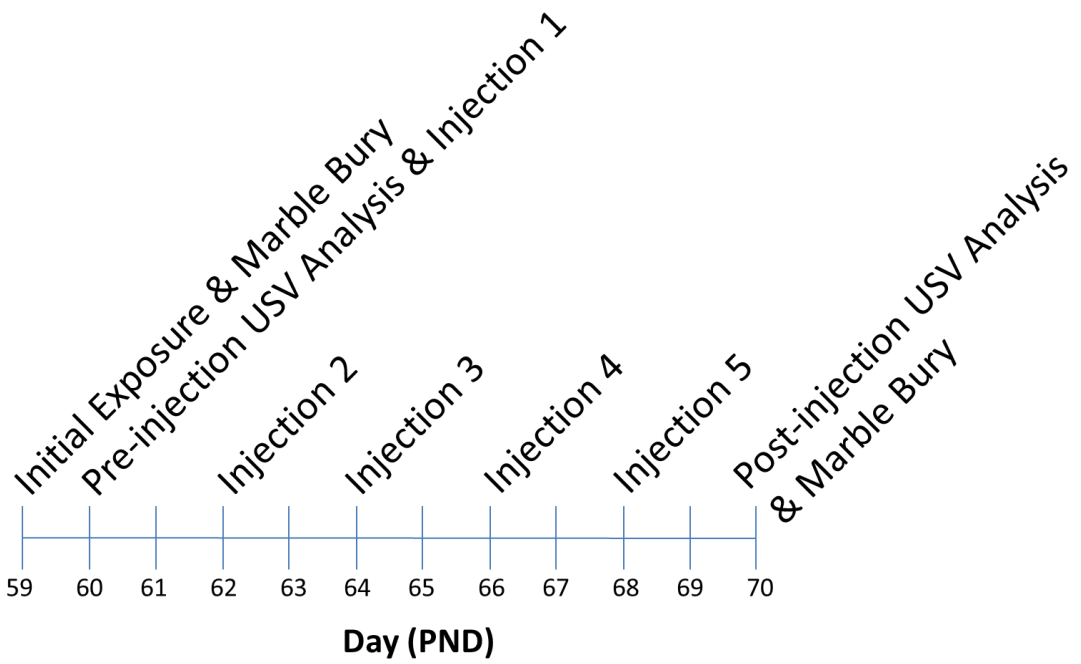

Figure 5.1: Schematic of injection scheme with time points (PND) for each behavioral assessment. Note, anxiety assessments were conducted on PND 69 mice from our prior study (Belagodu et al., 2017), that were treated starting on PND 60 as outlined above but did not receive any pre-injection treatments.

Open Field Assessment

To assess anxiety a modified Open Field assessment was used. Upon placing the mouse into a novel cage for 10 min the time spent in the center (Center 50%), edges, corners, crossings into center area, and the amount of time immobile in each of the aforementioned areas were assessed via Anymaze (v4.98) (Ennaceur, 2014). FXS mice have been observed to travel increased distances as well as spend more time mobile compared to their WT counterparts. Furthermore, FXS mice typically traverse a greater ratio of distance in the center region to total distance traveled compared to their WT counterparts, suggesting decreased anxiety-like behavior (Peier et al., 2000; Spencer et al., 2005).

Marble Bury Assessment

Marble Bury, a well-established paradigm of repetitive (stereotypy) behavior (Thomas et al., 2009), was used to explore the extent of benefits that Bevacizumab treatment can provide. This paradigm has been extensively used in studying repetitive behavior in autism models (Hoeffer et al., 2008; Jamain et al., 2008). Furthermore, studies in FXS mice have shown increases in the number of marbles buried compared to their WT counterparts (Spencer et al., 2011; Veeraragavan et al., 2012; Gholizadeh et al., 2014). To assess this stereotypic behavior, a modified protocol from (Deacon, 2006) was used. Briefly, mice were placed in a new cage consisting of 5 cm of woodchip bedding and 15 evenly spaced (at least 1 inch apart) glass marbles for 30 minutes. The mice were then removed, and the number of marbles buried was assessed. Marbles were considered fully buried if they were more than 50% covered. The Marble Bury Assessment was conducted prior to injections with a follow up test following drug treatment to obtain a within subject assessment.

USV Analysis

All social encounters and USV recordings were performed in a testing chamber (7"x11"x5") placed inside a larger sound attenuating chamber. An ultrasonic microphone (UltraSoundGate CM16/CMPA, Avisoft Bioacoustics) with a relatively flat frequency response (< 3 dB variability) up to 130 kHz was suspended 2 inches above the top of the testing chamber. The acoustic signal from the microphone was digitized at 375 kHz, 16 bits (UltraSoundGate 416H, Avisoft Bioacoustics) and saved as a wav file (Avisoft-RECORDER, Avisoft Bioacoustics) for later analysis.

All mice had prior exposure to the opposite sex. Following drug treatment, there were 3 main stages used to elicit and record USVs: Habituation, Interaction and Removal. The

Habituation step consisted of introducing the male mouse to the testing chamber for 2 minutes to minimize stressors from the novel environment. The Interaction step involved introducing a randomly assigned receptive female mouse into the testing chamber. The male and female mice were allowed to interact for up to one minute, or until mounting of the female occurred. The final stage, Removal, occurred immediately upon removing the female mouse from the testing chamber. Male mice were left in the testing chamber without the female for 10 minutes before returning to their home cage. USVs were only recorded during the Removal stage to ensure no female vocalizations were recorded.

USV Examination

Audio recordings from the Removal stage were processed and analyzed for USVs using the previously described custom MATLAB program (Belagodu et al., 2016). Spectrograms were created with a 512 FFT-length and 50% frame overlap, then bandpass filtered to remove sounds below 25 kHz and above 110 kHz. Background noise was then removed with an intensity threshold. Potential USV syllables were automatically identified and extracted based on mean frequency, spectral purity, and spectral discontinuity of neighboring spectrogram bins. These extracted USVs were identified as a syllable/phrase if they had a minimum duration of 5 ms, a spectral purity of 0.25 (at least 25% of the power in a single frequency, consistent with the narrow-band whistle of USVs vs. the broad-band noise associated with movement), and a spectral discontinuity of less than one, indicating a frequency change within the range previously reported for USV syllable frequency modulation. Those USVs that did not meet the classification for a pre-determined syllable referred to as "remainder" (Holy and Guo, 2005) were lumped into a miscellaneous category as our previous analysis showed no significant differences in any of the other mentioned categories previously listed (Belagodu et al., 2016).

Statistical Analysis

All data collection and analyses were conducted using a blind procedure to eliminate experimenter bias. Statistical analyses were conducted using a mixed model ANOVA on SAS (http://www.sas.com/en_us/home.html) with genotype as a between subject factor and behavioral assessments prior to and following drug treatments as within subject factors. For USV analyses the time between calls or percent of a certain type of call were also treated as within subject factors.

Results

Open Field Assessment

FXS and WT mice were assessed for general locomotor activity and anxiety-like behavior via an Open Field Paradigm. Consistent with previous studies (Peier et al., 2000; Spencer et al., 2005), FXS mice were found to exhibit increased distance traveled [Fig. 5.2a; $F_{(1,28)}=9.26$; $p<0.005$], average velocity [Fig. 5.2b; $F_{(1,28)}=9.54$; $p<0.005$], percent time mobile [Fig. 5.2c; $F_{(1,28)}=9.82$; $p<0.005$] and immobile [Fig. 5.2e; $F_{(1,28)}=9.83$; $p<0.005$], and bouts of mobility [Fig. 5.2d; $F_{(1,28)}=4.91$; $p<0.005$] and immobility [Fig. 5.2f; $F_{(1,28)}=4.89$; $p<0.005$]. FXS mice display increased distance traveled, velocity, and percent time mobile which are all indicative metrics of hyperactivity. FXS mice also had lower mobility bouts, but traveled a greater distance at a higher speed, suggesting that each instance of mobility consisted of greater locomotion than their WT counterparts. Furthermore, the aforementioned measures of increased motion suggested reduced anxiety and increased exploratory behavior. To further support this, FXS mice also spent a decreased amount of time immobile, with decreased bouts of immobility than their WT counterparts. Addressing stereotypy behavior from the Open Field Paradigm,

FXS had an increased amount of rotations [Fig. 5.2g; $F_{(1,26)}=6.08$; $p<0.005$], an indication of stereotypy behavior (Dolan et al., 2013), than their WT counterparts.

Figure 5.2. Open Field Assessment

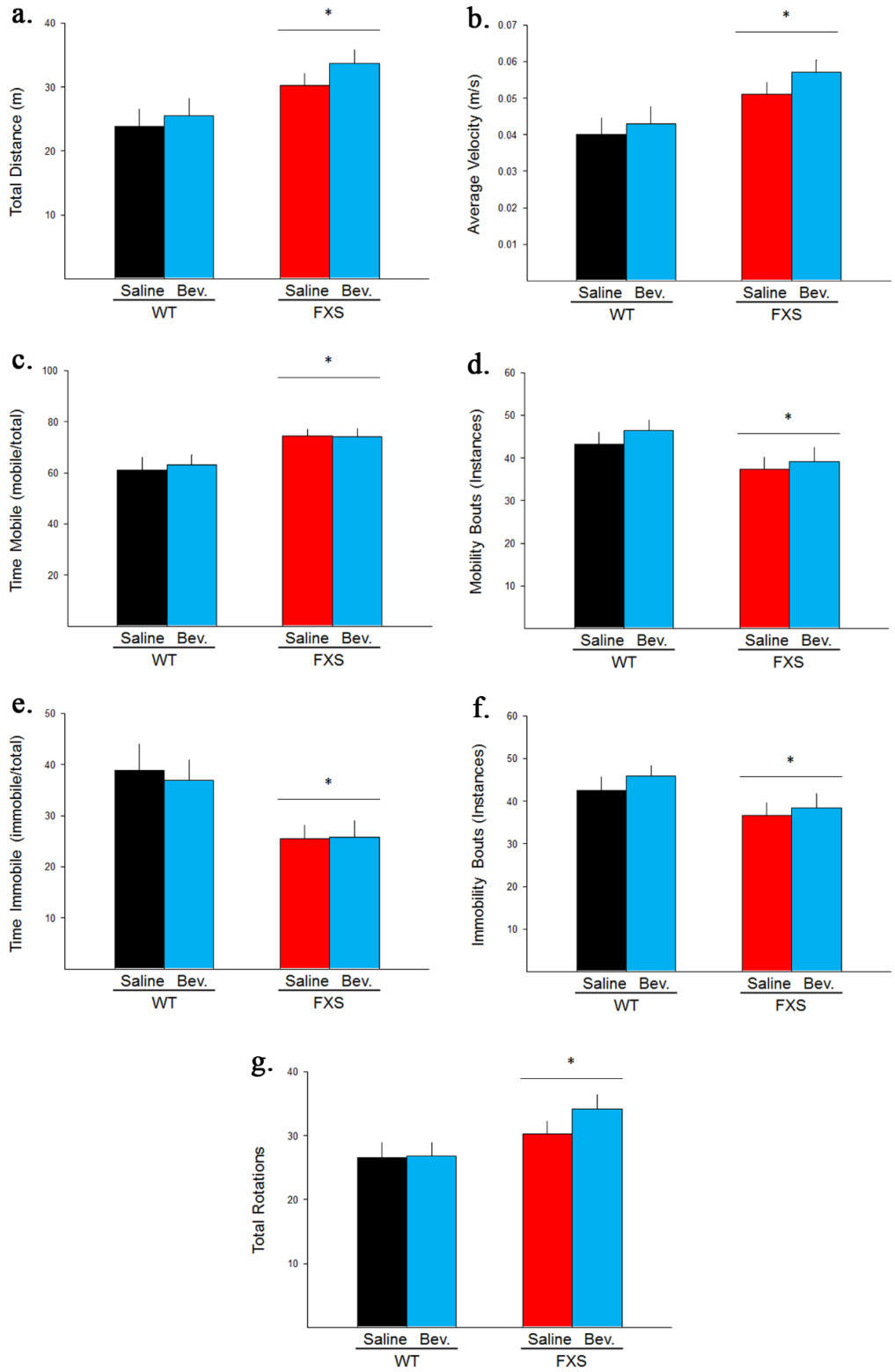

Figure 5.2 (cont.). Open Field Assessment metrics for locomotion (a.-d.), anxiety-like (c.-f.), and stereotypy behavior (g.) comparing WT vs FXS mice treated with Bevacizumab or Saline. Treatment yielded no effect in all metrics for either group. a. Total distance traversed in the training chamber. FXS mice had significantly more movement than WT mice. b. Average velocity of movement during the habituation stage. FXS mice had significantly faster movement than WT mice. c. Percent time in which the mice were mobile during the habituation stage. FXS mice were mobile for a significantly greater amount of time than WT mice. d. Mobility bouts during the habituation stage. FXS mice had significantly fewer instances where they began moving from rest than WT mice. e. Percent time in which the mice were immobile during the habituation stage. FXS mice were immobile for a significantly shorter amount of time than WT mice. f. Immobility bouts during the habituation stage. FXS mice had significantly fewer number of instances when they were immobile than WT mice. g. Total rotations of the mouse during the habituation stage. FXS mice rotated significantly more than WT mice. Bevacizumab = Bev. *<0.05.

Interestingly, anxiety-like behavioral effects in FXS mice were more pronounced in the first two minutes of the Open Field Paradigm, particularly with a decrease in the number of crossings into the center region [Fig. 5.3a; $F_{(1,59)}$=4.91; p<0.005], time spent in the center region [Fig. 5.3b; $F_{(1,59)}$=6.61; p<0.005], distance traveled in the center region [Fig. 5.3a; $F_{(1,59)}$=4.56; p<0.005], and finally the maximum instance in the center region [Fig. 5.3a; $F_{(1,59)}$=5.73; p<0.005]. A decrease in these metrics are indicative of increased exploratory behavior and reduced anxiety in mice (Peier et al., 2000; Spencer et al., 2005). Ultimately, there were no significant effects of Bevacizumab treatment on any of the aforementioned behavioral measures, suggesting that blocking VEGF-A does not alter hyperactivity or anxiety levels in FXS mice during the entire paradigm or during the initial two minutes in which the measures were more pronounced between FXS and WT Saline mice.

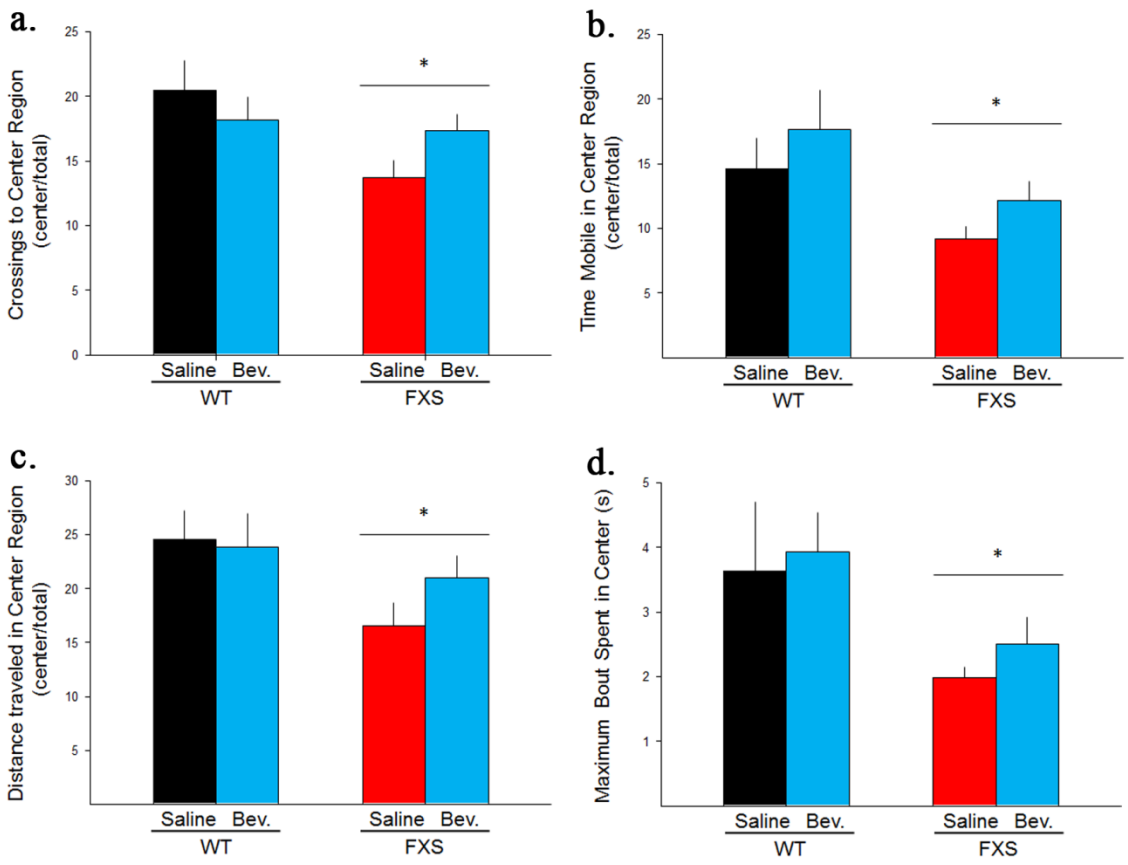

Figure 5.3. Open Field Assessment Center Region metrics for anxiety-like behavior per minute for the first two minutes of the paradigm comparing WT vs FXS mice treated with Bevacizumab or Saline. Treatment yielded no effect in any metrics for either group. a. Crossings to/from the center region. FXS mice had significantly fewer crossings to the center region compared to WT mice. b. Time in which the mice were mobile in the center region. FXS mice were mobile in the center region for a significantly shorter amount of time than WT mice. c. Total distance traversed in the center region. FXS mice had significantly less movement in the center region than WT mice. d. Maximum length of a bout spent in the center region. FXS mice maximum time moving in the center region was significantly lower than WT mice. Bevacizumab = Bev. *<0.05.

Marble Bury Assessment

Stereotypy behavior was further assess via Marble Bury, a prevailing phenotype in autism rodent models (Hoeffer et al., 2008; Jamain et al., 2008). Consistent with previous studies, FXS mice exhibited significantly increased burrowing behavior, resulting in an increased percentage (%) of marbles buried [Fig. 5.4; $F_{(2,80)}=2.79$; $p<0.005$] (Spencer et al., 2011; Veeraragavan et al., 2012; Gholizadeh et al., 2014). Unfortunately, Bevacizumab treatment did

not alleviate this difference in FXS mice. Interestingly, post-hoc analyses of post treatment groups (FXS/WT Saline/Bevacizumab) failed to detect a significant difference between groups [Fig. 5.4; $F_{(2,80)}$=1.63; p=0.2021]. These findings suggest that ten days of interacting with and treating FXS mice (Saline or Bevacizumab) impaired detection of the Marble Burying deficit. This is further discussed in the proceeding discussion below.

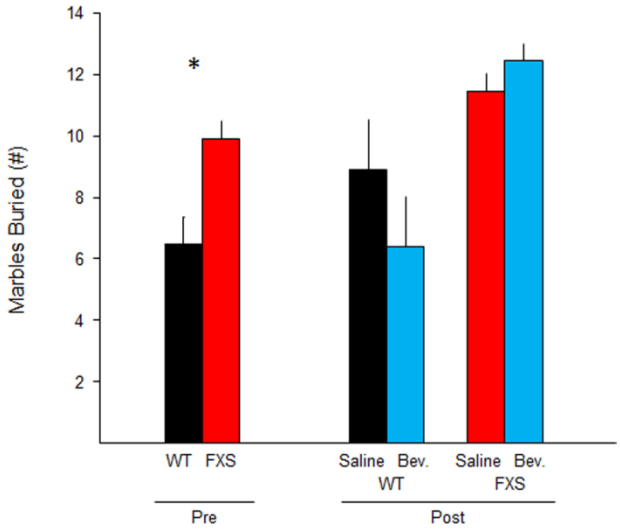

Figure 5.4. Marble burying behavior was not altered with 10 days of Bevacizumab treatment. FXS mice naturally bury more marbles than WT mice; however, Bevacizumab did not significantly alter the number of marbles buried for either group. Bevacizumab = Bev. *<0.05.

USV Examination

Examination of courtship induced vocalizations with Bevacizumab treatment yielded intriguing results. Our previous study demonstrated that sexually naïve FXS mice exhibited more syllables (frequency modulated vocalizations) (Holy and Guo, 2005) and a higher incidence of these syllables in phrases (vocalizations containing multiple syllables) (Belagodu et al., 2016). Consistent with these findings, the pre-treatment analyses demonstrated that FXS sexually experienced mice exhibited significantly increased percentage of syllables [Fig. 5.5a; $F_{(1,21)}$=5.63; p<0.005] and phrases [Fig. 5.5b; $F_{(2,40)}$=3.42; p<0.005]. FXS mice also exhibited a trend to produce longer phrases with more syllable units [Fig. 5.5c; $F_{(2,40)}$=3.41; p<0.005] and an

increase (~112%) in phrases with repeated syllable units (motifs) [Fig. 5.5d; $F_{(1,19)}$=4.84; p<0.005].

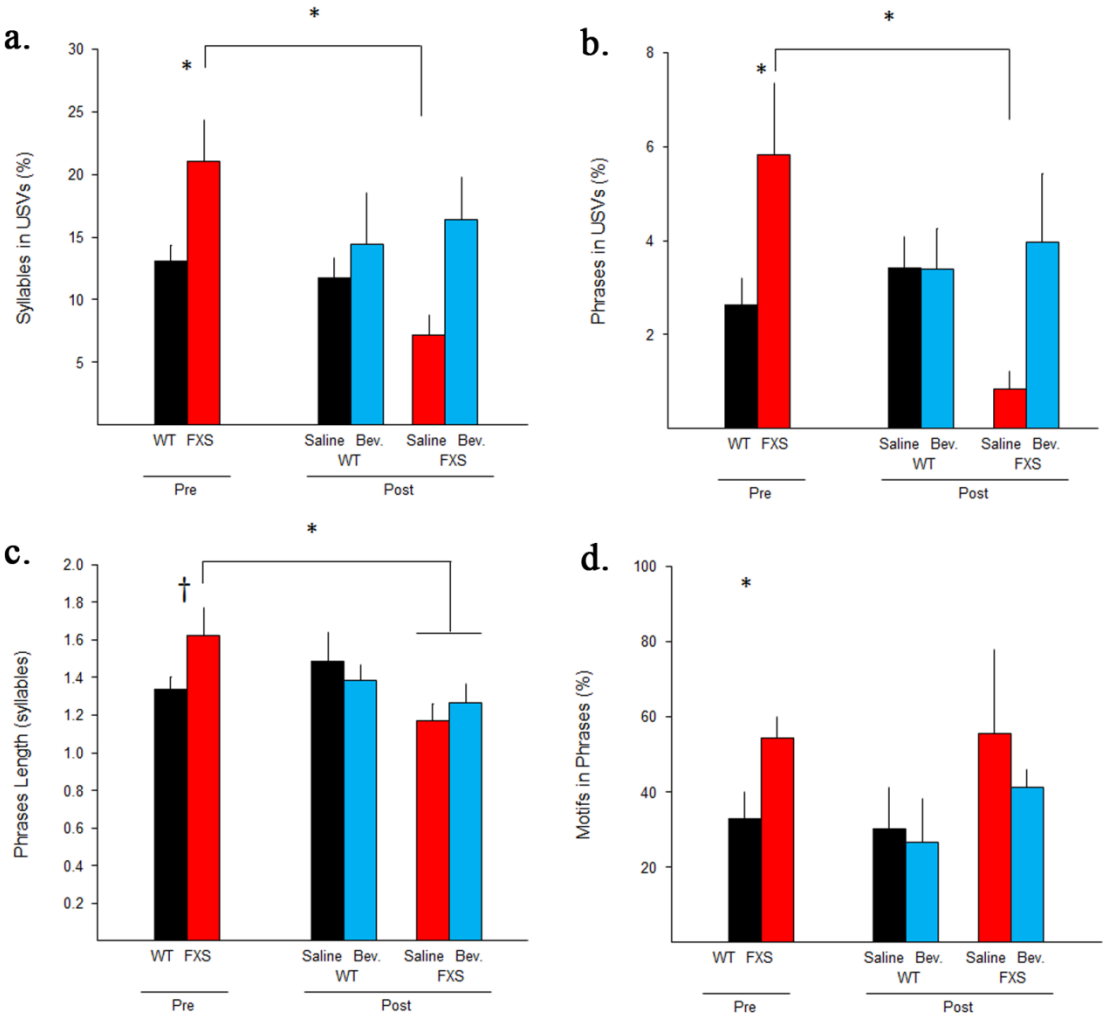

Figure 5.5. Treatment with Bevacizumab did not selectively alleviate pre-treated FXS mouse syllable and phrase vocalizations deficits. a. Percent of syllables in total vocalizations produced. Pretreated FXS mice produced more syllables than WT mice; however, Bevacizumab treatment had no effect, while posttreatment Saline FXS mice produced significantly fewer syllables than pretreated FXS mice. b. Percent of phrases in total vocalizations produced. Pretreated FXS mice produced more phrases than WT mice; however, Bevacizumab treatment had no effect, while posttreatment Saline FXS mice produced significantly fewer phrases than pretreated FXS mice. c. Average number of syllables in phrases. Pretreated FXS had a trend for increased phrase length compared to their WT counterparts. Treatment with either Bevacizumab or Saline had significantly reduced phrase length compared to pretreated FXS mice. d. Motif occurrence in phrases. Pretreated FXS mice had significantly more motifs in their phrases compared to their WT counterparts; however, there was no benefit from Bevacizumab treatment. Bevacizumab = Bev. †=0.0523. *<0.05.

Interestingly, treatment with either Saline or Bevacizumab, either significantly alleviated or had no effect on measured vocalization abnormalities in FXS mice. Specifically, FXS treated mice (Saline or Bevacizumab) exhibited a significant reduction to WT mouse levels in the percentage of syllables (difference seen only with Saline treatment) [Fig. 5.5a; $F_{(1,14)}=7.59$; $p<0.005$], phrases (difference seen only with Saline treatment) [Fig. 5.5b; $F_{(2,40)}=3.42$; $p<0.005$], length of syllable units in phrases [Fig. 5.5c; $F_{(2,40)}=3.41$; $p<0.005$], and no effect in the percentage of motifs in phrases. Interestingly, there were no significant differences in WT mouse vocalizations between pre- and post-treated USV profiles, suggesting that the change in vocalization patterns was specific to FXS mice.

Discussion

Blocking VEGF-A via Bevacizumab has been shown to have global effects on the brain; reducing Synapsin-1 levels in both the Visual Cortex and CA1 of the Hippocampus. These findings along with its ability to alleviate novel object recognition deficits (Belagodu et al., 2017), suggest that targeting the VEGF-A pathway could be a viable treatment option for a myriad of FXS behavioral phenotypes. The current study explored the extent of this intervention's ability (blocking VEGF-A with Bevacizumab) to alleviate various common FXS behavioral abnormalities. FXS mice typically exhibit increased locomotor activity coupled with decreased anxiety-like behaviors such as increased crossing and exploration with less time spent in the training chamber center region (Bakker et al., 1994; Peier et al., 2000; Spencer et al., 2005). Consistent with these studies, our analyses demonstrated that FXS Saline treated mice exhibited increased locomotion, stereotypy, along with decreased anxiety-like behavior, and altered USV production profiles with increased percentage of syllables, phrases and motifs (Peier et al., 2000; Spencer et al., 2005; Veeraragavan et al., 2012; Gholizadeh et al., 2014; Belagodu et

al., 2016). Interestingly, Bevacizumab treatment did not significantly alter anxiety-like behavior in FXS mice. This could be attested to a lack of Bevacizumab treatment on alleviating FXS hyperactivity (Belagodu et al., 2017), as increased FXS locomotor activity would increase overall exploratory behavior. Thus, further suggesting that any FXS behavior driven by increased activity levels would not be alleviated though blocking of VEGF-A.

In addition to the observed increased activity levels, stereotypy behavior is commonly observed in FXS mice with increased rotations (Dolan et al., 2013) and increased number of marbles buried in the Marble Bury Assessment (Spencer et al., 2005; Veeraragavan et al., 2012; Gholizadeh et al., 2014). Consistent with prior studies, our analyses demonstrated that FXS Saline treated mice rotated more and buried more marbles than their WT counter parts. However, Bevacizumab treated did not significantly change either metric of stereotypy. This could again be due to the inability of Bevacizumab to alleviate the hyperactivity deficit, which stereotypy behavior is heavily influenced by.

In addition to examination of hyperactivity/anxiety behaviors, the current study explored the effects of Bevacizumab in FXS on previously reported courtship induced vocalization deficits (Belagodu et al., 2016). Consistent with our previous study, the current study found that pretreated FXS mice exhibited increased syllable and phrase production, coupled with increased presence of motifs compared to their WT counterparts. Interestingly, both Saline and Bevacizumab treatment decreased the overall production of syllables, and subsequently phrases and motifs in FXS mice making them indistinguishable from WT mice. Although the underlying cause for this is not known, it is possible that the initial vocalization event allowed FXS mice to fine tune their vocalizations, so they better resemble those observed in WT mice. To explore this potential possibility, pre-exposure assessments should be eliminated in subsequent analyses.

This would mirror the pretreatment mice in this study, and those tested in our previous study (Belagodu et al., 2016)

The following study provided additional understanding of FXS mice vocalizations, ideal time points to assess differences in vocalizations, and potential causes for variations seen in published FXS vocalization studies. Currently these findings are limited to syllables, phrases and motifs. Further investigation of isolated syllables, particularly frequency components (max frequency and bandwidth of each isolated syllable) which were previously found to be significantly different (Belagodu et al., 2016) could be beneficial to obtain a more holistic understanding of potential beneficial effects of Bevacizumab on FXS vocalizations. Furthermore, our prior study showed that male FXS mice spend more time interacting with the female mouse (Belagodu et al., 2016). Thus, an assessment of the pre- and post-treatment courtship behavior could provide insight into potential Bevacizumab induced changes in FXS behavior.

CHAPTER 6: ASSESSING THE EFFECT OF BLOCKING VEGF RECEPTORS ON NON-VASCULATURE FRAGILE X SYNDROME ABNORMALITIES

Abstract

Fragile X Syndrome is the most common form of inherited mental retardation. Recent studies from our laboratory have demonstrated that Vascular Endothelial Growth Factor A (VEGF-A) is elevated in FXS mice and when reduced can alleviate many molecular and behavioral FXS phenotypes (Belagodu et al., 2017). However, VEGF-A is only one of five VEGF Family molecules which can bind to three VEGF Receptors. To assess which of these receptors, and subsequent mechanisms are driving the molecular and behavioral rescues observed in the aforementioned study, mice were dosed with VEGF Receptor blockers and the same molecular and behavioral abnormalities examined. Blocking VEGFR2 and VEGFR3 was found to significantly decrease Synapsin-1 expression in FXS mouse brain. Interestingly, our subsequent behavioral assessments demonstrated that blocking the receptors (VEGFR1, VEGFR2, or VEGFR3) had not effect on hyperactivity or any of the behavioral measures that are influenced by hyperactivity (locomotor activity, anxiety-like behavior, and marble bury). Blocking VEGFR2 was found to reduce the number of rotations per minute in FXS mice, a measure of stereotypy. These studies suggest that VEGFR2 is the primary driver through which VEGF-A mediates some FXS abnormalities; however, further exploration will be needed to obtain a better assessment of the specific behaviors that can be alleviated and drug optimal dosage.

Introduction

Fragile X Syndrome (FXS) is the leading form of inherited mental retardation, primarily affecting males at twice the incidence rate than females (Cornish et al., 2008). The primary

cause of FXS is the transcriptional silencing of *FMR1*, the gene that codes for the Fragile X Mental Retardation Protein (FMRP) (Pieretti et al., 1991; Verkerk et al., 1991). Although the cause of FXS is known, the mechanism by which an absence of FMRP alters anatomical, and cognitive properties is not known.

Previous studies from our laboratory have demonstrated that one mechanism mediating FXS abnormalities in adulthood is the abnormal expression of Vascular Endothelial Growth Factor A (VEGF-A) (Belagodu et al., 2017). Our studies demonstrated that adult FXS mice exhibit elevated VEGF-A expression and blocking VEGF-A can alleviate many adult FXS abnormalities (Belagodu et al., 2017). VEGF-A is the most prominent regulator of vascular growth (Neufeld et al., 1999) with proper expression being critical for normal vascular development and viability (Carmeliet et al., 1996; Ferrara et al., 1996). Consistent with these findings, FXS patients and mice have been shown to exhibit abnormal cerebral blood profusion (Balci et al., 2006; Kabakus et al., 2006) and increased brain vasculature (Galvan and Galvez, 2012), suggesting that increased VEGF-A is causing vascular abnormalities in FXS.

Interestingly, in addition to vascular regulation, VEGF-A has been shown to alter many neuronal properties that are disrupted in FXS. For example, increasing VEGF-A expression stimulates axonal growth, neurite outgrowth, and enhances cell survival (Silverman et al., 1999; Sondell et al., 1999; Sondell et al., 2000; Jin et al., 2002). Consistent with these findings, FXS is also associated with increased axonal material, elevated dendritic spine density, and excessive cell proliferation (Pan et al., 2004; Galvez and Greenough, 2005; Pan et al., 2010); further suggesting that altered VEGF-A expression is an underlying cause for FXS abnormalities. In support of this hypothesis our studies have shown that blocking VEGF-A binding to its receptor alleviates many FXS behavioral (Novel Object Recognition), physical (reduction in

macroorchidism), and molecular abnormalities (Synapsin-1 and VEGF-A levels) (Belagodu et al., 2017).

Unfortunately, the mechanism by which VEGF-A is able to alleviate these FXS abnormalities is not known. VEGF-A is known to bind to one of three VEGF receptors (VEGFR1, VEGFR2, and VEGFR3). VEGFR1 plays a critical role in vascular development (Fong et al., 1995) and more interestingly, is found with increased expression of astrocytes, suggesting that it aids in astroglial expression of various growth factors (Krum et al., 2008; Koyama et al., 2014). VEGFR2 is the primary driver of angiogenesis (Dvorak, 2002); however, there is growing evidence of increased functionality beyond blood vessel growth. VEGFR2 has been found on axonal growth cones (Sondell et al., 1999), implicated in driving microvascular permeability (Dvorak, 2002), as well as endothelial cell proliferation and survival (Millauer et al., 1993; Zeng et al., 2001). Furthermore, selective silencing of neuronal VEGFR2 has been indicated to impair hippocampal-dependent plasticity, memory consolidation, and learning (De Rossi et al., 2016), suggesting that it is vital in mediating learning mechanisms. Finally, VEGFR3 has been suggested to play a critical role in the development and plasticity of vascular networks during embryogenesis and drive lymphangiogenesis later in development (Kukk et al., 1996; Dumont et al., 1998; Paavonen et al., 2000; Alitalo and Carmeliet, 2002; Laakkonen et al., 2007). The current study used blockers for each of these receptors (MF-1; VEGFR1: DC101; VEGFR2: and mF4-31C1; VEGFR3) to determine the initial mechanism by which blocking VEGF-A binding is able to alleviate FXS abnormalities.

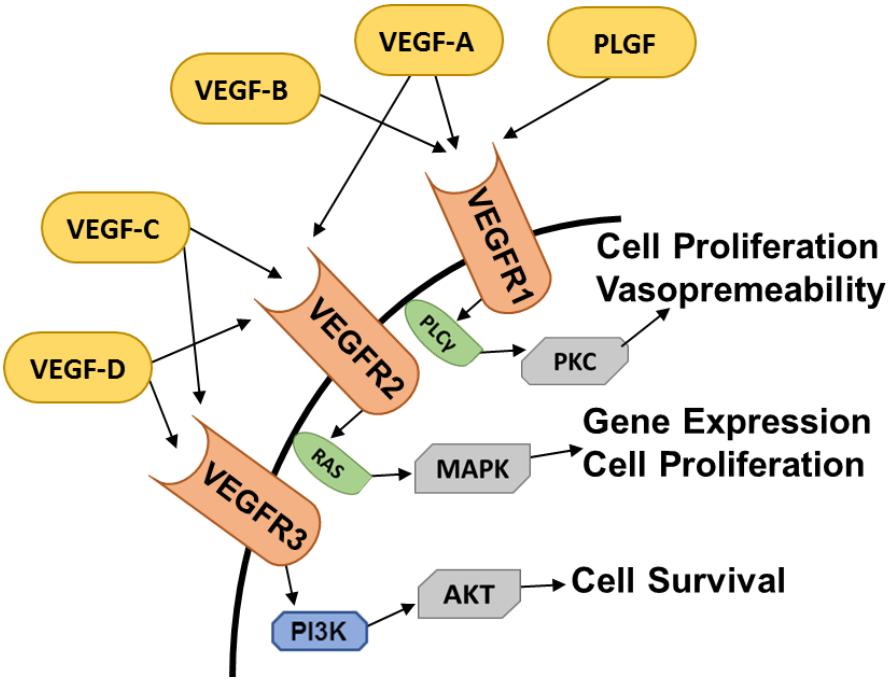

Figure 6.1. Schematic of binding affinities of VEGF Family of molecules to their various VEGF Receptors.

Methods & Analysis

Housing and Care of Animals

Adult (PND 60) male C57/B6 *FMR1* knockout (FXS) and wildtype (WT) mice were used. Mice were housed in standard laboratory conditions (12 hr-12 hr light/dark cycle with food and water provided *ad libitum*).

Blocking VEGF Receptors

For initial analysis of the effects of receptor blocking on synapse density, receptor blocking doses of 25 and 50 mg/kg every other day for 10 days intraperitoneal (IP) were selected. These doses were based upon prior studies exploring the blocker's efficiency for altering vascular properties [MF-1 (VEGFR1) (Wang et al., 2004; Huang et al., 2011), DC101 (VEGFR2) (Dias et al., 2001; De Bandt et al., 2003; Wang et al., 2004; Van de Veire et al., 2010; Huang et al., 2011), or mF4-31C1 (VEGFR3) (Pytowski et al., 2005; Roberts et al., 2006; Laakkonen et al., 2007)]. Based upon this initial assessment, our subsequent behavioral analyses

were conducted with 50 mg/kg IP every other day for 10 days. Note due to material transfer agreements with Eli Lilly only FXS mice were given the receptor blockers.

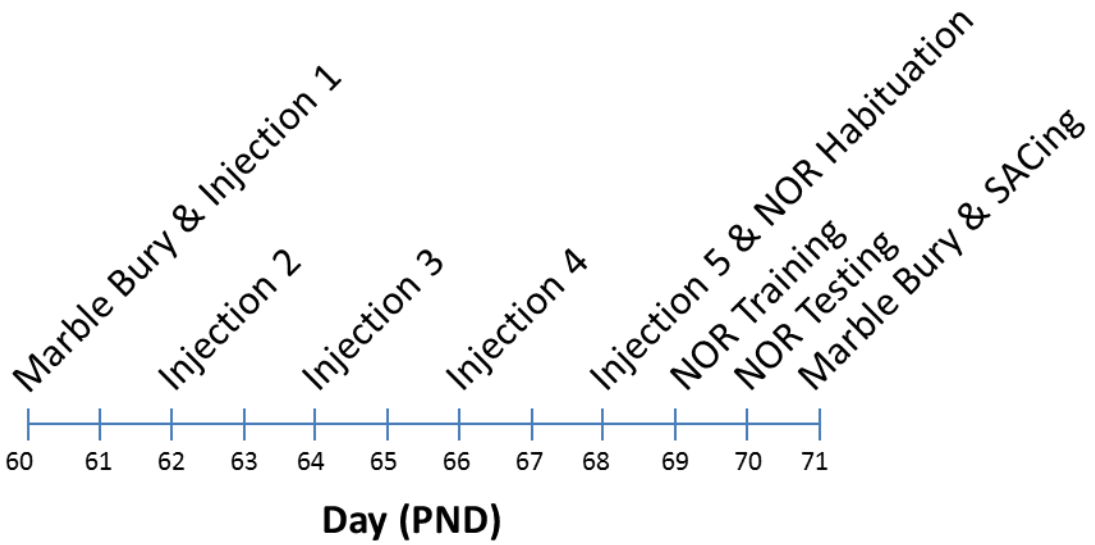

Figure 6.2: Schematic of injection scheme with time points (PND) for each behavioral assessment to be conducted.

Synapsin-1 Expression

To determine the effects of blocking VEGF Receptors on synapse density (determined via Synapsin-1 Expression), mice were given either MF-1, DC101, mF4-31C1, or Saline as outlined above. Postmortem samples were then processed for Synapsin-I expression as previously described (Belagodu et al., 2017). Briefly, following the last injection, mice [FXS (n=21) and WT (n=3)] were sacrificed and cortical hemispheres, including cortical white matter and hippocampus were dissected for Western Blot analysis. For Western Blot analysis, samples were homogenized and protein concentrations estimated via bicinchoninic acid assay (Thermo Scientific). Protein (10 µg) in a 1:1 loading buffer (450 µl Laemmli + 50 µl βME) ratio were loaded and run on a 4-15% electrophoresis gel (BioRad) at 100 V for 10 min followed by 200 V for 25 min. The separated proteins were then transferred to a nitrocellulose membrane at 100 V for 1 hr, blocked with 5% milk in TBS-T (Tris Buffered Saline with 0.05% Tween 20) and then

probed with Synapsin-1 antibody (1:1000; Sigma) and GAPDH (1:1000; Santa Cruz) to control for loading, overnight at 4°C. The membrane was then washed and incubated in anti-rabbit secondary antibody (1:1000; Cell Signaling Technology) for 2 hrs prior to chemiluminescent substrate (BioRad) exposed for 5 min and imaged via a BioRad ChemiDoc Touch Gel Imaging System (BioRad). To account for gel/run differences, each gel was loaded with a homogenate sample lane (sample which composed of multiple mouse brains pooled together). The relative intensity of Synapsin-1 was determined by dividing its optical density, determined using Image Lab v5.2.1 (BioRad), by GAPDH, and then divided by the homogenate sample lane's Synapsin-1/GAPDH Ratio.

Hyperactivity Assessment

FXS mice and subjects have been established to exhibit increased hyperactivity compared to controls (Bakker et al., 1994; Hagerman and Hagerman, 2003; Kazdoba et al., 2014). To assess the effects of each blocker on FXS hyperactivity, the total distance traveled, average velocity, and maximum velocity over 10 minutes was assessed using Anymaze (v4.98) during Novel Object Recognition Habituation as previously described (Belagodu et al., 2017).

Open Field Assessment

FXS patients and mice also exhibit increased anxiety levels (Hagerman and Hagerman, 2003; Cordeiro et al., 2011; Bailey et al., 2012). To assess anxiety, a standard Open Field assessment exploring the time spent in the center (Center 50%), corners, edges, crossings into center area, and the amount of time immobile in the center region of the training cage during habituation (10 min) was conducted using Anymaze (v4.98).

6.3.6. Marble Bury Analysis

Marble Bury, a well-established paradigm for repetitive (stereotypy) behavior (Thomas et al., 2009), was used to assess the beneficial effects of Receptor Blocker treatments. To assess stereotypic behavior, a modified protocol from (Deacon, 2006) was used. As previously described, mice were placed in a new cage consisting of 5 cm of woodchip bedding and 15 evenly spaced (at least 1 inch apart) glass marbles for 30 minutes. The mice were then removed, and the number of marbles buried was assessed. Marbles were considered fully buried if they were more than 50% covered. The Marble Bury Assessment was conducted prior to injections with a follow up test after drug treatment to obtain within subject assessments.

Testicle Weight

Macroorchidism is a prominent feature in FXS males, driven by excessive Sertoli cell proliferation (Slegtenhorst-Eegdeman et al., 1998). Testicular weight has been previously shown to be a viable metric for assessing macroorchidism in adult mice (Kooy et al., 1996; Belagodu et al., 2017). To assess each VEGF Receptor's influence on testicle weight, FXS (n=37) and WT (n=12) mice were dosed with either MF-1 (n=9), DC101 (n=9), mF4-31C1 (n=10), or Saline (n=21) in the aforementioned dosage scheme. Immediately following the last behavioral assessment, testicles were removed and post-fixed in 4% paraformaldehyde for 24 hrs. After post-fixing, testicles were desiccated for 2 days and then weighed. For statistical analyses, each testicle was considered an individual unit.

Statistical Analyses

All statistical analyses were conducted with a 2-way mixed model ANOVA on SAS (http://www.sas.com/en_us/home.html) with either genotype and/or drug as between subject factors. Marble burying also used pre/post injection as a within subject factor.

Results

Synapsin-1 Expression

VEGF-A's primary targets are VEGFR1 and VEGFR2, suggesting that the effects observed while utilizing the VEGF-A blocker Bevacizumab were primarily driven by one of these receptors. Furthermore, VEGFR3 is involved with lymphangiogenesis (Kukk et al., 1996; Paavonen et al., 2000; Alitalo and Carmeliet, 2002), is activated by VEGF-C and VEGF-D (Joukov et al., 1996; Achen et al., 1998), and could provide new insight into potential mechanisms mediating FXS deficits. Western Blot analyses demonstrated that the higher doses (50 mg/kg) of VEGFR2 (DC101) and VEGFR3 (mF4-31C1) receptor blockers significantly reduced Synapsin-1 expression. No significant effects were observed with the lower doses (25 mg/kg) [Fig. 6.3; $F_{(7,16)}=9.70$; $p<0.005$]. Based upon these findings, behavioral assessments mirroring those in our prior FXS VEGF-A blocker study were pursued; Hyperactivity and Open Field Assessments, Stereotypy Measures of Marble Bury and Rotations, and testicle weight (Belagodu et al., 2017).

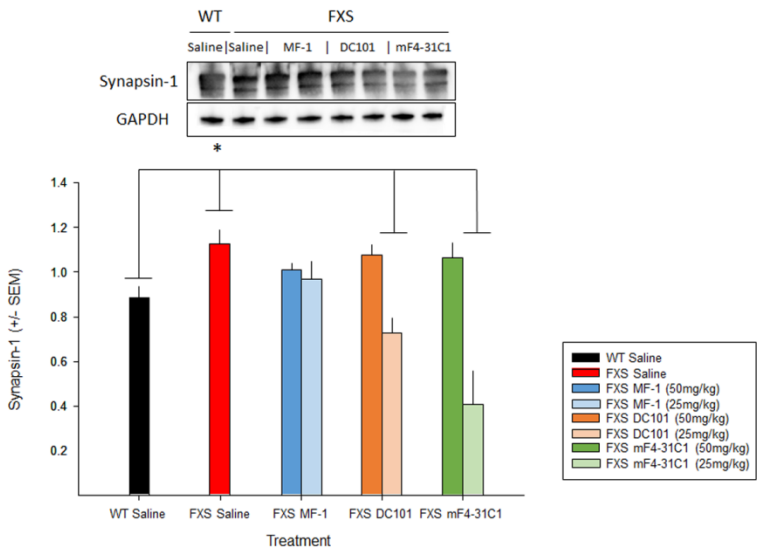

Figure 6.3. High doses of DC101 (VEGFR2 Blocker) and mF4-31C1 (VEGFR3 Blocker) decreased Synapsin-1 in FXS mouse brain. Synapsin-1 expression after 10 days of treatment with either Saline, MF-1 (VEGFR1 Blocker), DC101 (VEGFR2 Blocker), or mF4-31C1 (VEGFR3 Blocker). No significant reduction in Synapsin-1 expression was observed with a low dose (25mg/kg); however, the higher dose (50mg/kg) of DC101 and mF4-31C1 significantly reduced FXS brain Synapsin-1 levels. *<0.05.

Hyperactivity Assessment

Hyperactivity is a well-known FXS abnormality with FXS mice exhibiting increased total distance traveled, and velocity (Bakker et al., 1994; Belagodu et al., 2017). Consistent with previous studies, our study demonstrated that FXS saline treated mice displayed increased hyperactivity (distance traversed [Fig. 6.4a; $F_{(4,485)}$=13.03; p<0.005], overall mean velocity [Fig. 6.4b; $F_{(4,485)}$=13.02; p<0.005], and overall max velocity [Fig. 6.4c; $F_{(4,485)}$=8.00; p<0.005]). Interestingly, the receptor blockers did not alter overall hyperactivity in the aforementioned metrics. This is in line with our previous study assessed the effects of blocking VEGF-A, in which Bevacizumab did not alleviate FXS hyperactivity metrics (Belagodu et al., 2017).

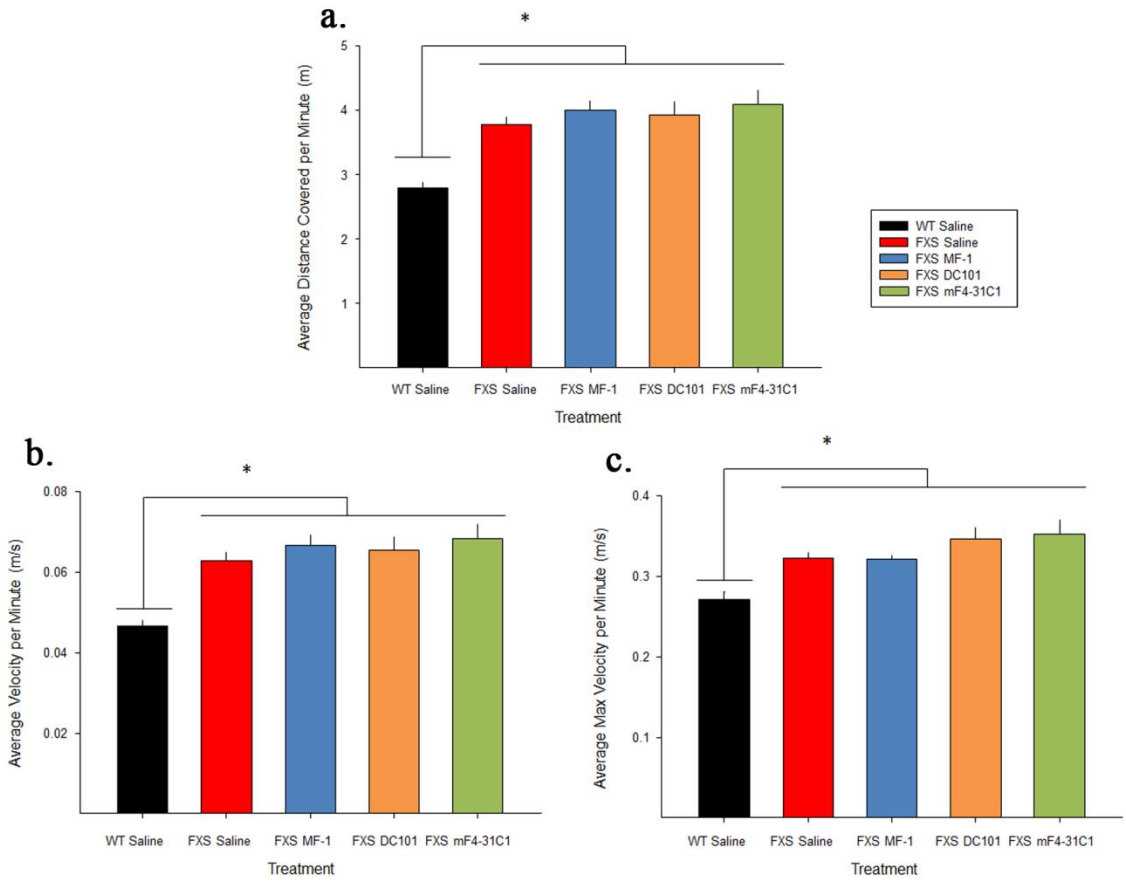

Figure 6.4. Measures of hyperactivity comparing WT mice to FXS mice treated with saline or one of three VEGF Receptor Blockers. None of the VEGF receptor blockers significantly alleviated any of the hyperactivity measures. a. Average distance covered per minute in the training chamber. FXS mice had significantly increased movement. b. Average velocity per minute in the training chamber. FXS mice moved significantly faster than WT mice. c. Average maximum velocity per minute. FXS mice reached significantly higher speeds than WT mice. *<0.05.

Open Field Assessment

The Open Field Paradigm was utilized to assess general locomotor activity and anxiety-like behavior. Previous studies have shown that FXS mice display decreased anxiety and increased overall levels of locomotion (Peier et al., 2000; Spencer et al., 2005). Although the initial metrics of locomotion (distance traveled, mean velocity, and max velocity) were already assessed in our discussion of hyperactivity this analysis found that FXS mice were also mobile for a greater amount of time [Fig. 6.5a; $F_{(4,485)}=12.92$; $p<0.005$] with more mobile episodes [Fig.

6.5b; $F_{(4,485)}$=10.95; p<0.005] and displayed less immobility time [Fig. 6.5c; $F_{(4,485)}$=12.93; p<0.005] with a decreased amount of immobile episodes [Fig. 6.5d; $F_{(4,485)}$=10.77; p<0.005]. These measures further suggest a reduction in anxiety and increased exploratory behavior. This was further corroborated with FXS mice exhibiting an increased number of crossings [Fig. 6.5e; $F_{(4,485)}$=11.95; p<0.005], particularly to/from the center zone [Fig. 6.5f; $F_{(4,484)}$=5.86; p<0.005]; a behavior consistent with reduced anxiety. Unfortunately, none of the receptor blockers significantly reduced any locomotor (Fig. 6.5a-d) or anxiety-like behavioral measures (Fig. 6.5c-f), suggesting that the VEGF Receptors are not involved in the pathways that dictate these phenotypes. Interestingly, our analysis of rotations, a measure of stereotypy, found that FXS mice, consistent with prior studies (Dolan et al., 2013), exhibit increased rotations (~32%); however, blocking VEGFR2 in FXS significantly reduced the number of rotations to control levels [Fig. 6.5g; $F_{(4,485)}$=11.16; p<0.005].

Figure 6.5. Open Field Assessment metrics

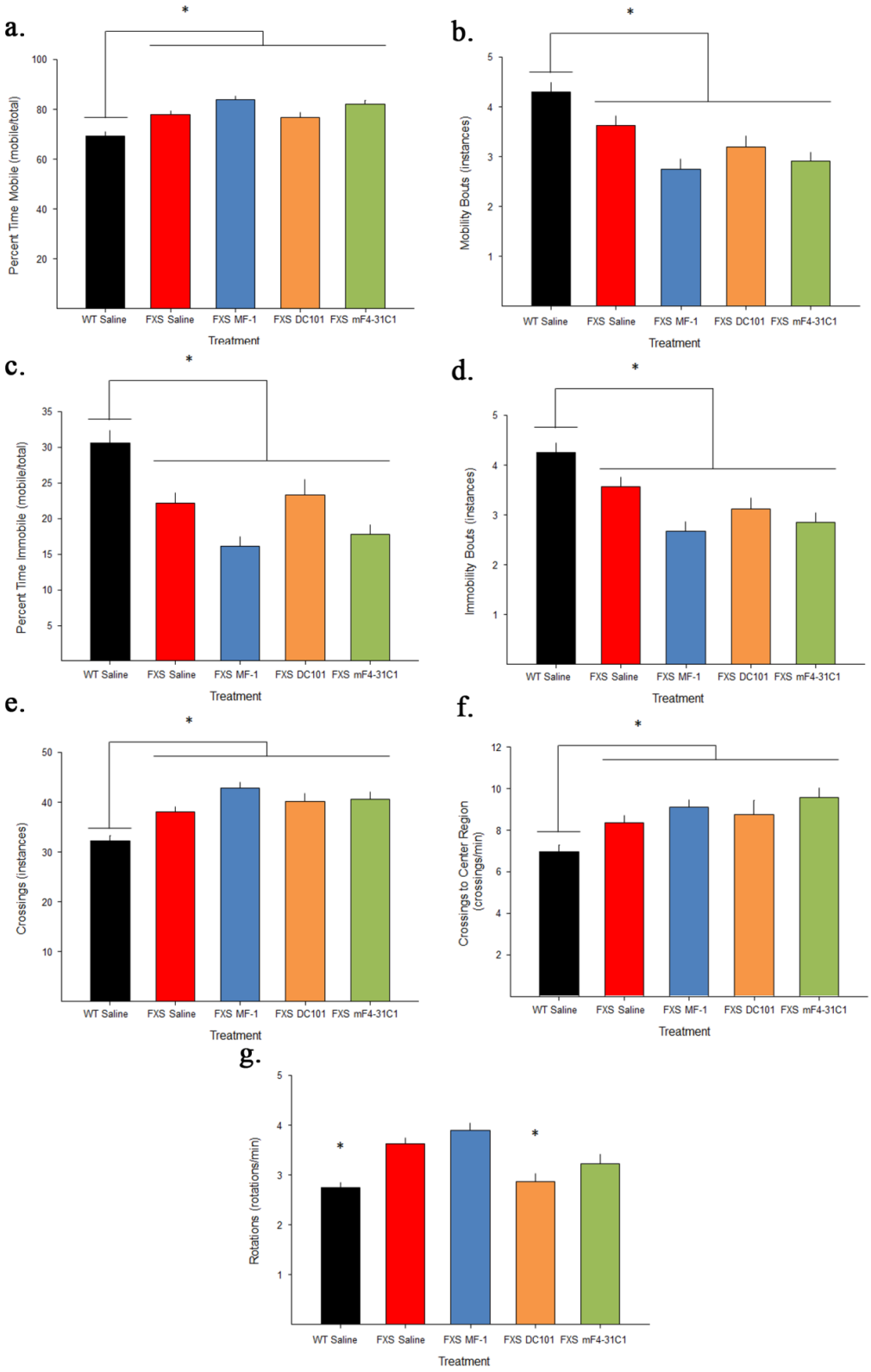

Figure 6.5 (cont.). Open Field Assessment metrics for locomotion (a.-d.), anxiety-like (c.-f.), and stereotypy behavior (g.) in WT vs FXS mice treated with saline or one of three VEGF Receptor Blockers. Treatment yielded no effect on locomotion or anxiety-like behaviors, but DC101 (VEGFR2 Blocker) was able to rescue stereotypy behaviors. a. Percent time in which the mice were mobile per minute in the training chamber. FXS mice were more mobile for significantly longer than WT mice. b. Mobility bouts per minute in the training chamber. FXS mice had significantly fewer number of instances in which they were mobile than WT mice. c. Percent time in which the mice were immobile per minute in the training chamber. FXS mice were immobile for significantly less time than WT mice. f. Immobility bouts per minute in the training chamber. FXS mice had significantly fewer instances in which they were immobile than WT mice. g. Total crossings per minute in the training chamber. FXS had significantly more crossings than WT mice. h. Crossings to/from the center region per minute in the training chamber. FXS mice had significantly more crossings in the center region than WT mice. g. Total rotations per minute in the training chamber. FXS rotated significantly more than WT mice and DC101 alleviated this deficit. *<0.05.

Marble Bury Analysis

The main metric for stereotypy behavior was assessed via Marble Bury. Consistent with previous FXS rodent studies (Spencer et al., 2011; Veeraragavan et al., 2012; Gholizadeh et al., 2014), FXS mice displayed increased stereotypy behavior expressed by increased burrowing behavior, and a (~46%) increase in the number of marbles buried. Two FXS (Saline), one FXS (VEGFR1) and one WT (Saline) mouse were removed from the analysis as their mean number of marbles buried were more than two standard deviations from their group mean. Our analyses demonstrated that the receptor blockers (MF-1, DC101, & mF4-31C1) did not alter the number of marbles buried [Fig. 6.6; $F_{(6,84)}=6.93$; $p<0.005$]. This is further addressed in the discussion below.

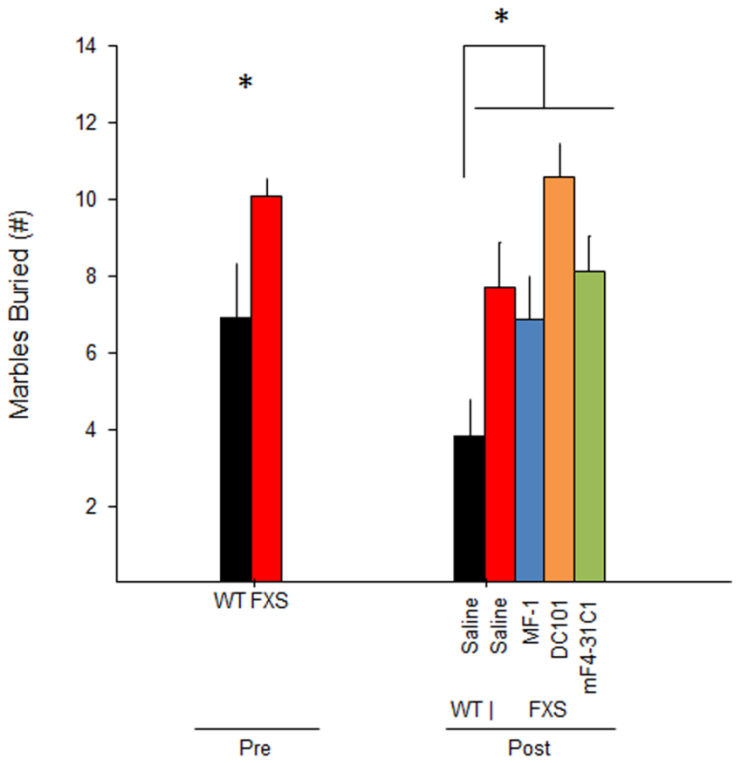

Figure 6.6. Stereotypy behavior of Marble Burying was not altered with 10 days of treatment with any VEGF Receptor Blocker. FXS mice bury more marbles than their WT counterparts. All FXS treatment groups buried significantly more marbles compared to WT Saline control mice. *<0.05.

Testicle Weight

Macroorchidism is a prominent phenotype of FXS subjects (McLennan et al., 2011) and FXS mice (Slegtenhorst-Eegdeman et al., 1998; Hagerman and Hagerman, 2003). Consistent with our previous findings (Belagodu et al., 2017), FXS mice displayed enlarged (~37%) testes compared to their WT counterparts [Fig. 6.7; $F_{(4,93)}$=14.65; p<0.005]. Interestingly, neither VEGFR1 or VEGFR2 significantly altered teste weight. However, mF4-31C1 (VEGFR3 Blocker) significantly decreased in teste weight (~11%) compared to FXS mice, but was still significantly elevated compared to WT mice (~23%) [Fig. 6.7; $F_{(4,93)}$=14.65; p<0.005].

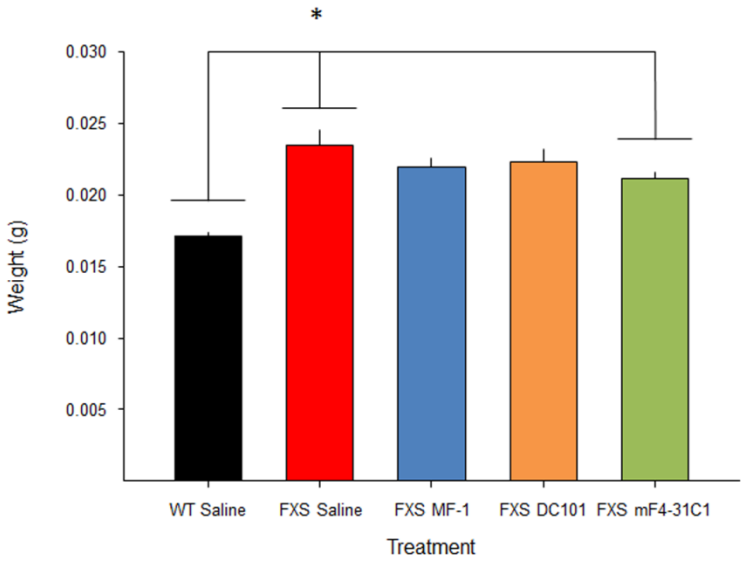

Figure 6.7. Blocking VEGF Receptors do not decrease FXS testicle weight to WT levels. However, blocking with mF4-31C1 (VEGFR3 Blocker), significantly decreases teste weight compared to FXS Saline controls. *<0.05.

Discussion

Prior studies have demonstrated that the VEGF Pathway may be a target for mediating FXS molecular and behavioral abnormalities (Belagodu et al., 2017). Specifically, our previous studies have demonstrated that blocking VEGF-A via Bevacizumab in FXS can reduce Synapsin-1 levels in both the visual cortex and CA1 of the Hippocampus. A reduction in Synapsin-1 levels suggests decreased synapse density, as Synapsin-1 expression has been shown to directly correlate with synapse number (Sudhof et al., 1989; Cesca et al., 2010). This reduction is believed to be the primary cause for the beneficial effects of Bevacizumab treatment on FXS Novel Object Recognition abnormalities (Belagodu et al., 2017). The following study sought to determine which of the VEGF Receptors were mediating these beneficial effects seen with blocking VEGF-A.

VEGF Receptors have been suggested to be involved in more than angiogenesis, particularly in adulthood. VEGFR1 has been extensively found on astrocytes, and is believed to regulate astroglial expression of various growth factors (Krum et al., 2008; Koyama et al., 2014).

However, blocking VEGFR1 with MF-1 did not significantly alter FXS Synapsin-1 levels in the brain.

VEGFR2 has been found on axonal growth cones (Sondell et al., 1999) with stimulation via VEGF-A promoting neurite outgrowth (Jin et al., 2006). Furthermore, it has been implicated as a key driver in microvascular permeability (Dvorak, 2002). Interestingly, VEGFR2 has recently been observed to influence learning mechanisms in rodents, as genetic removal of these receptors impairs contextual fear conditioning acquisition (De Rossi et al., 2016). Our findings suggest that blocking VEGF Receptors can alter synapse density; however, it has varying results on behavioral. Whole brain Synapsin-1 levels were significantly reduced with 50mg/kg of DC101. This is further corroborated with our previous study in which blocking VEGF-A, the primary ligand for VEGFR2 (Dvorak, 2002), resulted in a similar decrease in Synapsin-1 levels (Belagodu et al., 2017).

Finally, blocking VEGFR3 with 50 mg/kg of mF4-31C1 also significantly reduced FXS brain Synapsin-I expression. VEGFR3 is the main lymphangiogenic receptor, mediating the generation and proliferation of lymphatic vessels (Kukk et al., 1996; Paavonen et al., 2000; Alitalo and Carmeliet, 2002). Lymphatic vessels are lined with endothelium, which mediates the blood brain barrier and permeability (Feletou, 2011). Interestingly, VEGFR3 and the lymphatic vessels have recently been discovered to have a neuronal role in the Central Nervous System (CNS); lymphatic vessels have been discovered in the dural sinuses, and function to help mitigate fluid and immune cells to and from the Cerebral Spinal Fluid (CSF) and CNS (Louveau et al., 2015), thus suggesting their influence on mediating blood brain barrier permeability. Furthermore, application of VEGF-C and subsequent activation of VEGFR3 have been shown to increase hippocampal neurogenesis (Han et al., 2015). This increased neuronal function,

particularly the influence in hippocampal neurogenesis mirrors that of VEGFR2's ability to increase hippocampal neurogenesis (Jin et al., 2002), and thus could indicate a new potential mechanism for mediating FXS abnormalities.

Our behavioral findings of increased anxiety, hyperactivity, and stereotypy in FXS mice are consistent with those from other laboratories. FXS mice displayed phenotypic characteristics of reduced anxiety such as increased mobility and crossings to/from the center region (Peier et al., 2000; Spencer et al., 2005); however, blocking the VEGF receptors did not alter anxiety levels in FXS mice. Stereotypy behavior was primarily assessed through Marble Bury in which FXS mice exhibited increased number of marbles buried (Spencer et al., 2011; Veeraragavan et al., 2012; Gholizadeh et al., 2014); however, blocking the VEGF receptors did not alleviate this abnormality. Interestingly, another measure of stereotypy behavior, rotations per minute in which FXS mice tend to rotate more than WT mice during exploration, was alleviated with DC101 the VEGFR2 blocker. When combined with the Marble Bury assessment, these findings suggest a partial rescue of overall stereotypy behavior. Further analyses will be necessary to determine the biological pathways mediating these different aspects of stereotypy behavior, and how the VEGF pathway could be mediating them.

This inability to rescue stereotypy behavior could be attributed to an inability of these interventions in alleviating hyperactivity. Stereotypy behaviors are heavily influenced by the mouse's general locomotion levels, and thus could mask any potential benefits the VEGFR blockers are having. Further analysis into new behavioral paradigms and their connection with the VEGF pathway would be required to fully assess the effects of blocking VEGFR2 and the other receptors on measures of anxiety and stereotypy.

Our previous study demonstrated that the effects of blocking VEGF-A were global, as Bevacizumab treatment also reduced FXS teste weight (Belagodu et al., 2017). FXS mice displayed phenotypic macroorchidism (Slegtenhorst-Eegdeman et al., 1998; Hagerman and Hagerman, 2003); however, treatment with the receptor blockers were unable to reduce testicle weight to WT levels. Interestingly, mF4-31C1, the VEGFR3 blocker, did have a significant decrease in teste weight, but were still significantly heavier than WT mice.

The benefits of blocking VEGF receptors on FXS abnormalities require further investigation. While initial molecular effects, observed with the reduction in Synapsin-1 levels were promising, the subsequent behavioral analyses were unable to adequately delineate a beneficial effect for any of the VEGFR blockers. Understanding the full extent of the molecular influences can help to better ascertain the ability of the receptor blocks in mediating FXS cognitive and behavioral abnormalities. Furthermore, utilizing the observed anatomical/molecular changes can be used to determine an ideal dosing scheme for subsequent analyses. This study provides the ground work for a potential mechanism mediating some FXS abnormalities, and thus potentially providing new therapeutic targets for treating these abnormalities.

CHAPTER 7: GENERAL DISCUSSION

The studies in this Dissertation sought to examine the role of Vascular Endothelial Growth Factor (VEGF) and its effects on abnormalities in the mouse model of Fragile X Syndrome (FXS); a novel mechanism mediating FXS abnormalities. Our findings demonstrated a developmental dysregulation of brain blood vessel density (BVD). Specifically, we found that in WT mice, there was increased vasculature at PND 20 with a sharp reduction at PND 35; however, in FXS mice there was a gradual increase in BVD through development and into adulthood. These findings are consistent with our prior analyses demonstrating increased BVD in adult and aged FXS mice (Galvan and Galvez, 2012) and studies demonstrating abnormal blood perfusion in FXS patients (Balci et al., 2006). This BVD deficit in FXS mice could result in a developmental delay in vascular brain growth and proliferation at PND 20, that is overcorrected through adulthood with increased BVD at PND 60 (adulthood). Consistent with these findings we further demonstrated developmental dysregulation of the VEGF family of molecules and their respective receptors. However, further analyses will be needed to determine the specific implications of the altered protein expression on FXS neuronal properties and behavior. To ascertain a potential mechanism for this alteration in VEGF levels, rapamycin was utilized to inhibit mTORC1. Application of rapamycin resulted in decreased expression of VEGF-A in FXS. These findings suggest that VEGF-A production is downstream of mTORC1 and potentially involved in the mGluR pathway (Belagodu et al., 2017). The mGluR pathway is the prevailing theory for the abnormalities in FXS (Bear et al., 2004), and thus could provide a potential novel target for treating FXS abnormalities.

Our subsequent analyses found that blocking VEGF-A with Bevacizumab reduced FXS elevated Synapsin-1 levels in whole brain and specifically in the visual cortex and CA1 of the

hippocampus (Belagodu et al., 2017). Synapsin-1 is a pre-synaptic vesicle binding protein whose expression correlates with synapse number (Sudhof et al., 1989; Cesca et al., 2010). Interestingly, a follow up study utilizing VEGF receptor specific blockers demonstrated that blocking VEGFR2 or VEGFR3 resulted in a similar reduction in Synapsin-1 whole brain protein expression, suggesting that the effects of blocking VEGF-A on Synapsin-I expression are working through one of these receptors.

To assess if blocking VEGF-A mediated activity has any beneficial behavioral effects, FXS mice were initially tested on the Novel Object Recognition paradigm. Mice are ethologically exploratory in nature, and readily examine novel objects. However, FXS mice do not exhibit this preference as they are unable to recall which object had been previously explored (Ventura et al., 2004; Seese et al., 2014; Bhattacharya et al., 2016). Our findings demonstrated that treatment with Bevacizumab was able to alleviate this deficit, as Bevacizumab treated FXS mice had preferential exploration for the novel object during testing (Belagodu et al., 2017). To assess the extent that Bevacizumab and the Receptor Blockers can alleviate FXS abnormalities, we subsequently explored their effect on paradigms FXS mice are known to be deficit in: hyperactivity (Bakker et al., 1994; Hagerman and Hagerman, 2003; Kazdoba et al., 2014), anxiety (Hagerman and Hagerman, 2003; Cordeiro et al., 2011), and stereotypy (repetitive) behavior (Thomas et al., 2009; Spencer et al., 2011; Veeraragavan et al., 2012; Gholizadeh et al., 2014). In addition to these behavioral measures, there has been a push to establish more clinically relatable metrics to validate animal studies (Berry-Kravis et al., 2008; Berry-Kravis et al., 2013; Jacquemont et al., 2014). Thus, to address this concern, vocalization properties in FXS mice were also assessed.

FXS patients suffer communication deficits, manifesting in increased articulation errors, Palilalia, disfluency, and reduced quality of sentence structure (Van Borsel et al., 2008). Furthermore, many of the clinical measures, particularly those with higher reproducibility rely on communication and verbal responses (Berry-Kravis et al., 2008), furthering the need to find an analogous rodent model. Through testing adult mice in a courtship/separation paradigm, we found that FXS mice exhibit altered vocalization production. Specifically, FXS mice produced vocalizations with more frequency jumps (syllables) and more syllables in each call (phrases). These phrases contained more repeated units (motifs) compared to their WT counterparts. Furthermore, FXS mice produced fewer isolated syllables, suggesting an inability for proper vocalization formation (Belagodu et al., 2016). These findings suggest that assessing vocalization patterns could be a potential novel venue for assessing the efficacy of treatments in FXS mice, and thus was further explored following VEGF-A modulation in the subsequent studies.

Collectively, the aforementioned experiments suggest that modulating VEGF-A and the VEGF pathway could be a potential treatment mechanism for FXS deficits. Our previous studies demonstrated that treatment with Bevacizumab, VEGFR2, or VEGFR3 Blockers can reduce overall Synapsin-1 levels in FXS mice; however, neither of these or the VEGFR1 Blocker modulated hyperactivity (Belagodu et al., 2017), anxiety, marble burying, or vocalization deficits. Interesting, our analysis of the number of rotations per minute in FXS found that it was reduced by blocking VEGFR2 but not with Bevacizumab or any of the other receptor blockers. This suggests that there may be some influence of this pathway on these behaviors, but as previously mentioned, might not be the major contributing factor as other metrics were not altered.

Although blocking VEGF-A activity did not alleviate locomotor activity, anxiety-like behavior, stereotypy behaviors, or vocalization deficits, our previous studies demonstrated that it was able to rescue more cognitive paradigms such as Novel Object Recognition (Belagodu et al., 2017). This could suggest a potential limitation in modulating VEGF-A in FXS mice, as its benefits could be confined to more cognitive tasks. To ascertain this specificity, further investigation into not only which paradigms can be rescued, but region specific expression levels of Synapsin-1 would be beneficial. A focus on more cognitively demanding paradigms such as Morris Water Maze or Trace Fear Memory Tasks which FXS mice are known to be deficit in (Shang et al., 2009) could aid in understanding the full effects and potential benefits of VEGF-A modulation in adult FXS mice.

In moving forward with the findings from this dissertation, several lines of research should be pursued. An extensive region specific examination of alterations in Synapsin-1 levels via Western Blot and Immunohistochemistry (IHC) could offer important insight on the extent of Bevacizumab's influence in the brain and thus lead to a better understanding of which FXS behavioral phenotypes would benefit from such an intervention. Furthermore, understanding what changes are occurring on a cellular level to the neurons in these regions would be extremely beneficial. A reduction in Synapsin-1 was observed, but it is currently unknown if this translates to alterations in dendritic spine properties. A follow up anatomical study utilizing Golgi staining to ascertain neuron dendritic spine morphology can provide additional insight into which of these interventions can influence FXS mouse neuronal abnormalities. These studies could also help suggest if the treatment should be extended to obtain a greater effect on spine morphology, and potentially alleviate behavioral abnormalities. Utilizing these analyses to determine an ideal dosage, time point for intervention, and length of intervention could help further elucidate the

behavioral benefits of these interventions. Furthermore, this would be highly beneficial for translational research, as dosage, length, and adequate behavioral metrics are all growing concerns with FXS translational research (Jacquemont et al., 2014).

In addition to the neuronal effects, our analyses demonstrated that the effects of these interventions are global, as Bevacizumab treatment also reduced FXS overall teste weight to WT levels. Much to our surprise treatment with the receptor blockers only partially reduced teste weight. Further analyses will be needed to elucidate the underlying mechanisms mediating this effect and how blocking VEGF-A can alleviate it.

Collectively, the studies covered in this dissertation suggest that modulating VEGF-A and its receptors, particularly VEGFR2 and VEGFR3 can alter FXS behavioral, cellular and molecular properties. However, the observed rescue in FXS behavioral deficits are not universal, but rather specific towards particular abnormalities. Specifically, abnormalities in hyperactivity appear to be unaffected. These studies suggest that modulation the VEGF family of molecules and their receptors could be a novel mechanism for treating certain FXS abnormalities and that a cocktail of treatments will probably be necessary to cover the spectrum of abnormalities in FXS.

REFERENCES

Achen MG, Jeltsch M, Kukk E, Makinen T, Vitali A, Wilks AF, Alitalo K, Stacker SA (1998) Vascular endothelial growth factor D (VEGF-D) is a ligand for the tyrosine kinases VEGF receptor 2 (Flk1) and VEGF receptor 3 (Flt4). Proceedings of the National Academy of Sciences of the United States of America 95:548-553.

Adriani W, Granstrem O, Macri S, Izykenova G, Dambinova S, Laviola G (2004) Behavioral and neurochemical vulnerability during adolescence in mice: studies with nicotine. Neuropsychopharmacology : official publication of the American College of Neuropsychopharmacology 29:869-878.

Alitalo K, Carmeliet P (2002) Molecular mechanisms of lymphangiogenesis in health and disease. Cancer cell 1:219-227.

Ambros V (2004) The functions of animal microRNAs. Nature 431:350-355.

Anderson BR, Chopra P, Suhl JA, Warren ST, Bassell GJ (2016) Identification of consensus binding sites clarifies FMRP binding determinants. Nucleic acids research 44:6649-6659.

Antar LN, Dictenberg JB, Plociniak M, Afroz R, Bassell GJ (2005) Localization of FMRP-associated mRNA granules and requirement of microtubules for activity-dependent trafficking in hippocampal neurons. Genes, brain, and behavior 4:350-359.

Antar LN, Li C, Zhang H, Carroll RC, Bassell GJ (2006) Local functions for FMRP in axon growth cone motility and activity-dependent regulation of filopodia and spine synapses. Molecular and cellular neurosciences 32:37-48.

Arriaga G, Jarvis ED (2013) Mouse vocal communication system: are ultrasounds learned or innate? Brain and language 124:96-116.

Arriaga G, Zhou EP, Jarvis ED (2012) Of mice, birds, and men: the mouse ultrasonic song system has some features similar to humans and song-learning birds. PloS one 7:e46610.

Ascano M, Jr., Mukherjee N, Bandaru P, Miller JB, Nusbaum JD, Corcoran DL, Langlois C, Munschauer M, Dewell S, Hafner M, Williams Z, Ohler U, Tuschl T (2012) FMRP targets distinct mRNA sequence elements to regulate protein expression. Nature 492:382-386.

Aschrafi A, Cunningham BA, Edelman GM, Vanderklish PW (2005) The fragile X mental retardation protein and group I metabotropic glutamate receptors regulate levels of mRNA granules in brain. Proceedings of the National Academy of Sciences of the United States of America 102:2180-2185.

Ashley CT, Sutcliffe JS, Kunst CB, Leiner HA, Eichler EE, Nelson DL, Warren ST (1993) Human and murine FMR-1: alternative splicing and translational initiation downstream of the CGG-repeat. Nature genetics 4:244-251.

Aspelund A, Antila S, Proulx ST, Karlsen TV, Karaman S, Detmar M, Wiig H, Alitalo K (2015) A dural lymphatic vascular system that drains brain interstitial fluid and macromolecules. The Journal of experimental medicine 212:991-999.

Bailey DB, Jr., Raspa M, Bishop E, Olmsted M, Mallya UG, Berry-Kravis E (2012) Medication utilization for targeted symptoms in children and adults with fragile X syndrome: US survey. Journal of developmental and behavioral pediatrics : JDBP 33:62-69.

Bakker CE, Verheij C, Willemsen R, van der Helm R, Oerlemans F, Vermey M, Bygrave A, Hoogeveen A, Oostra BA (1994) Fmr1 knockout mice: a model to study fragile X mental retardation. The Dutch-Belgian Fragile X Consortium. Cell 78:23-33.

Balci TA, Ciftci I, Kabakus N, Aydin M (2006) Enhanced perfusion in eyes and cerebral perfusion defects in a patient with Fragile X Syndrome. The Tohoku journal of experimental medicine 210:169-173.
Baldwin ME, Roufail S, Halford MM, Alitalo K, Stacker SA, Achen MG (2001) Multiple forms of mouse vascular endothelial growth factor-D are generated by RNA splicing and proteolysis. The Journal of biological chemistry 276:44307-44314.
Banerjee P, Schoenfeld BP, Bell AJ, Choi CH, Bradley MP, Hinchey P, Kollaros M, Park JH, McBride SM, Dockendorff TC (2010) Short- and long-term memory are modulated by multiple isoforms of the fragile X mental retardation protein. The Journal of neuroscience : the official journal of the Society for Neuroscience 30:6782-6792.
Barleon B, Siemeister G, Martiny-Baron G, Weindel K, Herzog C, Marme D (1997) Vascular endothelial growth factor up-regulates its receptor fms-like tyrosine kinase 1 (FLT-1) and a soluble variant of FLT-1 in human vascular endothelial cells. Cancer research 57:5421-5425.
Bartel DP (2004) MicroRNAs: genomics, biogenesis, mechanism, and function. Cell 116:281-297.
Bear MF, Huber KM, Warren ST (2004) The mGluR theory of fragile X mental retardation. Trends in neurosciences 27:370-377.
Belagodu AP, Johnson AM, Galvez R (2016) Characterization of ultrasonic vocalizations of Fragile X mice. Behavioural brain research 310:76-83.
Belagodu AP, Zendeli L, Slater BJ, Galvez R (2017) Blocking elevated VEGF-A attenuates non-vasculature Fragile X syndrome abnormalities. Developmental neurobiology 77:14-25.
Belser RC, Sudhalter V (2001) Conversational characteristics of children with fragile X syndrome: repetitive speech. American journal of mental retardation : AJMR 106:28-38.
Berry-Kravis E (2002) Epilepsy in fragile X syndrome. Developmental medicine and child neurology 44:724-728.
Berry-Kravis E, Sumis A, Kim OK, Lara R, Wuu J (2008) Characterization of potential outcome measures for future clinical trials in fragile X syndrome. Journal of autism and developmental disorders 38:1751-1757.
Berry-Kravis E, Hessl D, Abbeduto L, Reiss AL, Beckel-Mitchener A, Urv TK, Outcome Measures Working G (2013) Outcome measures for clinical trials in fragile X syndrome. Journal of developmental and behavioral pediatrics : JDBP 34:508-522.
Berry-Kravis E, Hessl D, Coffey S, Hervey C, Schneider A, Yuhas J, Hutchison J, Snape M, Tranfaglia M, Nguyen DV, Hagerman R (2009) A pilot open label, single dose trial of fenobam in adults with fragile X syndrome. Journal of medical genetics 46:266-271.
Bhattacharya A, Kaphzan H, Alvarez-Dieppa AC, Murphy JP, Pierre P, Klann E (2012) Genetic removal of p70 S6 kinase 1 corrects molecular, synaptic, and behavioral phenotypes in fragile X syndrome mice. Neuron 76:325-337.
Bhattacharya A, Mamcarz M, Mullins C, Choudhury A, Boyle RG, Smith DG, Walker DW, Klann E (2016) Targeting Translation Control with p70 S6 Kinase 1 Inhibitors to Reverse Phenotypes in Fragile X Syndrome Mice. Neuropsychopharmacology : official publication of the American College of Neuropsychopharmacology 41:1991-2000.
Bilousova TV, Dansie L, Ngo M, Aye J, Charles JR, Ethell DW, Ethell IM (2009) Minocycline promotes dendritic spine maturation and improves behavioural performance in the fragile X mouse model. Journal of medical genetics 46:94-102.

Bolduc FV, Bell K, Cox H, Broadie KS, Tully T (2008) Excess protein synthesis in Drosophila fragile X mutants impairs long-term memory. Nature neuroscience 11:1143-1145.
Borghgraef M, Fryns JP, Dielkens A, Pyck K, Van den Berghe H (1987) Fragile (X) syndrome: a study of the psychological profile in 23 prepubertal patients. Clinical genetics 32:179-186.
Brody SA, Conquet F, Geyer MA (2003) Disruption of prepulse inhibition in mice lacking mGluR1. The European journal of neuroscience 18:3361-3366.
Brugarolas JB, Vazquez F, Reddy A, Sellers WR, Kaelin WG, Jr. (2003) TSC2 regulates VEGF through mTOR-dependent and -independent pathways. Cancer cell 4:147-158.
Burgdorf J, Panksepp J, Moskal JR (2011) Frequency-modulated 50 kHz ultrasonic vocalizations: a tool for uncovering the molecular substrates of positive affect. Neuroscience and biobehavioral reviews 35:1831-1836.
Busquets-Garcia A, Gomis-Gonzalez M, Guegan T, Agustin-Pavon C, Pastor A, Mato S, Perez-Samartin A, Matute C, de la Torre R, Dierssen M, Maldonado R, Ozaita A (2013) Targeting the endocannabinoid system in the treatment of fragile X syndrome. Nature medicine 19:603-607.
Carmeliet P, Storkebaum E (2002) Vascular and neuronal effects of VEGF in the nervous system: implications for neurological disorders. Seminars in cell & developmental biology 13:39-53.
Carmeliet P, Ferreira V, Breier G, Pollefeyt S, Kieckens L, Gertsenstein M, Fahrig M, Vandenhoeck A, Harpal K, Eberhardt C, Declercq C, Pawling J, Moons L, Collen D, Risau W, Nagy A (1996) Abnormal blood vessel development and lethality in embryos lacking a single VEGF allele. Nature 380:435-439.
Carmeliet P et al. (2001) Synergism between vascular endothelial growth factor and placental growth factor contributes to angiogenesis and plasma extravasation in pathological conditions. Nature medicine 7:575-583.
Carroll RC, Lissin DV, von Zastrow M, Nicoll RA, Malenka RC (1999) Rapid redistribution of glutamate receptors contributes to long-term depression in hippocampal cultures. Nature neuroscience 2:454-460.
Castren M, Paakkonen A, Tarkka IM, Ryynanen M, Partanen J (2003) Augmentation of auditory N1 in children with fragile X syndrome. Brain topography 15:165-171.
Caudy AA, Myers M, Hannon GJ, Hammond SM (2002) Fragile X-related protein and VIG associate with the RNA interference machinery. Genes & development 16:2491-2496.
Cesca F, Baldelli P, Valtorta F, Benfenati F (2010) The synapsins: key actors of synapse function and plasticity. Progress in neurobiology 91:313-348.
Chang S, Bray SM, Li Z, Zarnescu DC, He C, Jin P, Warren ST (2008) Identification of small molecules rescuing fragile X syndrome phenotypes in Drosophila. Nature chemical biology 4:256-263.
Chapman AG, Nanan K, Williams M, Meldrum BS (2000) Anticonvulsant activity of two metabotropic glutamate group I antagonists selective for the mGlu5 receptor: 2-methyl-6-(phenylethynyl)-pyridine (MPEP), and (E)-6-methyl-2-styryl-pyridine (SIB 1893). Neuropharmacology 39:1567-1574.
Chen L, Toth M (2001) Fragile X mice develop sensory hyperreactivity to auditory stimuli. Neuroscience 103:1043-1050.

Choi CH et al. (2015) PDE-4 inhibition rescues aberrant synaptic plasticity in Drosophila and mouse models of fragile X syndrome. The Journal of neuroscience : the official journal of the Society for Neuroscience 35:396-408.
Chu Z, Hablitz JJ (2000) Quisqualate induces an inward current via mGluR activation in neocortical pyramidal neurons. Brain research 879:88-92.
Chua CC, Hamdy RC, Chua BH (1998) Upregulation of vascular endothelial growth factor by H2O2 in rat heart endothelial cells. Free radical biology & medicine 25:891-897.
Chuang SC, Zhao W, Bauchwitz R, Yan Q, Bianchi R, Wong RK (2005) Prolonged epileptiform discharges induced by altered group I metabotropic glutamate receptor-mediated synaptic responses in hippocampal slices of a fragile X mouse model. The Journal of neuroscience : the official journal of the Society for Neuroscience 25:8048-8055.
Chubykin AA, Roach EB, Bear MF, Shuler MG (2013) A cholinergic mechanism for reward timing within primary visual cortex. Neuron 77:723-735.
Cooke SF, Bear MF (2010) Visual experience induces long-term potentiation in the primary visual cortex. The Journal of neuroscience : the official journal of the Society for Neuroscience 30:16304-16313.
Cooke SF, Bear MF (2012) Stimulus-selective response plasticity in the visual cortex: an assay for the assessment of pathophysiology and treatment of cognitive impairment associated with psychiatric disorders. Biological psychiatry 71:487-495.
Cordeiro L, Ballinger E, Hagerman R, Hessl D (2011) Clinical assessment of DSM-IV anxiety disorders in fragile X syndrome: prevalence and characterization. Journal of neurodevelopmental disorders 3:57-67.
Cornish K, Turk J, Hagerman R (2008) The fragile X continuum: new advances and perspectives. Journal of intellectual disability research : JIDR 52:469-482.
Cornish KM, Turk J, Wilding J, Sudhalter V, Munir F, Kooy F, Hagerman R (2004) Annotation: Deconstructing the attention deficit in fragile X syndrome: a developmental neuropsychological approach. Journal of child psychology and psychiatry, and allied disciplines 45:1042-1053.
Dahlhaus M, Li KW, van der Schors RC, Saiepour MH, van Nierop P, Heimel JA, Hermans JM, Loos M, Smit AB, Levelt CN (2011) The synaptic proteome during development and plasticity of the mouse visual cortex. Molecular & cellular proteomics : MCP 10:M110 005413.
Dansie LE, Phommahaxay K, Okusanya AG, Uwadia J, Huang M, Rotschafer SE, Razak KA, Ethell DW, Ethell IM (2013) Long-lasting effects of minocycline on behavior in young but not adult Fragile X mice. Neuroscience 246:186-198.
Darnell JC, Jensen KB, Jin P, Brown V, Warren ST, Darnell RB (2001) Fragile X mental retardation protein targets G quartet mRNAs important for neuronal function. Cell 107:489-499.
Darnell JC, Fraser CE, Mostovetsky O, Stefani G, Jones TA, Eddy SR, Darnell RB (2005) Kissing complex RNAs mediate interaction between the Fragile-X mental retardation protein KH2 domain and brain polyribosomes. Genes & development 19:903-918.
Darnell JC, Van Driesche SJ, Zhang C, Hung KY, Mele A, Fraser CE, Stone EF, Chen C, Fak JJ, Chi SW, Licatalosi DD, Richter JD, Darnell RB (2011) FMRP stalls ribosomal translocation on mRNAs linked to synaptic function and autism. Cell 146:247-261.
De Bandt M, Ben Mahdi MH, Ollivier V, Grossin M, Dupuis M, Gaudry M, Bohlen P, Lipson KE, Rice A, Wu Y, Gougerot-Pocidalo MA, Pasquier C (2003) Blockade of vascular

endothelial growth factor receptor I (VEGF-RI), but not VEGF-RII, suppresses joint destruction in the K/BxN model of rheumatoid arthritis. Journal of immunology 171:4853-4859.
De Boulle K, Verkerk AJ, Reyniers E, Vits L, Hendrickx J, Van Roy B, Van den Bos F, de Graaff E, Oostra BA, Willems PJ (1993) A point mutation in the FMR-1 gene associated with fragile X mental retardation. Nature genetics 3:31-35.
De Felipe J, Marco P, Fairen A, Jones EG (1997) Inhibitory synaptogenesis in mouse somatosensory cortex. Cerebral cortex 7:619-634.
De Rossi P, Harde E, Dupuis JP, Martin L, Chounlamountri N, Bardin M, Watrin C, Benetollo C, Pernet-Gallay K, Luhmann HJ, Honnorat J, Malleret G, Groc L, Acker-Palmer A, Salin PA, Meissirel C (2016) A critical role for VEGF and VEGFR2 in NMDA receptor synaptic function and fear-related behavior. Molecular psychiatry.
de Vries C, Escobedo JA, Ueno H, Houck K, Ferrara N, Williams LT (1992) The fms-like tyrosine kinase, a receptor for vascular endothelial growth factor. Science 255:989-991.
de Vrij FM, Levenga J, van der Linde HC, Koekkoek SK, De Zeeuw CI, Nelson DL, Oostra BA, Willemsen R (2008) Rescue of behavioral phenotype and neuronal protrusion morphology in Fmr1 KO mice. Neurobiology of disease 31:127-132.
Deacon RM (2006) Digging and marble burying in mice: simple methods for in vivo identification of biological impacts. Nature protocols 1:122-124.
Devys D, Lutz Y, Rouyer N, Bellocq JP, Mandel JL (1993) The FMR-1 protein is cytoplasmic, most abundant in neurons and appears normal in carriers of a fragile X premutation. Nature genetics 4:335-340.
Dias S, Hattori K, Heissig B, Zhu Z, Wu Y, Witte L, Hicklin DJ, Tateno M, Bohlen P, Moore MA, Rafii S (2001) Inhibition of both paracrine and autocrine VEGF/ VEGFR-2 signaling pathways is essential to induce long-term remission of xenotransplanted human leukemias. Proceedings of the National Academy of Sciences of the United States of America 98:10857-10862.
Dockendorff TC, Su HS, McBride SM, Yang Z, Choi CH, Siwicki KK, Sehgal A, Jongens TA (2002) Drosophila lacking dfmr1 activity show defects in circadian output and fail to maintain courtship interest. Neuron 34:973-984.
Dodd KM, Yang J, Shen MH, Sampson JR, Tee AR (2015) mTORC1 drives HIF-1alpha and VEGF-A signalling via multiple mechanisms involving 4E-BP1, S6K1 and STAT3. Oncogene 34:2239-2250.
Dolan BM, Duron SG, Campbell DA, Vollrath B, Shankaranarayana Rao BS, Ko HY, Lin GG, Govindarajan A, Choi SY, Tonegawa S (2013) Rescue of fragile X syndrome phenotypes in Fmr1 KO mice by the small-molecule PAK inhibitor FRAX486. Proceedings of the National Academy of Sciences of the United States of America 110:5671-5676.
Dolen G, Osterweil E, Rao BS, Smith GB, Auerbach BD, Chattarji S, Bear MF (2007) Correction of fragile X syndrome in mice. Neuron 56:955-962.
Dumont DJ, Jussila L, Taipale J, Lymboussaki A, Mustonen T, Pajusola K, Breitman M, Alitalo K (1998) Cardiovascular failure in mouse embryos deficient in VEGF receptor-3. Science 282:946-949.
Dvorak HF (2002) Vascular permeability factor/vascular endothelial growth factor: a critical cytokine in tumor angiogenesis and a potential target for diagnosis and therapy. Journal of clinical oncology : official journal of the American Society of Clinical Oncology 20:4368-4380.

Edbauer D, Neilson JR, Foster KA, Wang CF, Seeburg DP, Batterton MN, Tada T, Dolan BM, Sharp PA, Sheng M (2010) Regulation of synaptic structure and function by FMRP-associated microRNAs miR-125b and miR-132. Neuron 65:373-384.
Ennaceur A (2014) Tests of unconditioned anxiety - pitfalls and disappointments. Physiology & behavior 135:55-71.
Feletou M (2011) In: The Endothelium: Part 1: Multiple Functions of the Endothelial Cells-Focus on Endothelium-Derived Vasoactive Mediators. San Rafael (CA).
Ferrara N, Gerber HP, LeCouter J (2003) The biology of VEGF and its receptors. Nature medicine 9:669-676.
Ferrara N, Carver-Moore K, Chen H, Dowd M, Lu L, O'Shea KS, Powell-Braxton L, Hillan KJ, Moore MW (1996) Heterozygous embryonic lethality induced by targeted inactivation of the VEGF gene. Nature 380:439-442.
Ferrier LJ, Bashir AS, Meryash DL, Johnston J, Wolff P (1991) Conversational skills of individuals with fragile-X syndrome: a comparison with autism and Down syndrome. Developmental medicine and child neurology 33:776-788.
Floody OR, DeBold JF (2004) Effects of midbrain lesions on lordosis and ultrasound production. Physiology & behavior 82:791-804.
Fong GH, Rossant J, Gertsenstein M, Breitman ML (1995) Role of the Flt-1 receptor tyrosine kinase in regulating the assembly of vascular endothelium. Nature 376:66-70.
Frenkel MY, Sawtell NB, Diogo AC, Yoon B, Neve RL, Bear MF (2006) Instructive effect of visual experience in mouse visual cortex. Neuron 51:339-349.
Fu YH, Kuhl DP, Pizzuti A, Pieretti M, Sutcliffe JS, Richards S, Verkerk AJ, Holden JJ, Fenwick RG, Jr., Warren ST, et al. (1991) Variation of the CGG repeat at the fragile X site results in genetic instability: resolution of the Sherman paradox. Cell 67:1047-1058.
Galea I, Bechmann I, Perry VH (2007) What is immune privilege (not)? Trends in immunology 28:12-18.
Galvan AM, Galvez R (2012) Neocortical vasculature abnormalities in the Fragile X mental retardation syndrome. Brain research 1471:155-161.
Galvez R, Greenough WT (2005) Sequence of abnormal dendritic spine development in primary somatosensory cortex of a mouse model of the fragile X mental retardation syndrome. American journal of medical genetics Part A 135:155-160.
Galvez R, Gopal AR, Greenough WT (2003) Somatosensory cortical barrel dendritic abnormalities in a mouse model of the fragile X mental retardation syndrome. Brain research 971:83-89.
Gasparini F, Lingenhohl K, Stoehr N, Flor PJ, Heinrich M, Vranesic I, Biollaz M, Allgeier H, Heckendorn R, Urwyler S, Varney MA, Johnson EC, Hess SD, Rao SP, Sacaan AI, Santori EM, Velicelebi G, Kuhn R (1999) 2-Methyl-6-(phenylethynyl)-pyridine (MPEP), a potent, selective and systemically active mGlu5 receptor antagonist. Neuropharmacology 38:1493-1503.
Gaub S, Groszer M, Fisher SE, Ehret G (2010) The structure of innate vocalizations in Foxp2-deficient mouse pups. Genes, brain, and behavior 9:390-401.
Gavornik JP, Bear MF (2014) Learned spatiotemporal sequence recognition and prediction in primary visual cortex. Nature neuroscience 17:732-737.
Gholizadeh S, Arsenault J, Xuan IC, Pacey LK, Hampson DR (2014) Reduced phenotypic severity following adeno-associated virus-mediated Fmr1 gene delivery in fragile X

mice. Neuropsychopharmacology : official publication of the American College of Neuropsychopharmacology 39:3100-3111.
Gkogkas CG, Khoutorsky A, Cao R, Jafarnejad SM, Prager-Khoutorsky M, Giannakas N, Kaminari A, Fragkouli A, Nader K, Price TJ, Konicek BW, Graff JR, Tzinia AK, Lacaille JC, Sonenberg N (2014) Pharmacogenetic inhibition of eIF4E-dependent Mmp9 mRNA translation reverses fragile X syndrome-like phenotypes. Cell reports 9:1742-1755.
Goldstein S, Reynolds CR (1999) Handbook of neurodevelopmental and genetic disorders in children. New York: Guilford Press.
Gothelf D, Furfaro JA, Hoeft F, Eckert MA, Hall SS, O'Hara R, Erba HW, Ringel J, Hayashi KM, Patnaik S, Golianu B, Kraemer HC, Thompson PM, Piven J, Reiss AL (2008) Neuroanatomy of fragile X syndrome is associated with aberrant behavior and the fragile X mental retardation protein (FMRP). Annals of neurology 63:40-51.
Graybiel AM (1998) The basal ganglia and chunking of action repertoires. Neurobiology of learning and memory 70:119-136.
Greenough WT, Chang FL (1988) Dendritic pattern formation involves both oriented regression and oriented growth in the barrels of mouse somatosensory cortex. Brain research 471:148-152.
Gross C, Bassell GJ (2012) Excess protein synthesis in FXS patient lymphoblastoid cells can be rescued with a p110beta-selective inhibitor. Molecular medicine 18:336-345.
Grossman AW, Elisseou NM, McKinney BC, Greenough WT (2006) Hippocampal pyramidal cells in adult Fmr1 knockout mice exhibit an immature-appearing profile of dendritic spines. Brain research 1084:158-164.
Gubellini P, Saulle E, Centonze D, Costa C, Tropepi D, Bernardi G, Conquet F, Calabresi P (2003) Corticostriatal LTP requires combined mGluR1 and mGluR5 activation. Neuropharmacology 44:8-16.
Guo W, Murthy AC, Zhang L, Johnson EB, Schaller EG, Allan AM, Zhao X (2012) Inhibition of GSK3beta improves hippocampus-dependent learning and rescues neurogenesis in a mouse model of fragile X syndrome. Human molecular genetics 21:681-691.
Hagerman RJ, Hagerman PJ (2003) Fragile X Syndrome: Diagnosis, Treatment, and Research: John Hopkins University Press, Baltimore.
Hallahan BP, Craig MC, Toal F, Daly EM, Moore CJ, Ambikapathy A, Robertson D, Murphy KC, Murphy DG (2011) In vivo brain anatomy of adult males with Fragile X syndrome: an MRI study. NeuroImage 54:16-24.
Han J, Calvo CF, Kang TH, Baker KL, Park JH, Parras C, Levittas M, Birba U, Pibouin-Fragner L, Fragner P, Bilguvar K, Duman RS, Nurmi H, Alitalo K, Eichmann AC, Thomas JL (2015) Vascular endothelial growth factor receptor 3 controls neural stem cell activation in mice and humans. Cell reports 10:1158-1172.
Hanover JL, Huang ZJ, Tonegawa S, Stryker MP (1999) Brain-derived neurotrophic factor overexpression induces precocious critical period in mouse visual cortex. The Journal of neuroscience : the official journal of the Society for Neuroscience 19:RC40.
Hazlett HC, Poe MD, Lightbody AA, Styner M, MacFall JR, Reiss AL, Piven J (2012) Trajectories of early brain volume development in fragile X syndrome and autism. Journal of the American Academy of Child and Adolescent Psychiatry 51:921-933.

He Q, Nomura T, Xu J, Contractor A (2014) The developmental switch in GABA polarity is delayed in fragile X mice. The Journal of neuroscience : the official journal of the Society for Neuroscience 34:446-450.
Herbst DS (1980) Nonspecific X-linked mental retardation I: a review with information from 24 new families. American journal of medical genetics 7:443-460.
Hoeffer CA, Tang W, Wong H, Santillan A, Patterson RJ, Martinez LA, Tejada-Simon MV, Paylor R, Hamilton SL, Klann E (2008) Removal of FKBP12 enhances mTOR-Raptor interactions, LTP, memory, and perseverative/repetitive behavior. Neuron 60:832-845.
Hoeffer CA, Sanchez E, Hagerman RJ, Mu Y, Nguyen DV, Wong H, Whelan AM, Zukin RS, Klann E, Tassone F (2012) Altered mTOR signaling and enhanced CYFIP2 expression levels in subjects with fragile X syndrome. Genes, brain, and behavior 11:332-341.
Holy TE, Guo Z (2005) Ultrasonic songs of male mice. PLoS biology 3:e386.
Hu Y, Chen Z, Fu Y, He Q, Jiang L, Zheng J, Gao Y, Mei P, Chen Z, Ren X (2015) The amino-terminal structure of human fragile X mental retardation protein obtained using precipitant-immobilized imprinted polymers. Nature communications 6:6634.
Huang F, Chotiner JK, Steward O (2005) The mRNA for elongation factor 1alpha is localized in dendrites and translated in response to treatments that induce long-term depression. The Journal of neuroscience : the official journal of the Society for Neuroscience 25:7199-7209.
Huang H, Shen J, Vinores SA (2011) Blockade of VEGFR1 and 2 suppresses pathological angiogenesis and vascular leakage in the eye. PloS one 6:e21411.
Huang ZJ, Kirkwood A, Pizzorusso T, Porciatti V, Morales B, Bear MF, Maffei L, Tonegawa S (1999) BDNF regulates the maturation of inhibition and the critical period of plasticity in mouse visual cortex. Cell 98:739-755.
Huber KM, Kayser MS, Bear MF (2000) Role for rapid dendritic protein synthesis in hippocampal mGluR-dependent long-term depression. Science 288:1254-1257.
Huber KM, Roder JC, Bear MF (2001) Chemical induction of mGluR5- and protein synthesis--dependent long-term depression in hippocampal area CA1. Journal of neurophysiology 86:321-325.
Iliff JJ, Wang M, Liao Y, Plogg BA, Peng W, Gundersen GA, Benveniste H, Vates GE, Deane R, Goldman SA, Nagelhus EA, Nedergaard M (2012) A paravascular pathway facilitates CSF flow through the brain parenchyma and the clearance of interstitial solutes, including amyloid beta. Science translational medicine 4:147ra111.
Incorpora G, Sorge G, Sorge A, Pavone L (2002) Epilepsy in fragile X syndrome. Brain & development 24:766-769.
Inoue S, Shimoda M, Nishinokubi I, Siomi MC, Okamura M, Nakamura A, Kobayashi S, Ishida N, Siomi H (2002) A role for the Drosophila fragile X-related gene in circadian output. Current biology : CB 12:1331-1335.
Irwin SA, Galvez R, Greenough WT (2000) Dendritic spine structural anomalies in fragile-X mental retardation syndrome. Cerebral cortex 10:1038-1044.
Irwin SA, Patel B, Idupulapati M, Harris JB, Crisostomo RA, Larsen BP, Kooy F, Willems PJ, Cras P, Kozlowski PB, Swain RA, Weiler IJ, Greenough WT (2001) Abnormal dendritic spine characteristics in the temporal and visual cortices of patients with fragile-X syndrome: a quantitative examination. American journal of medical genetics 98:161-167.
Irwin SA, Idupulapati M, Gilbert ME, Harris JB, Chakravarti AB, Rogers EJ, Crisostomo RA, Larsen BP, Mehta A, Alcantara CJ, Patel B, Swain RA, Weiler IJ, Oostra BA, Greenough

WT (2002) Dendritic spine and dendritic field characteristics of layer V pyramidal neurons in the visual cortex of fragile-X knockout mice. American journal of medical genetics 111:140-146.
Jacquemont S, Berry-Kravis E, Hagerman R, von Raison F, Gasparini F, Apostol G, Ufer M, Des Portes V, Gomez-Mancilla B (2014) The challenges of clinical trials in fragile X syndrome. Psychopharmacology 231:1237-1250.
Jacquemont S et al. (2011) Epigenetic modification of the FMR1 gene in fragile X syndrome is associated with differential response to the mGluR5 antagonist AFQ056. Science translational medicine 3:64ra61.
Jamain S, Radyushkin K, Hammerschmidt K, Granon S, Boretius S, Varoqueaux F, Ramanantsoa N, Gallego J, Ronnenberg A, Winter D, Frahm J, Fischer J, Bourgeron T, Ehrenreich H, Brose N (2008) Reduced social interaction and ultrasonic communication in a mouse model of monogenic heritable autism. Proceedings of the National Academy of Sciences of the United States of America 105:1710-1715.
Jeltsch M, Kaipainen A, Joukov V, Meng X, Lakso M, Rauvala H, Swartz M, Fukumura D, Jain RK, Alitalo K (1997) Hyperplasia of lymphatic vessels in VEGF-C transgenic mice. Science 276:1423-1425.
Jin K, Mao XO, Greenberg DA (2006) Vascular endothelial growth factor stimulates neurite outgrowth from cerebral cortical neurons via Rho kinase signaling. Journal of neurobiology 66:236-242.
Jin K, Zhu Y, Sun Y, Mao XO, Xie L, Greenberg DA (2002) Vascular endothelial growth factor (VEGF) stimulates neurogenesis in vitro and in vivo. Proceedings of the National Academy of Sciences of the United States of America 99:11946-11950.
Jin KL, Mao XO, Greenberg DA (2000) Vascular endothelial growth factor rescues HN33 neural cells from death induced by serum withdrawal. Journal of molecular neuroscience : MN 14:197-203.
Josko J, Gwozdz B, Jedrzejowska-Szypulka H, Hendryk S (2000) Vascular endothelial growth factor (VEGF) and its effect on angiogenesis. Medical science monitor : international medical journal of experimental and clinical research 6:1047-1052.
Joukov V, Pajusola K, Kaipainen A, Chilov D, Lahtinen I, Kukk E, Saksela O, Kalkkinen N, Alitalo K (1996) A novel vascular endothelial growth factor, VEGF-C, is a ligand for the Flt4 (VEGFR-3) and KDR (VEGFR-2) receptor tyrosine kinases. The EMBO journal 15:290-298.
Jurgens U (1998) Neuronal control of mammalian vocalization, with special reference to the squirrel monkey. Die Naturwissenschaften 85:376-388.
Jurgens U, Ehrenreich L (2007) The descending motorcortical pathway to the laryngeal motoneurons in the squirrel monkey. Brain research 1148:90-95.
Kabakus N, Aydin M, Akin H, Balci TA, Kurt A, Kekilli E (2006) Fragile X syndrome and cerebral perfusion abnormalities: single-photon emission computed tomographic study. Journal of child neurology 21:1040-1046.
Karkkainen MJ, Makinen T, Alitalo K (2002) Lymphatic endothelium: a new frontier of metastasis research. Nature cell biology 4:E2-5.
Kazdoba TM, Leach PT, Silverman JL, Crawley JN (2014) Modeling fragile X syndrome in the Fmr1 knockout mouse. Intractable & rare diseases research 3:118-133.
Kirzinger A, Jurgens U (1985) The effects of brainstem lesions on vocalization in the squirrel monkey. Brain research 358:150-162.

Koga K, Liu MG, Qiu S, Song Q, O'Den G, Chen T, Zhuo M (2015) Impaired presynaptic long-term potentiation in the anterior cingulate cortex of Fmr1 knock-out mice. The Journal of neuroscience : the official journal of the Society for Neuroscience 35:2033-2043.

Kooy RF, D'Hooge R, Reyniers E, Bakker CE, Nagels G, De Boulle K, Storm K, Clincke G, De Deyn PP, Oostra BA, Willems PJ (1996) Transgenic mouse model for the fragile X syndrome. American journal of medical genetics 64:241-245.

Koyama Y, Hayashi M, Nagae R, Tokuyama S, Konishi T (2014) Endothelin-1 increases the expression of VEGF-R1/Flt-1 receptors in rat cultured astrocytes through ETB receptors. Journal of neurochemistry 130:759-769.

Kronk R, Bishop EE, Raspa M, Bickel JO, Mandel DA, Bailey DB, Jr. (2010) Prevalence, nature, and correlates of sleep problems among children with fragile X syndrome based on a large scale parent survey. Sleep 33:679-687.

Krum JM, Mani N, Rosenstein JM (2008) Roles of the endogenous VEGF receptors flt-1 and flk-1 in astroglial and vascular remodeling after brain injury. Experimental neurology 212:108-117.

Kukk E, Lymboussaki A, Taira S, Kaipainen A, Jeltsch M, Joukov V, Alitalo K (1996) VEGF-C receptor binding and pattern of expression with VEGFR-3 suggests a role in lymphatic vascular development. Development 122:3829-3837.

Kumari D, Bhattacharya A, Nadel J, Moulton K, Zeak NM, Glicksman A, Dobkin C, Brick DJ, Schwartz PH, Smith CB, Klann E, Usdin K (2014) Identification of fragile X syndrome specific molecular markers in human fibroblasts: a useful model to test the efficacy of therapeutic drugs. Human mutation 35:1485-1494.

Kunkel P, Ulbricht U, Bohlen P, Brockmann MA, Fillbrandt R, Stavrou D, Westphal M, Lamszus K (2001) Inhibition of glioma angiogenesis and growth in vivo by systemic treatment with a monoclonal antibody against vascular endothelial growth factor receptor-2. Cancer research 61:6624-6628.

Kurz A, Wohr M, Walter M, Bonin M, Auburger G, Gispert S, Schwarting RK (2010) Alpha-synuclein deficiency affects brain Foxp1 expression and ultrasonic vocalization. Neuroscience 166:785-795.

Laakkonen P, Waltari M, Holopainen T, Takahashi T, Pytowski B, Steiner P, Hicklin D, Persaud K, Tonra JR, Witte L, Alitalo K (2007) Vascular endothelial growth factor receptor 3 is involved in tumor angiogenesis and growth. Cancer research 67:593-599.

Laggerbauer B, Ostareck D, Keidel EM, Ostareck-Lederer A, Fischer U (2001) Evidence that fragile X mental retardation protein is a negative regulator of translation. Human molecular genetics 10:329-338.

Lai JK, Sobala-Drozdowski M, Zhou L, Doering LC, Faure PA, Foster JA (2014) Temporal and spectral differences in the ultrasonic vocalizations of fragile X knock out mice during postnatal development. Behavioural brain research 259:119-130.

Largo RH, Schinzel A (1985) Developmental and behavioural disturbances in 13 boys with fragile X syndrome. European journal of pediatrics 143:269-275.

Lee J, Gray A, Yuan J, Luoh SM, Avraham H, Wood WI (1996) Vascular endothelial growth factor-related protein: a ligand and specific activator of the tyrosine kinase receptor Flt4. Proceedings of the National Academy of Sciences of the United States of America 93:1988-1992.

Leigh MJ, Nguyen DV, Mu Y, Winarni TI, Schneider A, Chechi T, Polussa J, Doucet P, Tassone F, Rivera SM, Hessl D, Hagerman RJ (2013) A randomized double-blind, placebo-

controlled trial of minocycline in children and adolescents with fragile x syndrome. Journal of developmental and behavioral pediatrics : JDBP 34:147-155.
Levelt CN, Hubener M (2012) Critical-period plasticity in the visual cortex. Annual review of neuroscience 35:309-330.
Li G, Shan C, Liu L, Zhou T, Zhou J, Hu X, Chen Y, Cui H, Gao N (2015) Tanshinone IIA inhibits HIF-1alpha and VEGF expression in breast cancer cells via mTOR/p70S6K/RPS6/4E-BP1 signaling pathway. PloS one 10:e0117440.
Li J, Pelletier MR, Perez Velazquez JL, Carlen PL (2002) Reduced cortical synaptic plasticity and GluR1 expression associated with fragile X mental retardation protein deficiency. Molecular and cellular neurosciences 19:138-151.
Li Y, Stockton ME, Bhuiyan I, Eisinger BE, Gao Y, Miller JL, Bhattacharyya A, Zhao X (2016) MDM2 inhibition rescues neurogenic and cognitive deficits in a mouse model of fragile X syndrome. Science translational medicine 8:336ra361.
Lindemann L et al. (2015) Pharmacology of basimglurant (RO4917523, RG7090), a unique metabotropic glutamate receptor 5 negative allosteric modulator in clinical development for depression. The Journal of pharmacology and experimental therapeutics 353:213-233.
Liu ZH, Chuang DM, Smith CB (2011) Lithium ameliorates phenotypic deficits in a mouse model of fragile X syndrome. The international journal of neuropsychopharmacology / official scientific journal of the Collegium Internationale Neuropsychopharmacologicum 14:618-630.
Liu ZH, Huang T, Smith CB (2012) Lithium reverses increased rates of cerebral protein synthesis in a mouse model of fragile X syndrome. Neurobiology of disease 45:1145-1152.
Loesch D, Hagerman R (2012) Unstable mutations in the FMR1 gene and the phenotypes. Advances in experimental medicine and biology 769:78-114.
Louveau A, Smirnov I, Keyes TJ, Eccles JD, Rouhani SJ, Peske JD, Derecki NC, Castle D, Mandell JW, Lee KS, Harris TH, Kipnis J (2015) Structural and functional features of central nervous system lymphatic vessels. Nature 523:337-341.
Lu KV, Chang JP, Parachoniak CA, Pandika MM, Aghi MK, Meyronet D, Isachenko N, Fouse SD, Phillips JJ, Cheresh DA, Park M, Bergers G (2012) VEGF inhibits tumor cell invasion and mesenchymal transition through a MET/VEGFR2 complex. Cancer cell 22:21-35.
Lubs H, Travers H, Lujan E, Carroll A (1984) A large kindred with X-linked mental retardation, marker X and macroorchidism. American journal of medical genetics 17:145-157.
Luo Y, Shan G, Guo W, Smrt RD, Johnson EB, Li X, Pfeiffer RL, Szulwach KE, Duan R, Barkho BZ, Li W, Liu C, Jin P, Zhao X (2010) Fragile x mental retardation protein regulates proliferation and differentiation of adult neural stem/progenitor cells. PLoS genetics 6:e1000898.
Maenner MJ, Baker MW, Broman KW, Tian J, Barnes JK, Atkins A, McPherson E, Hong J, Brilliant MH, Mailick MR (2013) FMR1 CGG expansions: prevalence and sex ratios. American journal of medical genetics Part B, Neuropsychiatric genetics : the official publication of the International Society of Psychiatric Genetics 162B:466-473.
Matsuzaki H, Tamatani M, Yamaguchi A, Namikawa K, Kiyama H, Vitek MP, Mitsuda N, Tohyama M (2001) Vascular endothelial growth factor rescues hippocampal neurons from glutamate-induced toxicity: signal transduction cascades. FASEB journal : official

publication of the Federation of American Societies for Experimental Biology 15:1218-1220.
McBride SM, Choi CH, Wang Y, Liebelt D, Braunstein E, Ferreiro D, Sehgal A, Siwicki KK, Dockendorff TC, Nguyen HT, McDonald TV, Jongens TA (2005) Pharmacological rescue of synaptic plasticity, courtship behavior, and mushroom body defects in a Drosophila model of fragile X syndrome. Neuron 45:753-764.
McLennan Y, Polussa J, Tassone F, Hagerman R (2011) Fragile x syndrome. Current genomics 12:216-224.
McNaughton CH, Moon J, Strawderman MS, Maclean KN, Evans J, Strupp BJ (2008) Evidence for social anxiety and impaired social cognition in a mouse model of fragile X syndrome. Behavioral neuroscience 122:293-300.
Menon L, Mihailescu MR (2007) Interactions of the G quartet forming semaphorin 3F RNA with the RGG box domain of the fragile X protein family. Nucleic acids research 35:5379-5392.
Menon L, Mader SA, Mihailescu MR (2008) Fragile X mental retardation protein interactions with the microtubule associated protein 1B RNA. Rna 14:1644-1655.
Millauer B, Wizigmann-Voos S, Schnurch H, Martinez R, Moller NP, Risau W, Ullrich A (1993) High affinity VEGF binding and developmental expression suggest Flk-1 as a major regulator of vasculogenesis and angiogenesis. Cell 72:835-846.
Miller LJ, McIntosh DN, McGrath J, Shyu V, Lampe M, Taylor AK, Tassone F, Neitzel K, Stackhouse T, Hagerman RJ (1999) Electrodermal responses to sensory stimuli in individuals with fragile X syndrome: a preliminary report. American journal of medical genetics 83:268-279.
Min WW, Yuskaitis CJ, Yan Q, Sikorski C, Chen S, Jope RS, Bauchwitz RP (2009) Elevated glycogen synthase kinase-3 activity in Fragile X mice: key metabolic regulator with evidence for treatment potential. Neuropharmacology 56:463-472.
Mines MA, Yuskaitis CJ, King MK, Beurel E, Jope RS (2010) GSK3 influences social preference and anxiety-related behaviors during social interaction in a mouse model of fragile X syndrome and autism. PloS one 5:e9706.
Mirrett P, Roberts J, Price J (2003) Early intervention practices and communication intervention strategies for young males with fragile X syndrome. Language, Speech, and Hearing Services in Schools 34:320-331.
Miyashiro KY, Beckel-Mitchener A, Purk TP, Becker KG, Barret T, Liu L, Carbonetto S, Weiler IJ, Greenough WT, Eberwine J (2003) RNA cargoes associating with FMRP reveal deficits in cellular functioning in Fmr1 null mice. Neuron 37:417-431.
Monyak RE, Emerson D, Schoenfeld BP, Zheng X, Chambers DB, Rosenfelt C, Langer S, Hinchey P, Choi CH, McDonald TV, Bolduc FV, Sehgal A, McBride SM, Jongens TA (2016) Insulin signaling misregulation underlies circadian and cognitive deficits in a Drosophila fragile X model. Molecular psychiatry.
Morales J, Hiesinger PR, Schroeder AJ, Kume K, Verstreken P, Jackson FR, Nelson DL, Hassan BA (2002) Drosophila fragile X protein, DFXR, regulates neuronal morphology and function in the brain. Neuron 34:961-972.
Muddashetty RS, Kelic S, Gross C, Xu M, Bassell GJ (2007) Dysregulated metabotropic glutamate receptor-dependent translation of AMPA receptor and postsynaptic density-95 mRNAs at synapses in a mouse model of fragile X syndrome. The Journal of neuroscience : the official journal of the Society for Neuroscience 27:5338-5348.

Napoli I, Mercaldo V, Boyl PP, Eleuteri B, Zalfa F, De Rubeis S, Di Marino D, Mohr E, Massimi M, Falconi M, Witke W, Costa-Mattioli M, Sonenberg N, Achsel T, Bagni C (2008) The fragile X syndrome protein represses activity-dependent translation through CYFIP1, a new 4E-BP. Cell 134:1042-1054.

Neufeld G, Cohen T, Gengrinovitch S, Poltorak Z (1999) Vascular endothelial growth factor (VEGF) and its receptors. FASEB journal : official publication of the Federation of American Societies for Experimental Biology 13:9-22.

Neugebauer V, Chen PS, Willis WD (1999) Role of metabotropic glutamate receptor subtype mGluR1 in brief nociception and central sensitization of primate STT cells. Journal of neurophysiology 82:272-282.

Neunuebel JP, Taylor AL, Arthur BJ, Egnor SE (2015) Female mice ultrasonically interact with males during courtship displays. eLife 4.

Nielsen DM, Derber WJ, McClellan DA, Crnic LS (2002) Alterations in the auditory startle response in Fmr1 targeted mutant mouse models of fragile X syndrome. Brain research 927:8-17.

Oberle I, Rousseau F, Heitz D, Kretz C, Devys D, Hanauer A, Boue J, Bertheas MF, Mandel JL (1991) Instability of a 550-base pair DNA segment and abnormal methylation in fragile X syndrome. Science 252:1097-1102.

Ogunshola OO, Stewart WB, Mihalcik V, Solli T, Madri JA, Ment LR (2000) Neuronal VEGF expression correlates with angiogenesis in postnatal developing rat brain. Brain research Developmental brain research 119:139-153.

Ohashi H, Maruyama T, Higashi-Matsumoto H, Nomoto T, Nishimura S, Takeuchi Y (2002) A novel binding assay for metabotropic glutamate receptors using [3H] L-quisqualic acid and recombinant receptors. Zeitschrift fur Naturforschung C, Journal of biosciences 57:348-355.

Oliet SH, Malenka RC, Nicoll RA (1997) Two distinct forms of long-term depression coexist in CA1 hippocampal pyramidal cells. Neuron 18:969-982.

Olofsson B, Pajusola K, von Euler G, Chilov D, Alitalo K, Eriksson U (1996) Genomic organization of the mouse and human genes for vascular endothelial growth factor B (VEGF-B) and characterization of a second splice isoform. The Journal of biological chemistry 271:19310-19317.

Olofsson B, Korpelainen E, Pepper MS, Mandriota SJ, Aase K, Kumar V, Gunji Y, Jeltsch MM, Shibuya M, Alitalo K, Eriksson U (1998) Vascular endothelial growth factor B (VEGF-B) binds to VEGF receptor-1 and regulates plasminogen activator activity in endothelial cells. Proceedings of the National Academy of Sciences of the United States of America 95:11709-11714.

Opitz JM, Sutherland GR (1984) Conference report: International Workshop on the fragile X and X-linked mental retardation. American journal of medical genetics 17:5-94.

Osterweil EK, Krueger DD, Reinhold K, Bear MF (2010) Hypersensitivity to mGluR5 and ERK1/2 leads to excessive protein synthesis in the hippocampus of a mouse model of fragile X syndrome. The Journal of neuroscience : the official journal of the Society for Neuroscience 30:15616-15627.

Paavonen K, Puolakkainen P, Jussila L, Jahkola T, Alitalo K (2000) Vascular endothelial growth factor receptor-3 in lymphangiogenesis in wound healing. The American journal of pathology 156:1499-1504.

Padmashri R, Reiner BC, Suresh A, Spartz E, Dunaevsky A (2013) Altered structural and functional synaptic plasticity with motor skill learning in a mouse model of fragile X syndrome. The Journal of neuroscience : the official journal of the Society for Neuroscience 33:19715-19723.

Pan F, Aldridge GM, Greenough WT, Gan WB (2010) Dendritic spine instability and insensitivity to modulation by sensory experience in a mouse model of fragile X syndrome. Proceedings of the National Academy of Sciences of the United States of America 107:17768-17773.

Pan L, Broadie KS (2007) Drosophila fragile X mental retardation protein and metabotropic glutamate receptor A convergently regulate the synaptic ratio of ionotropic glutamate receptor subclasses. The Journal of neuroscience : the official journal of the Society for Neuroscience 27:12378-12389.

Pan L, Zhang YQ, Woodruff E, Broadie K (2004) The Drosophila fragile X gene negatively regulates neuronal elaboration and synaptic differentiation. Current biology : CB 14:1863-1870.

Pan L, Woodruff E, 3rd, Liang P, Broadie K (2008) Mechanistic relationships between Drosophila fragile X mental retardation protein and metabotropic glutamate receptor A signaling. Molecular and cellular neurosciences 37:747-760.

Paradee W, Melikian HE, Rasmussen DL, Kenneson A, Conn PJ, Warren ST (1999) Fragile X mouse: strain effects of knockout phenotype and evidence suggesting deficient amygdala function. Neuroscience 94:185-192.

Paribello C, Tao L, Folino A, Berry-Kravis E, Tranfaglia M, Ethell IM, Ethell DW (2010) Open-label add-on treatment trial of minocycline in fragile X syndrome. BMC neurology 10:91.

Park D, Lee S, Jun K, Hong YM, Kim DY, Kim YI, Shin HS (2003) Translation of clock rhythmicity into neural firing in suprachiasmatic nucleus requires mGluR-PLCbeta4 signaling. Nature neuroscience 6:337-338.

Park JE, Chen HH, Winer J, Houck KA, Ferrara N (1994) Placenta growth factor. Potentiation of vascular endothelial growth factor bioactivity, in vitro and in vivo, and high affinity binding to Flt-1 but not to Flk-1/KDR. The Journal of biological chemistry 269:25646-25654.

Paxinos G, Franklin, K. (2008) The Mouse Brain in Stereotaxic Coordinates: Academic Press.

Pearson CE, Tam M, Wang YH, Montgomery SE, Dar AC, Cleary JD, Nichol K (2002) Slipped-strand DNAs formed by long (CAG)*(CTG) repeats: slipped-out repeats and slip-out junctions. Nucleic acids research 30:4534-4547.

Peier AM, McIlwain KL, Kenneson A, Warren ST, Paylor R, Nelson DL (2000) (Over)correction of FMR1 deficiency with YAC transgenics: behavioral and physical features. Human molecular genetics 9:1145-1159.

Pieretti M, Zhang FP, Fu YH, Warren ST, Oostra BA, Caskey CT, Nelson DL (1991) Absence of expression of the FMR-1 gene in fragile X syndrome. Cell 66:817-822.

Pietropaolo S, Guilleminot A, Martin B, D'Amato FR, Crusio WE (2011) Genetic-background modulation of core and variable autistic-like symptoms in Fmr1 knock-out mice. PloS one 6:e17073.

Porter RH, Jaeschke G, Spooren W, Ballard TM, Buttelmann B, Kolczewski S, Peters JU, Prinssen E, Wichmann J, Vieira E, Muhlemann A, Gatti S, Mutel V, Malherbe P (2005) Fenobam: a clinically validated nonbenzodiazepine anxiolytic is a potent, selective, and

noncompetitive mGlu5 receptor antagonist with inverse agonist activity. The Journal of pharmacology and experimental therapeutics 315:711-721.
Pretto DI, Kumar M, Cao Z, Cunningham CL, Durbin-Johnson B, Qi L, Berman R, Noctor SC, Hagerman RJ, Pessah IN, Tassone F (2014) Reduced excitatory amino acid transporter 1 and metabotropic glutamate receptor 5 expression in the cerebellum of fragile X mental retardation gene 1 premutation carriers with fragile X-associated tremor/ataxia syndrome. Neurobiology of aging 35:1189-1197.
Pytowski B, Goldman J, Persaud K, Wu Y, Witte L, Hicklin DJ, Skobe M, Boardman KC, Swartz MA (2005) Complete and specific inhibition of adult lymphatic regeneration by a novel VEGFR-3 neutralizing antibody. Journal of the National Cancer Institute 97:14-21.
Radyushkin K, Hammerschmidt K, Boretius S, Varoqueaux F, El-Kordi A, Ronnenberg A, Winter D, Frahm J, Fischer J, Brose N, Ehrenreich H (2009) Neuroligin-3-deficient mice: model of a monogenic heritable form of autism with an olfactory deficit. Genes, brain, and behavior 8:416-425.
Raspa M, Bailey DB, Bishop E, Holiday D, Olmsted M (2010) Obesity, food selectivity, and physical activity in individuals with fragile X syndrome. American journal on intellectual and developmental disabilities 115:482-495.
Repicky S, Broadie K (2009) Metabotropic glutamate receptor-mediated use-dependent down-regulation of synaptic excitability involves the fragile X mental retardation protein. Journal of neurophysiology 101:672-687.
Rhoads FA (1984) Fragile-X syndrome in Hawaii: a summary of clinical experience. American journal of medical genetics 17:209-214.
Roberts J, Long SH, Malkin C, Barnes E, Skinner M, Hennon EA, Anderson K (2005) A comparison of phonological skills of boys with fragile X syndrome and Down syndrome. Journal of speech, language, and hearing research : JSLHR 48:980-995.
Roberts N, Kloos B, Cassella M, Podgrabinska S, Persaud K, Wu Y, Pytowski B, Skobe M (2006) Inhibition of VEGFR-3 activation with the antagonistic antibody more potently suppresses lymph node and distant metastases than inactivation of VEGFR-2. Cancer research 66:2650-2657.
Rodrigues SM, Bauer EP, Farb CR, Schafe GE, LeDoux JE (2002) The group I metabotropic glutamate receptor mGluR5 is required for fear memory formation and long-term potentiation in the lateral amygdala. The Journal of neuroscience : the official journal of the Society for Neuroscience 22:5219-5229.
Rotschafer SE, Trujillo MS, Dansie LE, Ethell IM, Razak KA (2012) Minocycline treatment reverses ultrasonic vocalization production deficit in a mouse model of Fragile X Syndrome. Brain research 1439:7-14.
Roy S, Watkins N, Heck D (2012) Comprehensive analysis of ultrasonic vocalizations in a mouse model of fragile X syndrome reveals limited, call type specific deficits. PloS one 7:e44816.
Sajikumar S, Frey JU (2003) Anisomycin inhibits the late maintenance of long-term depression in rat hippocampal slices in vitro. Neuroscience letters 338:147-150.
Santoro MR, Bray SM, Warren ST (2012) Molecular mechanisms of fragile X syndrome: a twenty-year perspective. Annual review of pathology 7:219-245.
Sawtell NB, Frenkel MY, Philpot BD, Nakazawa K, Tonegawa S, Bear MF (2003) NMDA receptor-dependent ocular dominance plasticity in adult visual cortex. Neuron 38:977-985.

Scharf SH, Jaeschke G, Wettstein JG, Lindemann L (2015) Metabotropic glutamate receptor 5 as drug target for Fragile X syndrome. Current opinion in pharmacology 20:124-134.
Schiera G, Proia P, Alberti C, Mineo M, Savettieri G, Di Liegro I (2007) Neurons produce FGF2 and VEGF and secrete them at least in part by shedding extracellular vesicles. Journal of cellular and molecular medicine 11:1384-1394.
Seese RR, Wang K, Yao YQ, Lynch G, Gall CM (2014) Spaced training rescues memory and ERK1/2 signaling in fragile X syndrome model mice. Proceedings of the National Academy of Sciences of the United States of America 111:16907-16912.
Selvaraj D, Gangadharan V, Michalski CW, Kurejova M, Stosser S, Srivastava K, Schweizerhof M, Waltenberger J, Ferrara N, Heppenstall P, Shibuya M, Augustin HG, Kuner R (2015) A Functional Role for VEGFR1 Expressed in Peripheral Sensory Neurons in Cancer Pain. Cancer cell 27:780-796.
Shang Y, Wang H, Mercaldo V, Li X, Chen T, Zhuo M (2009) Fragile X mental retardation protein is required for chemically-induced long-term potentiation of the hippocampus in adult mice. Journal of neurochemistry 111:635-646.
Sharma A, Hoeffer CA, Takayasu Y, Miyawaki T, McBride SM, Klann E, Zukin RS (2010) Dysregulation of mTOR signaling in fragile X syndrome. The Journal of neuroscience : the official journal of the Society for Neuroscience 30:694-702.
Shuler MG, Bear MF (2006) Reward timing in the primary visual cortex. Science 311:1606-1609.
Silverman WF, Krum JM, Mani N, Rosenstein JM (1999) Vascular, glial and neuronal effects of vascular endothelial growth factor in mesencephalic explant cultures. Neuroscience 90:1529-1541.
Siomi H, Siomi MC, Nussbaum RL, Dreyfuss G (1993) The protein product of the fragile X gene, FMR1, has characteristics of an RNA-binding protein. Cell 74:291-298.
Slegtenhorst-Eegdeman KE, de Rooij DG, Verhoef-Post M, van de Kant HJ, Bakker CE, Oostra BA, Grootegoed JA, Themmen AP (1998) Macroorchidism in FMR1 knockout mice is caused by increased Sertoli cell proliferation during testicular development. Endocrinology 139:156-162.
Smeets HJ, Smits AP, Verheij CE, Theelen JP, Willemsen R, van de Burgt I, Hoogeveen AT, Oosterwijk JC, Oostra BA (1995) Normal phenotype in two brothers with a full FMR1 mutation. Human molecular genetics 4:2103-2108.
Snyder EM, Philpot BD, Huber KM, Dong X, Fallon JR, Bear MF (2001) Internalization of ionotropic glutamate receptors in response to mGluR activation. Nature neuroscience 4:1079-1085.
Sondell M, Lundborg G, Kanje M (1999) Vascular endothelial growth factor has neurotrophic activity and stimulates axonal outgrowth, enhancing cell survival and Schwann cell proliferation in the peripheral nervous system. The Journal of neuroscience : the official journal of the Society for Neuroscience 19:5731-5740.
Sondell M, Sundler F, Kanje M (2000) Vascular endothelial growth factor is a neurotrophic factor which stimulates axonal outgrowth through the flk-1 receptor. The European journal of neuroscience 12:4243-4254.
Sourdet V, Russier M, Daoudal G, Ankri N, Debanne D (2003) Long-term enhancement of neuronal excitability and temporal fidelity mediated by metabotropic glutamate receptor subtype 5. The Journal of neuroscience : the official journal of the Society for Neuroscience 23:10238-10248.

Spencer CM, Alekseyenko O, Serysheva E, Yuva-Paylor LA, Paylor R (2005) Altered anxiety-related and social behaviors in the Fmr1 knockout mouse model of fragile X syndrome. Genes, brain, and behavior 4:420-430.

Spencer CM, Alekseyenko O, Hamilton SM, Thomas AM, Serysheva E, Yuva-Paylor LA, Paylor R (2011) Modifying behavioral phenotypes in Fmr1KO mice: genetic background differences reveal autistic-like responses. Autism research : official journal of the International Society for Autism Research 4:40-56.

Spiridogliozzi GA, Lachiewicz AM, Mirrett P, McConkie-Rosell A (2000) Fragile X syndrome in young children. In: Handbook of early language impairment in children: Nature (Layton TL, Crais ER, R.Watson L, eds). Delmar: Thomson Learning.

Stefani G, Fraser CE, Darnell JC, Darnell RB (2004) Fragile X mental retardation protein is associated with translating polyribosomes in neuronal cells. The Journal of neuroscience : the official journal of the Society for Neuroscience 24:7272-7276.

Sudhof TC, Czernik AJ, Kao HT, Takei K, Johnston PA, Horiuchi A, Kanazir SD, Wagner MA, Perin MS, De Camilli P, et al. (1989) Synapsins: mosaics of shared and individual domains in a family of synaptic vesicle phosphoproteins. Science 245:1474-1480.

Sun MK, Hongpaisan J, Lim CS, Alkon DL (2014) Bryostatin-1 restores hippocampal synapses and spatial learning and memory in adult fragile x mice. The Journal of pharmacology and experimental therapeutics 349:393-401.

Sutcliffe JS, Nelson DL, Zhang F, Pieretti M, Caskey CT, Saxe D, Warren ST (1992) DNA methylation represses FMR-1 transcription in fragile X syndrome. Human molecular genetics 1:397-400.

Tachibana T, Endoh M, Kumakami R, Nawa T (2003) Immunohistochemical expressions of mGluR5, P2Y2 receptor, PLC-beta1, and IP3R-I and -II in Merkel cells in rat sinus hair follicles. Histochemistry and cell biology 120:13-21.

Tatarczynska E, Klodzinska A, Chojnacka-Wojcik E, Palucha A, Gasparini F, Kuhn R, Pilc A (2001) Potential anxiolytic- and antidepressant-like effects of MPEP, a potent, selective and systemically active mGlu5 receptor antagonist. British journal of pharmacology 132:1423-1430.

Telias M, Segal M, Ben-Yosef D (2013) Neural differentiation of Fragile X human Embryonic Stem Cells reveals abnormal patterns of development despite successful neurogenesis. Developmental biology 374:32-45.

Thomas A, Burant A, Bui N, Graham D, Yuva-Paylor LA, Paylor R (2009) Marble burying reflects a repetitive and perseverative behavior more than novelty-induced anxiety. Psychopharmacology 204:361-373.

Tierney CD, Gupta VB, Angel AP, Augustyn M (2012) Teasing out specific language impairment from an autism spectrum disorder. Journal of developmental and behavioral pediatrics : JDBP 33:272-274.

Till SM, Wijetunge LS, Seidel VG, Harlow E, Wright AK, Bagni C, Contractor A, Gillingwater TH, Kind PC (2012) Altered maturation of the primary somatosensory cortex in a mouse model of fragile X syndrome. Human molecular genetics 21:2143-2156.

Tucker B, Richards RI, Lardelli M (2006) Contribution of mGluR and Fmr1 functional pathways to neurite morphogenesis, craniofacial development and fragile X syndrome. Human molecular genetics 15:3446-3458.

Utari A, Chonchaiya W, Rivera SM, Schneider A, Hagerman RJ, Faradz SM, Ethell IM, Nguyen DV (2010) Side effects of minocycline treatment in patients with fragile X syndrome and

exploration of outcome measures. American journal on intellectual and developmental disabilities 115:433-443.
Van Borsel J, Dor O, Rondal J (2008) Speech fluency in fragile X syndrome. Clinical linguistics & phonetics 22:1-11.
Van de Veire S et al. (2010) Further pharmacological and genetic evidence for the efficacy of PlGF inhibition in cancer and eye disease. Cell 141:178-190.
Veeraragavan S, Graham D, Bui N, Yuva-Paylor LA, Wess J, Paylor R (2012) Genetic reduction of muscarinic M4 receptor modulates analgesic response and acoustic startle response in a mouse model of fragile X syndrome (FXS). Behavioural brain research 228:1-8.
Veikkola T, Jussila L, Makinen T, Karpanen T, Jeltsch M, Petrova TV, Kubo H, Thurston G, McDonald DM, Achen MG, Stacker SA, Alitalo K (2001) Signalling via vascular endothelial growth factor receptor-3 is sufficient for lymphangiogenesis in transgenic mice. The EMBO journal 20:1223-1231.
Ventura R, Pascucci T, Catania MV, Musumeci SA, Puglisi-Allegra S (2004) Object recognition impairment in Fmr1 knockout mice is reversed by amphetamine: involvement of dopamine in the medial prefrontal cortex. Behavioural pharmacology 15:433-442.
Vergouwen RP, Huiskamp R, Bas RJ, Roepers-Gajadien HL, Davids JA, de Rooij DG (1993) Postnatal development of testicular cell populations in mice. Journal of reproduction and fertility 99:479-485.
Verkerk AJ, Pieretti M, Sutcliffe JS, Fu YH, Kuhl DP, Pizzuti A, Reiner O, Richards S, Victoria MF, Zhang FP, et al. (1991) Identification of a gene (FMR-1) containing a CGG repeat coincident with a breakpoint cluster region exhibiting length variation in fragile X syndrome. Cell 65:905-914.
Verkerk AJ, de Graaff E, De Boulle K, Eichler EE, Konecki DS, Reyniers E, Manca A, Poustka A, Willems PJ, Nelson DL, et al. (1993) Alternative splicing in the fragile X gene FMR1. Human molecular genetics 2:399-404.
Vilkman E, Niemi J, Ikonen U (1988) Fragile X speech phonology in Finnish. Brain and language 34:203-221.
von Leden RE, Curley LC, Greenberg GD, Hunsaker MR, Willemsen R, Berman RF (2014) Reduced activity-dependent protein levels in a mouse model of the fragile X premutation. Neurobiology of learning and memory 109:160-168.
Walker EJ, Su H, Shen F, Degos V, Amend G, Jun K, Young WL (2012) Bevacizumab attenuates VEGF-induced angiogenesis and vascular malformations in the adult mouse brain. Stroke; a journal of cerebral circulation 43:1925-1930.
Walker K, Reeve A, Bowes M, Winter J, Wotherspoon G, Davis A, Schmid P, Gasparini F, Kuhn R, Urban L (2001) mGlu5 receptors and nociceptive function II. mGlu5 receptors functionally expressed on peripheral sensory neurones mediate inflammatory hyperalgesia. Neuropharmacology 40:10-19.
Wang ES, Teruya-Feldstein J, Wu Y, Zhu Z, Hicklin DJ, Moore MA (2004) Targeting autocrine and paracrine VEGF receptor pathways inhibits human lymphoma xenografts in vivo. Blood 104:2893-2902.
Westmark CJ, Malter JS (2007) FMRP mediates mGluR5-dependent translation of amyloid precursor protein. PLoS biology 5:e52.
White EL, Weinfeld L, Lev DL (1997) A survey of morphogenesis during the early postnatal period in PMBSF barrels of mouse SmI cortex with emphasis on barrel D4. Somatosensory & motor research 14:34-55.

Winograd C, Clayton D, Ceman S (2008) Expression of fragile X mental retardation protein within the vocal control system of developing and adult male zebra finches. Neuroscience 157:132-142.
Wohr M, Roullet FI, Crawley JN (2011) Reduced scent marking and ultrasonic vocalizations in the BTBR T+tf/J mouse model of autism. Genes, brain, and behavior 10:35-43.
Xiao Z, Kong Y, Yang S, Li M, Wen J, Li L (2007) Upregulation of Flk-1 by bFGF via the ERK pathway is essential for VEGF-mediated promotion of neural stem cell proliferation. Cell research 17:73-79.
Yan QJ, Rammal M, Tranfaglia M, Bauchwitz RP (2005) Suppression of two major Fragile X Syndrome mouse model phenotypes by the mGluR5 antagonist MPEP. Neuropharmacology 49:1053-1066.
Yu F, Zhong P, Liu X, Sun D, Gao HQ, Liu QS (2013) Metabotropic glutamate receptor I (mGluR1) antagonism impairs cocaine-induced conditioned place preference via inhibition of protein synthesis. Neuropsychopharmacology : official publication of the American College of Neuropsychopharmacology 38:1308-1321.
Zampieri BL, Fernandez F, Pearson JN, Stasko MR, Costa AC (2014) Ultrasonic vocalizations during male-female interaction in the mouse model of Down syndrome Ts65Dn. Physiology & behavior 128:119-125.
Zeidler S, Hukema RK, Willemsen R (2015) The quest for targeted therapy in fragile X syndrome. Expert opinion on therapeutic targets 19:1277-1281.
Zeng H, Dvorak HF, Mukhopadhyay D (2001) Vascular permeability factor (VPF)/vascular endothelial growth factor (VEGF) peceptor-1 down-modulates VPF/VEGF receptor-2-mediated endothelial cell proliferation, but not migration, through phosphatidylinositol 3-kinase-dependent pathways. The Journal of biological chemistry 276:26969-26979.
Zhang L, Cooper-Kuhn CM, Nannmark U, Blomgren K, Kuhn HG (2010) Stimulatory effects of thyroid hormone on brain angiogenesis in vivo and in vitro. Journal of cerebral blood flow and metabolism : official journal of the International Society of Cerebral Blood Flow and Metabolism 30:323-335.
Zhang YQ, Bailey AM, Matthies HJ, Renden RB, Smith MA, Speese SD, Rubin GM, Broadie K (2001) Drosophila fragile X-related gene regulates the MAP1B homolog Futsch to control synaptic structure and function. Cell 107:591-603.
Zola-Morgan S, Squire LR, Amaral DG (1986) Human amnesia and the medial temporal region: enduring memory impairment following a bilateral lesion limited to field CA1 of the hippocampus. The Journal of neuroscience : the official journal of the Society for Neuroscience 6:2950-2967.

APPENDIX A: SUPPLEMENTARY FILES FOR USV PROFILES

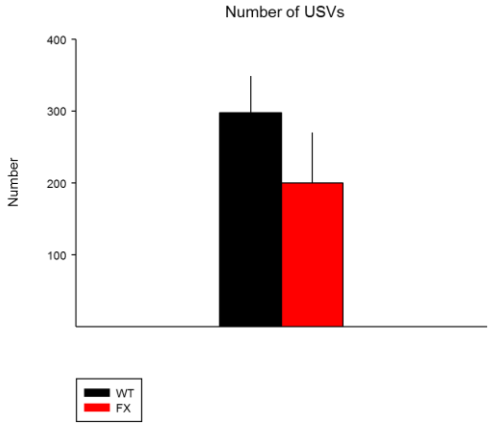

Figure A1. Total number of USVs generated.

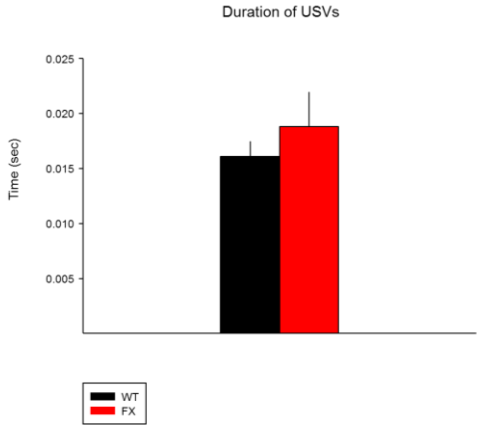

Figure A2. Average duration in seconds of generated USVs.

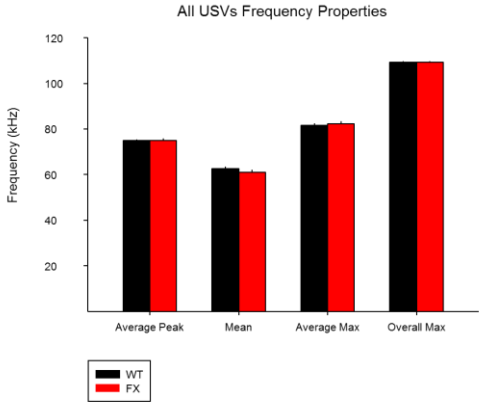

Figure A3. General frequency properties of all produced USVs. Note: Average Max is the average of the max frequencies of all USVs while Overall Max is the absolute maximum frequency reached.

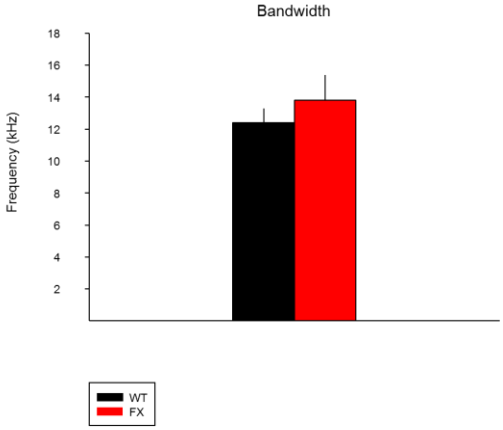

Figure A4. Frequency range of generated USVs.

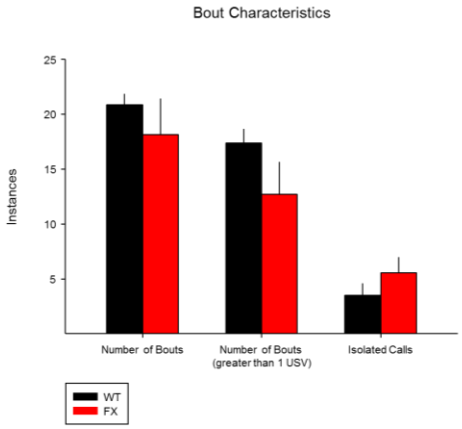

Figure A5. Number of various bouts and isolated calls.

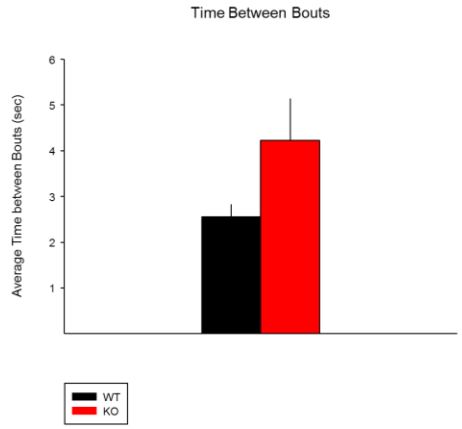

Figure A6. Time between bouts.

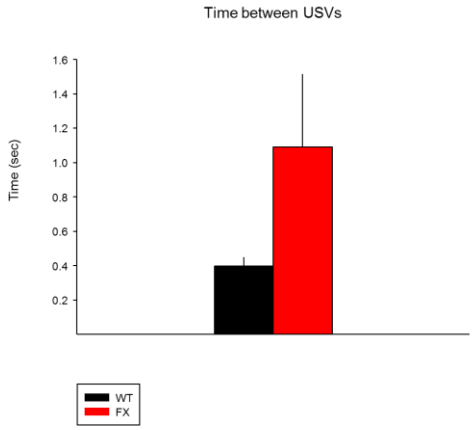

Figure A7. Time between all generated USVs.

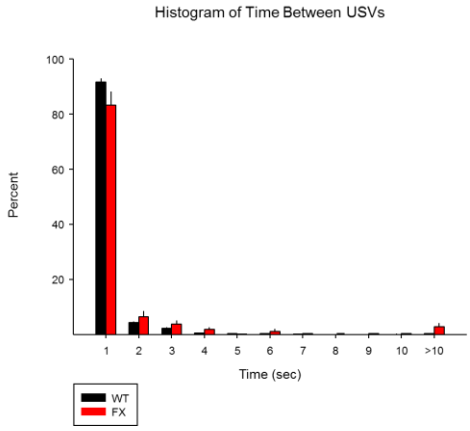

Figure A8. Histogram distribution of time between all generated USVs in one second bins.

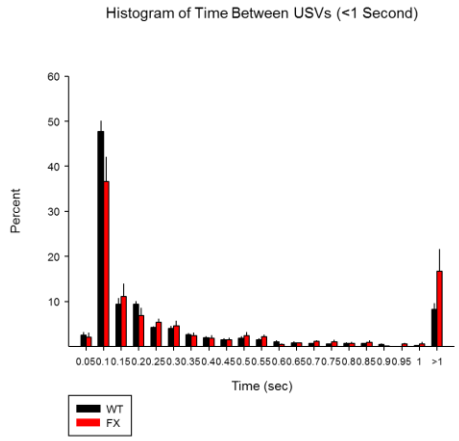

Figure A9. Histogram distribution of generated USVs with less than one second between calls in 0.05 second bins.

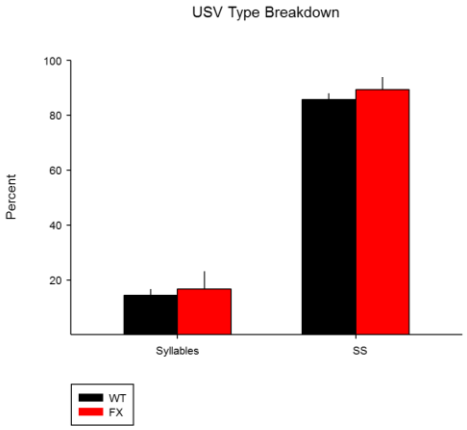

Figure A10. Distribution of USVs between syllables and sinusoidal sweeps (SS).

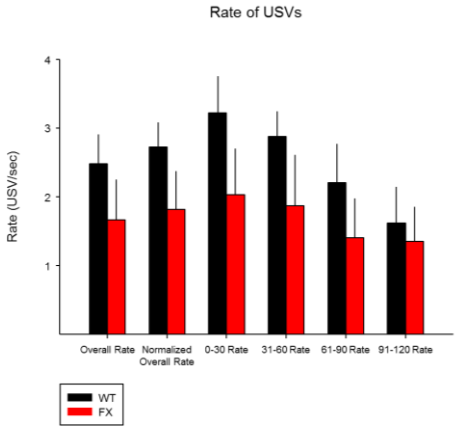

Figure A11. Rate of calling, overall and 30 second time bins.

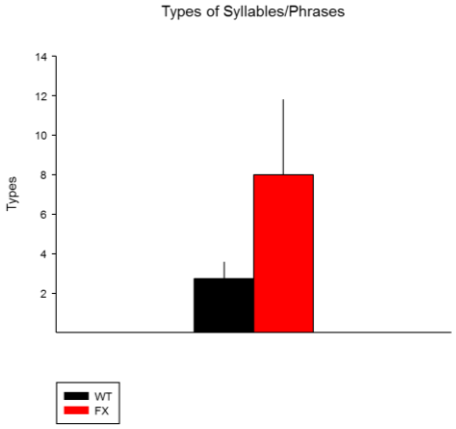

Figure A12. Number of types of generated syllables and phrases.

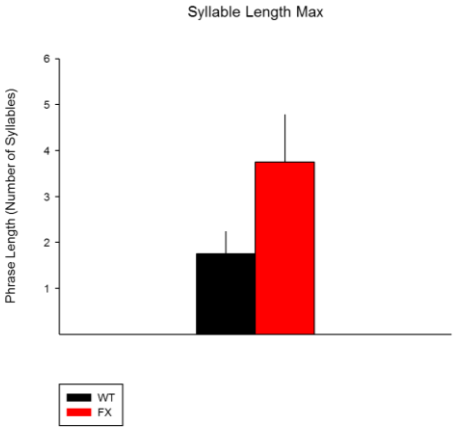

Figure A13. Max Length of all syllables and phrases.

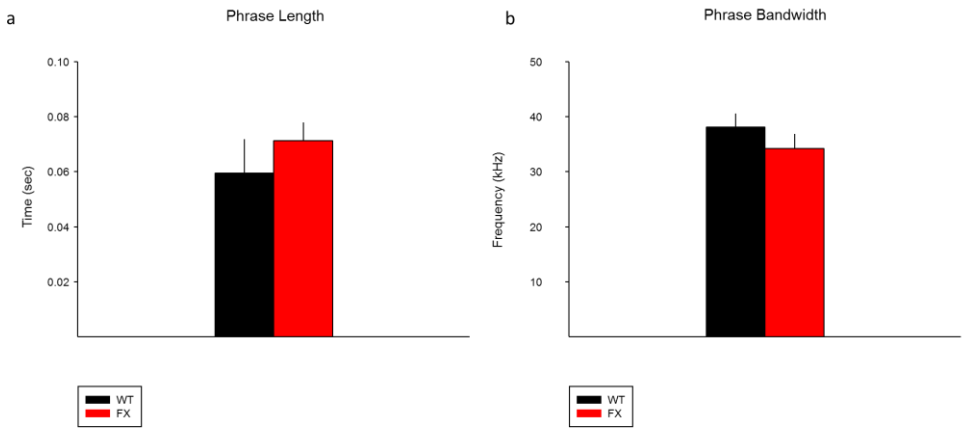

Figure A14. Characteristics of Phrases. a. Duration in seconds of each phrase. b. Frequency range of all phrases.

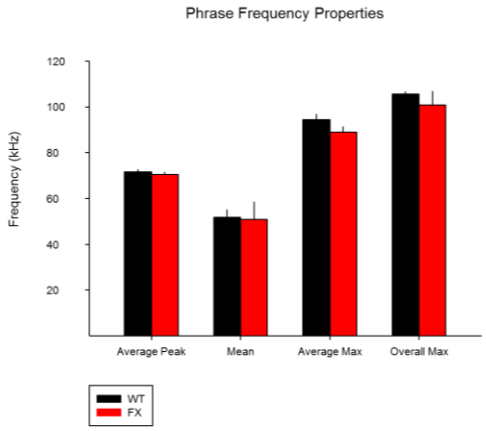

Figure A15. Frequency properties of all generated phrases.

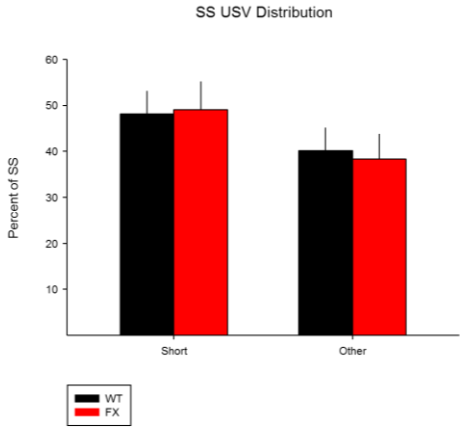

Figure A16. Percent of sinusoidal sweeps (SS) which were classified as short or other.

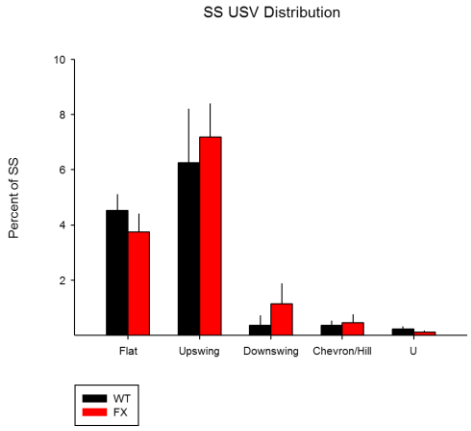

Figure A17. Distribution of the various sinusoidal sweep (SS) categories.

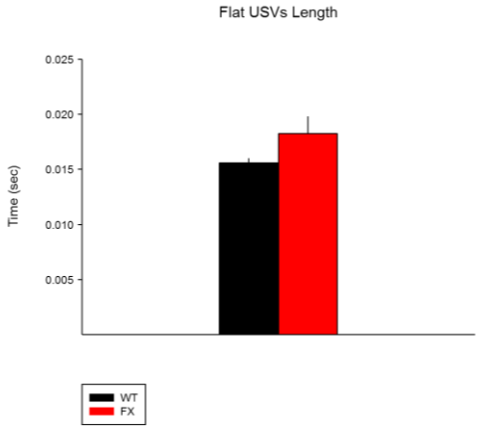

Figure A18. Duration of all generated flat USVs.

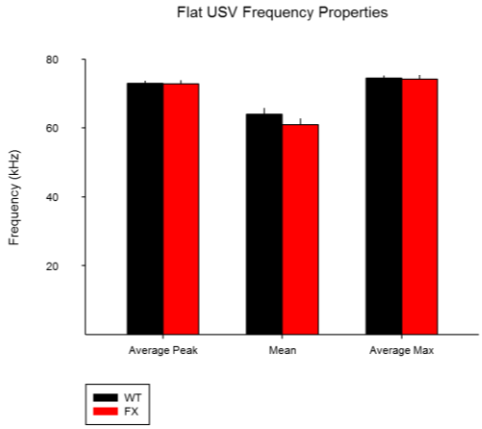

Figure A19. Frequency properties of all generated flat USVs.

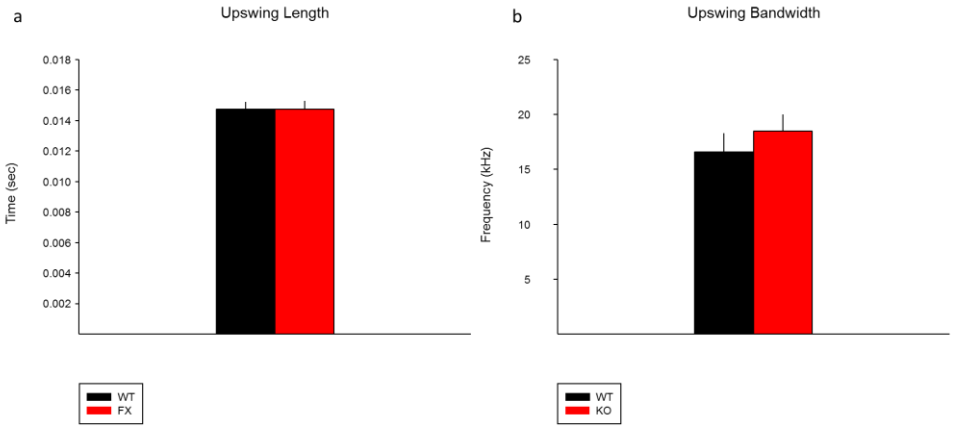

Figure A20. Characteristics of upswing USVs. a. Duration in seconds of all upswings. b. Frequency range of all upswings.

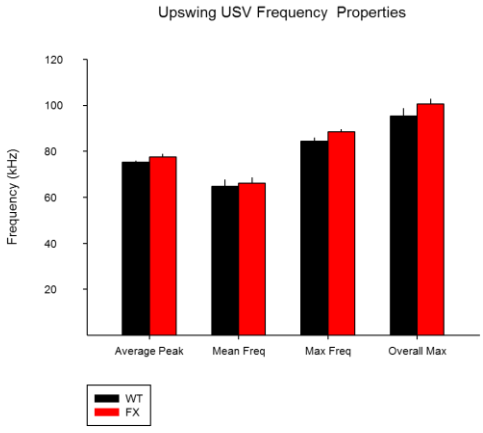

Figure A21. Frequency properties of all generated upswing USVs.

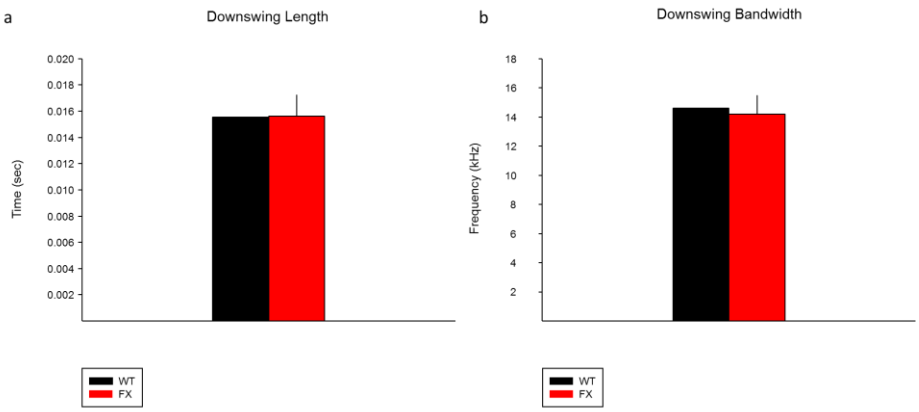

Figure A22. Characteristics of downswing USVs. a. Duration in seconds of all downswings. b. Frequency range of all downswings.

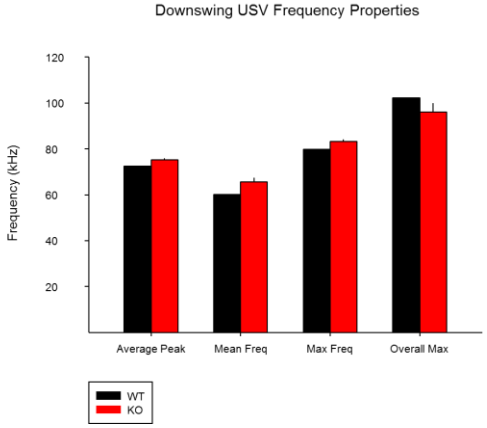

Figure A23. Frequency properties of all generated downswing USVs.

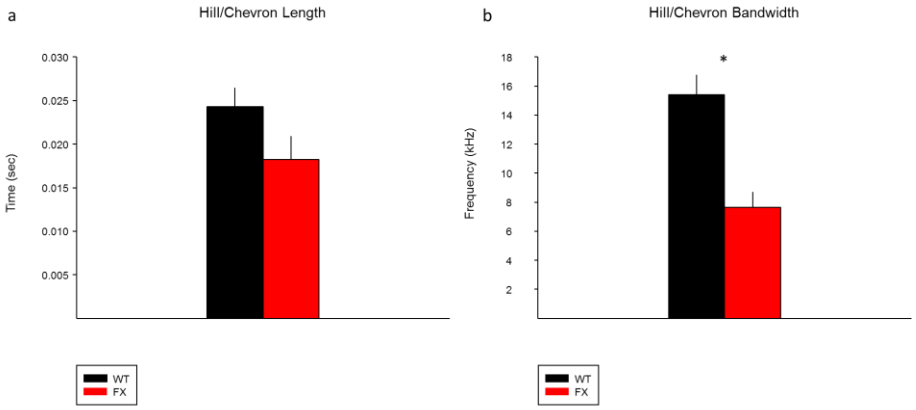

Figure A24. Characteristics of hill/chevron USVs. a. Duration in seconds of all hill/chevron. b. Frequency range of all hill/chevron. *<0.05

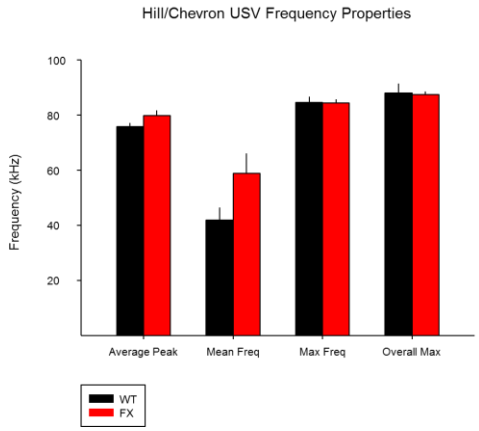

Figure A25. Frequency properties of all generated hill/chevron USVs.

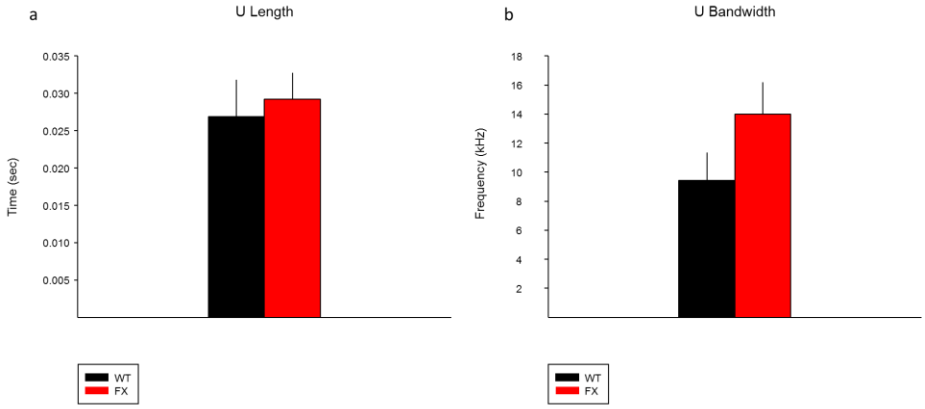

Figure A26. Characteristics of U sinusoidal sweep USVs. a. Duration in seconds of all U sinusoidal sweeps. b. Frequency range of all U sinusoidal sweeps.

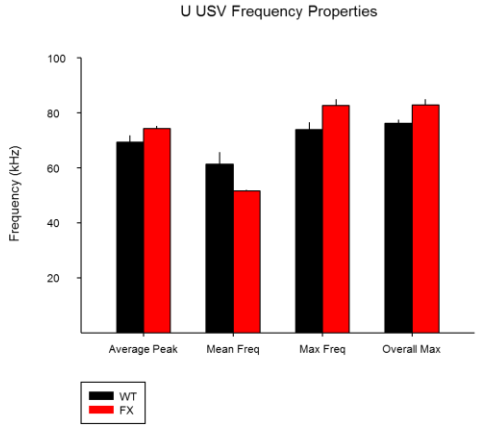

Figure A27. Frequency properties of all generated U sinusoidal sweep USVs.